Report from
Proceedings of
ForestSat 2005
in Borås May 31 - June 3

forestsat
2005

Håkan Olsson

Table of contents

Session 2b,
Edges and Ecotones

Session 3a,
Wind and other damages

Content in Report 8b
Session 3b,
Classification studies

Session 5b,
Radar studies

Content in Report 8c
Session 6a,
Change detection and time series

Session 6b,
Needs and use of Remote Sensing in Russia

Closing Session

Poster contributions

Large area mapping and monitoring

Methods for estimation and change detection

Habitat models and landscape metrics

Preface

ForestSat 2005 is the final conference of the EU-Life project ForestSafe. The conference is arranged by the Swedish partners in the project: the Swedish Forest Administration, which is the main organiser, and the Swedish University of Agricultural Sciences, which is responsible for the scientific aspects of the meeting. The conference is also a follow-up to ForestSat 2002, which was arranged by the UK partners of ForestSafe: the Forestry Commission and the University of Durham.

The ForestSafe project is about the practical use of new remote sensing techniques and we have divided the conference in two parts. The first part is a scientific workshop May 31 – June 1, which is co-sponsored by the relevant working groups in the concerned scientific organizations:

The special interest group on forestry within the European Association of Remote Sensing Laboratories (EARSeL);

The Remote Sensing Technology and Geographic Information Systems (GIS) unit (4.02.08) within the International Union of Forest Research Organisations (IUFRO);

Working group VIII/11, Sustainable Forest and Landscape Management, within the International Society of Photogrammetry and Remote Sensing (ISPRS).

This proceedings volume, in which only the abstracts have been reviewed, is a documentation of the scientific workshop, May 31-June 1, 2005. Furthermore, full peer-reviewed versions of selected articles will be published in a special issue of Remote Sensing of Environment, with Ronald McRoberts, US Forest Service and Daniel Donoghue, University of Durham, as guest editors. Summaries of the conference will also be communicated in the networks of EARSeL, IUFRO, and ISPRS. Even after the ForestSafe project ends in 2005, there is still a need for a meeting point for European forestry remote sensing, and the above mentioned working groups are prepared to sponsor a "ForestSat 2007" as well.

The host organisation, the Swedish Forest Administration, is a large operational user of satellite remote sensing. SPOT HRG or similar satellite data for all of Sweden is acquired yearly and used for, among other things, mapping of clearfelled areas. The Swedish University of Agricultural Sciences also uses satellite data on a nation-wide scale. In combination with National Forest Inventory plots, the satellite data is used both for forest parameter mapping using kNN and post stratification. We have tried to target the scientific workshop towards issues related to large-area practical use of forestry remote sensing and we are glad to have a large number of representatives for national forest inventories attend. It is also welcomed that we have a large delegation from Russia, where the need for forest monitoring is currently large. Optical satellite remote sensing is now a maturing technology, however, a major bottleneck for operational users is a secure future access to data. Important international processes are currently ongoing in this area, such as the prioritising of satellite missions within the European GMES programme, and the establishment of a Global Earth Observation System of Systems (GEOSS), which will be co-

ordinated by the GEO secretariat in Geneva. It is our hope that the ForestSAT 2005 conference will help highlight the forestry needs in these processes.

In addition to satellite remote sensing and interpretation of aerial photos, a number of new powerful techniques are also maturing, such as laser scanning, interferometric SAR and automatic interpretation of digital images. The presence of a number of papers in these areas gives a full picture of European forestry remote sensing. These technologies are also expected to be covered more in depth in an upcoming EARSeL / ISPRS workshop, "3D Remote Sensing in Forestry" in Vienna, February 13-15, 2006, (http://ivfl.boku.ac.at/3DRSForestry).

The scientific part of ForestSat, reported here, is followed by a "Practical Workshop" June 2, 2005 where user needs and existing methods in forestry remote sensing and GIS are demonstrated and where the intended audience is widened. ForestSat then ends with a field excursion, June 3.

We would like to thank the scientific committee: Daniel Donoghue, Ronald McRoberts, Erkki Tomppo, Anders Persson, Mathias Schardt, Werner Schneider and Juan Suarez for the work with selecting contributions and for their advice in organising the workshop.

Finally, we would like to thank the economic sponsors: The Nordic Forest Research Co-operation Committee (SNS), The Swedish Environmental Protection Agency and the Swedish National Space Board.

Håkan Olsson, Swedish University of Agricultural Sciences, Chairman of the ForestSat 2005 scientific committee.

Staffan Norin, Swedish Forest Administration, Chairman of the organising committee.

REMOTE SENSING SUPPORT FOR THE NATIONAL FOREST INVENTORY OF THE UNITED STATES OF AMERICA

Ronald E. McRoberts
North Central Research Station
USDA Forest Service
1992 Folwell Avenue
Saint Paul, Minnesota USA 55108
e-mail: rmcroberts@fs.fed.us

ABSTRACT

The Forest Inventory and Analysis (FIA) program of the United States Forest Service conducts inventories of the nation to estimate the area of forest land; the volume, growth, and removal of forest resources; and the health of the forest. Users of FIA data, estimates, and related products include land managers, policy and decision-makers, forest industry, environmental organizations, and university researchers. To accomplish its mission, the FIA program has established a plot configuration, a sampling design, and estimation routines that are all nationally consistent. The inventory program releases data on an annual basis and reports estimates at the county level for each state every five years. Remote sensing applications enhance the data acquisition, estimation, and information distribution components of the program. Primary remote sensing applications include initial observation of plot locations, stratification to increase the precision of estimates, circumventing the consequences of the prohibition on release of exact plot locations, and mapping.

Keywords. Stratification, mapping, plot location security, uncertainty.

1   THE FOREST INVENTORY AND ANALYSIS PROGRAM

The national forest inventory of the United States of America (USA) is conducted by the Forest Inventory and Analysis (FIA) program of the Forest Service, U.S. Department of Agriculture, and has been in continuous operation since the 1930s. The program collects and analyzes inventory data and reports on the status and trends of the nation's forests. In 1998, the five regional FIA units adopted common data collection procedures, an action which greatly simplified construction of a data distribution database and national reporting tools. The national FIA plot consists of four 7.32-m (24-ft) radius circular subplots. The subplots are configured as a central subplot and three peripheral subplots with centers located at 36.58 m (120 ft) and azimuths of 0°, 120°, and 240° from the center of the central subplot. The plot configuration includes smaller components for sampling other forest attributes such as small trees, non-woody vegetation, down woody material, soils, and vegetation diversity and structure. The national sampling design was derived from the world wide sampling array developed by the U.S. Environmental Protection Agency as part of the Environmental Monitoring and Assessment Program (White *et al*. 1992). Initially, the nation was tessellated using an array of approximately 65,000-ha hexagons that formed the basis for the Forest Health and Monitoring (FHM) program sampling design. This array was used as a framework for generating smaller FIA hexagons of which each contains approximately 2,400 ha (6,000 ac) (Figure 1). The FIA sampling design was implemented by establishing a permanent plot in each FIA hexagon. The latter array of plots is designated the federal base sample and is considered to be an equal probability sample. Thus, the FIA sampling design is nationally consistent, provides systematic coverage of all lands, and is fully integrated with the FHM sampling design. The federal base sample was systematically divided into five interpenetrating, non-overlapping panels. Panels are selected for measurement on approximate 5-, 7-, or 10-year rotating bases, depending on the region of the country, and measurement of all accessible plots in one panel is completed before measurement of plots in a subsequent panel is initiated.

FIA inventories are conducted in three phases. Phase 1 entails the use of remotely sensed data to obtain initial observations of land cover and to stratify land area in the population of interest with the objective of increasing the precision of estimates. Phase 2 entails field crew visits to the physical locations of permanent field plots determined in Phase 1 to include accessible forest land that is at least 10-percent stocked, 0.4 ha (1.0 ac) in area, and 36.58 m (120 ft) wide. For each tree, field crews record a variety of

observations and measurements including species, live/dead status, lean, diameter, height, crown ratio (percent of tree height represented by crown), crown class (e.g., dominant, co-dominant, overtopped), damage, and decay status. Stand-level observations include ownership, land cover, forest type, stand origin, stand age, stand size, site productivity, forest disturbance history, slope, aspect, physiographic class, and land use. Inventory specialists use field crew measurements to calculate values for additional variables including individual tree volume and per unit area estimates of number of trees, volume, and biomass by subplot, by species groups, by live/dead status, and by ownership.
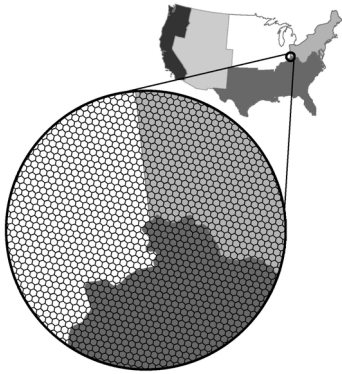
Figure 1. 2,400-ha sampling hexagons.

Phase 3 focuses on forest health and is administered cooperatively by the FIA program, other Forest Service programs, other federal agencies, state natural resource agencies, and universities and is partially integrated with the FHM program. The FHM program consists of four interrelated and complementary activities: Detection Monitoring, Evaluation Monitoring, Intensive Site Ecosystem Monitoring, and Research on Monitoring Techniques. Detection Monitoring consists of systematic aerial and ground surveys designed to collect baseline information on the current condition of forest ecosystems and to detect changes from those baselines over time. Evaluation Monitoring studies examine the extent, severity, and probable causes of changes in forest health identified through the Detection Monitoring surveys. The Intensive Site Ecosystem Monitoring program conducts research into regionally specific ecological processes at a network of sites located in representative forested ecosystems. Finally, Research on Monitoring Techniques focuses on developing and refining indicator measurements to improve the efficiency and reliability of data collection and analysis at all levels of the program.

The ground survey portion of the FHM Detection Monitoring program was integrated with the FIA program as Phase 3 in 1999. The Phase 3 sample consists of a 1:16 subset of the Phase 2 plots with one Phase 3 plot for approximately every 38,450 ha (96,000 ac). Phase 3 measurements are obtained by field crews during the growing season and include an extended suite of ecological data: lichen diversity and abundance, soil quality (erosion, compaction, and chemistry), vegetation diversity and structure, and down woody material. The incidence and severity of ozone injury for selected indicator species are also monitored as part of an associated sampling scheme. Because each Phase 3 plot is also a Phase 2 plot, the entire suite of Phase 2 measurements is also collected on each Phase 3 plot.

2 PRODUCTS AND USERS

A variety of products are based on or derived from FIA data and made available to the public: (1) annual and 5-year statistical reports that include tables and graphical depictions of estimates by species, ownership classes, and political units such as counties, national forests, and states; (2) assessments of sustainable forest management; (3) assessments of ecological and environmental issues identified from analyses accompanying the statistical reports; (4) raw and summarized plot data; and (5) maps depicting the spatial distribution of forest attributes. Users of FIA data and the derived products are drawn from government, forest industry, environmental groups, and university researchers. Examples of uses include government monitoring of the sustainability of forest management for both ecological and economic purposes, industrial decision-making and resource assessments, and monitoring of sustainability and wildlife habitat by environmental groups. University researchers often focus on development of tools and methods to support other users. Increasingly, university researchers seek access to FIA plot data as a source of training or accuracy assessment data for satellite image-based classification, prediction, and map-making. The latter

uses are hampered by the constraint imposed by the U.S. Government that exact plot locations and proprietary plot information may not be disclosed to the public.

3 REMOTE SENSING APPLICATIONS

Remotely sensed information in the form of aerial photographs and satellite imagery is used extensively to enhance data acquisition, estimation, mapping, and to alleviate the effects of the constraint prohibiting disclosure of exact plot locations. Four primary applications are discussed: (1) initial plot observation, (2) stratification, (3) compensating for the prohibition on release of exact plot locations, and (4) map construction.

3.1 INITIAL PLOT OBSERVATION

The federal base sample includes at least one permanent plot location in each 2,400-ha hexagon, regardless of whether the plot location has complete, partial, or no forest cover. However, many large portions of the USA, particularly in the Midwestern plains, have little forest land. Because the greatest portion of the expense of field measurement of an FIA plot is the cost of travel to and from the plot, considerable savings may be realized by not field measuring plots that do not have tree cover qualifying as forest land. In these regions, an initial assessment of the land cover at each plot location is made using scanned aerial photographs, GIS layers, and historical information. If this initial assessment indicates that a plot has no forest land, no field visit is made to the plot. To avoid bias as a result of misinterpretation of the remotely sensed data, all plots with questionable land cover are field visited, as are plots that were forested at the time of the most recent field visit or that are in close proximity to forest land. In addition, a sample of plots determined to have no accessible forest land are field visited as a means of assessing the accuracy of the initial plot observation.

3.2 STRATIFICATION TO INCREASE THE PRECISION OF ESTIMATES

Due to budgetary constraints and natural variability among plots, sufficient numbers of plots frequently cannot be measured to satisfy precision guidelines for the estimates of many variables unless the estimation process is enhanced using ancillary data. Classified satellite imagery has been accepted as a source of ancillary data that can be used with stratified estimation techniques to increase the precision of estimates with little corresponding increase in costs (Poso 1990, Muinonen and Tokola 1990, McRoberts *et al.* 2002a, Hoppus and Lister 2003, Nilsson *et al.* 2003). McRoberts *et al.* (2002a) used three steps to derive four strata from the National Landcover Dataset, (NLCD) (Vogelmann *et al.* 2001, Homer *et al.* 2004), a 21-class land cover map of the conterminous USA. First, the NLCD transitional, deciduous forest, evergreen forest, mixed forest, shrubland, and woody wetland classes are aggregated into a forest stratum, and the remaining classes are aggregated into a non-forest stratum. Second, isolated groups of small numbers of contiguous forest pixels are reassigned to the non-forest stratum to comply with the 0.40-ha minimum area necessary to be designated FIA forest land. Third, two additional strata are created by subdividing the forest stratum into forest and forest edge strata and by subdividing the non-forest stratum into non-forest and non-forest edge strata. The edge strata are created by assigning pixels in the original forest stratum within two pixels of the forest/non-forest boundary to the forest edge stratum and pixels in the original non-forest stratum within two pixels of the forest/non-forest boundary to the non-forest edge stratum (Figure 2). The increase in precision realized with this approach to stratification typically ranges from 2.00 to 3.50 for estimating forest area and from 1.25 to 1.75 for estimating volume per unit area.
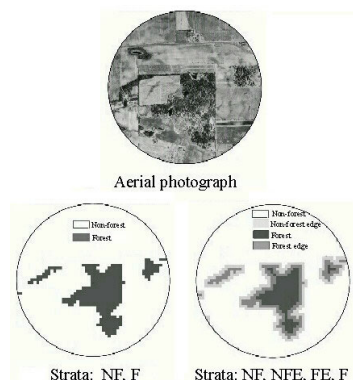
Figure 2. Stratification based on classified satellite imagery.

McRoberts *et al.* (in review) proposed an approach to stratification in which a logistic regression model was used to predict proportion forest land for each Landsat TM/ETM+ pixel. Strata were defined in terms of categories of predictions, $\bar{p}$, of proportion forest; for example: $0.0 \leq \bar{p} \leq 0.1$, $0.1 < \bar{p} \leq 0.5$, $0.5 < \bar{p} \leq 0.9$, and $0.9 < \bar{p} \leq 1.0$. With this approach, precision was increased by approximately 50% for estimates of forest area and approximately 20% for estimates of volume per unit area relative to the NLCD-based stratifications.

3.3 CIRCUMVENTING THE EFFECTS OF PERTUBED PLOT LOCATIONS

For a variety of privacy and sample integrity reasons, the FIA program is prohibited by law from disclosing the exact locations of inventory plots to the public. To comply with the law, all plot locations are perturbed as much as 0.8 km before being released. One potential effect of perturbed plot locations is to decrease the utility of FIA data for use in training or evaluating the accuracy of classifiers of satellite imagery by non-FIA users. If the pixel resolution is substantially greater than the perturbing radius, then there are few difficulties, but for moderate resolution imagery such as 250-m MODIS and 30-m Landsat TM/ETM+ the pixel resolution is much less than the perturbing radius. If the combination of spectral values for the pixel associated with a plot is unique within the Landsat scene, then the possibility exists that the plot may be located to within the pixel resolution by searching the satellite image for that particular combination of spectral values. With one or two dates of Landsat imagery the probability of locating plots is small, but with three dates the probability is unacceptably large. McRoberts *et al.* (in press) investigated the effects of perturbed plot locations on model-based forest/nonforest maps and on estimates of forest area obtained from a logistic regression model calibrated using inventory data and the spectral values of three dates of Landsat imagery. They found that both estimates of forest area and the spatial distributions of pixels predicted to be forested and nonforested were biased. However, they also found that by adding a randomly selected, uniformly distributed integer between -5 and +5 to each spectral value of the three dates of Landsat imagery, the probability of locating plots was negligible, while the estimates of forest area based on perturbed spectral values exhibited much less bias.

3.4 MAPPING APPLICATIONS

With the widespread availability of reasonably priced, moderate resolution satellite imagery, mapping forest attributes has become an increasingly high priority activity. If unbiased and sufficiently precise areal estimates of forest attributes could be obtained by aggregating pixel predictions, then several advantages would accrue. First, in addition to plot-based estimates for medium and large regions, users would obtain spatial distributions of forest attributes from which estimates for small areas could be obtained. Second, because map-based approaches that use the full range of spectral values of satellite imagery use more information than do stratification approaches, the precision of map-based estimates may be greater than corresponding stratified estimates. Third, for many applications, map-based estimation at least partially alleviates the effects of the prohibition on disclosure of exact plot locations, because predictions are aggregations of observations for multiple plots, and the particular plots, their locations, and their ownerships need not be revealed. Fifth, efficiencies would be gained by simultaneously addressing both the estimation and mapping issues.

A crucial challenge in this type of mapping effort is to ensure the consistent, compatible, and unbiased prediction of multiple forest attributes simultaneously. This almost certainly requires a multivariate approach to prediction; otherwise, for example, some pixels that are predicted to have no forest cover may also be predicted to have a large amount of tree volume, and vice versa. An additional difficulty is that most parametric approaches to multivariate prediction are constrained by distributional assumptions. The non-parametric, multivariate k-Nearest Neighbors method seems ready made for this application (Franco-Lopez *et al.* 2001, Katila and Tomppo 2001, McRoberts *et al.* 2002b). Investigations for six test areas, three each in Minnesota and Indiana, USA, indicate that map-based estimates of forest area and volume per unit area for circular areas with radii ranging from 6 km to 15 km are not statistically significantly different than plot-based estimates (Table 1). Further, estimates may be obtained for small areas for which there are not enough plots for plot-based estimates. An Internet-based application that permits users to submit an arbitrary polygon and receive both plot- and map-based estimates in return is under construction. The

challenge will be to develop estimation algorithms that are sufficiently fast to accommodate users' tolerance thresholds.

Table 1. Results for Test Area 1

Radius (km)	No. plots	Proportion forest area				Volume per unit area (m³/ha)			
		Plot-based		Map-based		Plot-based		Map-based	
		$\bar{\mu}_{plot}$	SE_{plot}	$\bar{\mu}_{map}$	τ[1]	$\bar{\mu}_{plot}$	SE_{plot}	$\bar{\mu}_{map}$	τ[1]
6	10	0.80	0.12	0.73	0.58	15.7	5.8	19.7	-0.69
7	13	0.71	0.11	0.70	0.09	14.0	4.6	19.3	-1.15
8	15	0.75	0.09	0.68	0.78	16.6	4.6	19.0	-0.52
9	20	0.68	0.09	0.65	0.33	13.8	3.7	18.7	-1.32
10	25	0.57	0.09	0.62	-0.56	11.6	3.1	18.0	-2.06
11	29	0.60	0.08	0.63	-0.38	13.2	3.3	18.2	-1.52
12	33	0.59	0.07	0.63	-0.57	14.6	3.3	18.6	-1.21
13	40	0.57	0.07	0.64	-1.00	14.0	2.9	18.7	-1.62
14	45	0.58	0.06	0.65	-1.17	13.9	2.6	18.7	-1.85
15	50	0.62	0.06	0.65	-0.50	15.6	2.6	18.7	-1.19

[1] $\tau = \dfrac{\bar{\mu}_{plot} - \bar{\mu}_{map}}{SE_{plot}}$; $\tau \leq 2.0$ suggests no statistically significant difference

4 SUMMARY

Before 1998, forest inventory data for the USA was collected, stored, and distributed using regional systems. The adoption by the national FIA program of a national plot configuration, a national sampling design, nationally consistent compilation algorithms, and data storage procedures has dramatically increased the utility of FIA data. The advent of readily available aerial photographs in electronic formats and moderate resolution satellite imagery has led to cost savings in data acquisition, increases in the precision of estimates, greater distribution of inventory data, and partial alleviation of the negative effects of constraints on disclosure of exact plot locations and proprietary information.

REFERENCES

Franco-Lopez, H. Ek, A.R., and Bauer, M.E. 2001. Estimation and mapping of forest stand density, volume, and cover type using the k-Nearest Neighbour method, *Remote Sensing of Environment* 77: 251-274.

Homer, C., Huang, C., Yang, L., Wylie, B., and Coan, M. 2004. Development of a 2001 national landcover database for the United States. *Photogrammetric Engineering and Remote Sensing* 70(7): 829-840.

Hoppus, M.L., and Lister, A.J. 2003. A statistically valid method for using FIA plots to guide spectral class rejection in producing stratification maps. In: R.E. McRoberts, G.A. Reams, P.C. Van Deusen, and J.W. Moser (Eds.) *Proceedings of the third annual forest inventory and analysis symposium*; 2001 October 17-19; Traverse City, Michigan. Gen. Tech. Rep. NC-230. St. Paul, MN: U.S. Department of Agriculture, Forest Service, North Central Research Station. pp. 44-49.

Katila, M., and Tomppo, E. 2001. Selecting estimation parameters for the Finnish multisource National Forest Inventory. *Remote Sensing of Environment* 76: 16-32.

McRoberts, R.E., Wendt, D.G., Nelson, M.D., and Hansen, M.H. 2002a. Using a land cover classification based on satellite imagery to improve the precision of forest inventory area estimates. *Remote Sensing of Environment* 81: 36-44.

McRoberts, R.E., Nelson, M.D., and Wendt, D.G. 2002b. Stratified estimation of forest area using satellite imagery, inventory data, and the k-Nearest Neighbors technique. *Remote Sensing of Environment* 82: 457-468.

McRoberts, R.E., Holden, G.R., Nelson, M.D., Liknes, G.C., and Gormanson, D.D. In review. Increasing the precision of forest inventory estimates using satellite imagery as ancillary data. *Canadian Journal of Forest Research.*

McRoberts, R.E., Holden, G.R., Nelson, M.D., Liknes, G.C., Moser, W.K., Lister, A.J., King, S.L., LaPoint, E.B., Coulston, J.W., Smith, W.B., and Reams, R.A. In press. Estimating and circumventing the effects of perturbing and swapping inventory plot locations. *Journal of Forestry.*

Muoinonen, E., and Tokola, T. 1990. An application of remote sensing for communal forest inventory. In: *The usability of remote sensing for forest inventory and planning, proceedings from SNS/IUFRO workshop, Report 4.* Remote Sensing Laboratory, Swedish University of Agricultural Sciences, Umeå, Sweden. pp. 35-42.

Nilsson, M., Folving, S., Kennedy, P., Puumalainen, J., Chirici, G., Corona, P., Marchetti, M., Olsson, H., Ricotta, C., Ringvall, A., Stahl, G. and Tommpo, E. 2003. Combining remote sensing and field data for deriving unbiased estimates of parameters over large regions. In: P.Corona, M. Köhl, and M. Marchetti (Eds.) *Advances in forest inventory for sustainable forest management and biodiversity monitoring.* Kluwer Academic Publishers, Dordrecht, The Netherlands. pp. 19-32.

Poso, S. 1990. Frame for using remote sensing in forestry planning. In: *The usability of remote sensing for forest inventory and planning, proceedings from SNS/IUFRO workshop, Report 4.* Remote Sensing Laboratory, Swedish University of Agricultural Sciences, Umeå, Sweden. pp. 31-34.

Vogelmann, J.E., Howard, S.M., Yang, L., Larson, C.R., Wylie, B.K., and Van Driel, N. 2001. Completion of the 1990s National Land Cover Data Set for the conterminous United States from Landsat Thematic Mapper data and ancillary data sources. *Photogrammetric Engineering and Remote Sensing* 67: 650-662.

White, D., J. Kimerling, and S.W. Overton. 1992. Cartographic and geometric components of a global sampling design for environmental monitoring. *Cartography and Geographic Information Systems* 19: 5-22.

ACCURACY OF FOREST MAPPING BASED ON LANDSAT TM DATA AND A kNN-BASED METHOD

A.K. Gjertsen

Norwegian Institute of Land Inventory, Raveien 9, N-1430 Ås, Norway, email: akg@nijos.no

ABSTRACT

A multi-source forest inventory method has been developed. It is based on a k-nearest neighbour classification rule and uses field data from the National Forest Inventory, land cover maps, and satellite image data. The inventory method is used to produce maps and to make estimates of selected forest parameters for large areas such as municipalities. For maps the accuracy at pixel level is relevant; for large area estimation the size of the error mean is important. In this paper the focus has been on the accuracy of the inventory method at pixel level.

Keywords: forest inventory, nearest neighbour classification, Landsat TM.

1 INTRODUCTION

The National Forest Inventory (NFI) of Norway is based on a regular 3x3 km network of permanent sample plots. Each plot is defined as a circle with 250-m^2 area (r = 8.92 m), and the diameter at breast height (DBH) of trees with DBH > 5 cm is measured and species recorded. Tree height is measured for a sample of the trees. Based on these measures, total volume and volumes per species are calculated. Forest stand parameters, such as site index, development class, stand species class, are assessed based on a 1000 m^2 area (0.1 hectare) of a homogenous stand that the plot falls inside.

The NFI delivers statistical reports for counties and the whole country. The system has limitations and is neither able to report reliable statistics for small areas such as municipalities or maps showing where inside a county certain forest resources are localised. To solve these limitations, a multi-source forest inventory method based on the k-nearest neighbour rule was tested in 1998 (Gjertsen *et al.* 1998). The objective of the test was to find out which forest parameters could be estimated with the method. The test included both parameters that describe the condition of the forest floor and parameters describing attributes of the canopy. Of all the 28 parameters tested only a few showed reasonable good results, and of these dominating species and generalised development classes were the most promising (Gjertsen *et al.*, 1998; Gjertsen *et al.*, 1999). Today, both maps and statistics for municipalities are produced using the method. A study has been made to analyse the accuracy of the maps and how the accuracy depends on the input variables to the model (Gjertsen *et al.*, 2004). This paper reports on some of the findings of this work.

2 DATA AND STUDY AREA

A set of 1075 NFI plots inside the coverage of Landsat Thematic Mapper (TM) scene frame (path 197, row 18) was used as ground reference data. A Landsat 5 TM acquisition from July 31, 1999 was obtained. The image was orthorectified using digital terrain data, derived from a 1:50,000 topographic map, and a detailed topographic map. In the rectification process, the nearest neighbour algorithm was used to interpolate digital values, and the reason for this choice was that the original values should not be distorted. From a physical point of view, however, it can be argued that cubic convolution would be more appropriate. Atmospheric correction has not been done.

The NFI plots have been georeferenced with GPS and the accuracy was expected to be within 10 meters for 99 % of the plots. However, two independent tests of GPS localisation gave a deviation of more than 10 meters for 7 % of the plots, and of these 3 % had a deviation of more than 15 meters. All plots are marked by a metal pole securing exact identification of the plot centre in the field. Each year 1/5 of the plots is visited, and in 5 years all plots inside a county is measured. For this study plot data from the period 1995–99 was used. In Table 1 statistics show how the plots are distributed by dominating species groups and development classes. In development class I species class is not recorded. We see that spruce is quite evenly distributed over development classes, that more that 1/3 of the pine dominated plots are in mature forest (class V), and that more than half of the deciduous dominated plots are found in regenerated plots

(class II). These patterns are as expected. The study area lies between 59 and 61 degrees north centred on Oslo. This is a nemo-boreal area dominated by conifers and only with pockets of deciduous woods in the most favourable sites, and are mainly found in ecotones between open areas and forests, water bodies and forest, and as pioneer species in recently disturbed areas.

Table 1. Statistics from the NFI dataset showing a cross tabulation of dominating species class by development class[a]. a. I: under regeneration, II: regenerated area, III: young thinning stand, IV: advanced thinning stand, V: mature forest.

Dominating species		Development classes				
		I	II	III	IV	V
Spruce	%	0	26	28	21	25
Pine	%	0	20	25	19	36
Deciduous	%	0	61	14	19	6

3 METHODS

The multi-source inventory method has been described in earlier publication (Gjertsen *et al*, 1998; Gjertsen *et al.*, 2004), and it will therefore only be shortly described here. The method is based on the k-NN classification rule, and the procedure is quite simple. We compute the distance from an observation vector y_i to all calibration vectors y_j for all $j = 1, ..., n$, where n is the number of NFI plots in the calibration dataset. The vector y consists of the six measurements in the TM bands used. Several distance measures can be employed, and one of the simplest is the Euclidean distance $d(x,y) = sqrt[(x − y)'(x − y)]$. To adjust for differing variances and covariances among the six TM bands, the statistical distance $sqrt[(x − y)'S^{-1}(x − y)]$ can be used, where S is the sample covariance matrix. To classify y_i, the k points nearest to y_i are examined. For a forest parameter measured on nominal or ordinal scales, the class with a majority among the k points is assigned to y_i; for parameters measured on interval or ratio scales a distance weighted estimate based on the k nearest points is calculated. If the sample sizes n_i differ, proportions k_i/n_i can be used instead of counts. A decision must be made as to the value of k. It has been suggested to choose k near $sqrt(n_i)$ for typical n_i. In practise, we test several values for k and use the one with the best error rate.

Thematic maps of the inventory area can be used in the process. One method that is implemented in our method is to use a site index map to filter the points y_j, such that only points assigned to the same site index class as the observation vector y_i are used. This makes sense from an ecological point of view, since the different tree species occupy different ecological niches.

The image sensor measures reflected EM energy in seven bands. The accuracy of the inventory method depends heavily on the association between the spectral variables and the forest parameters. When the association is weak, we can expect results from the inventory that we would get by using the calibration dataset alone. To test the level of association univariate and multivariate analysis of variance has been performed. The analyses were used to show whether the spectral variables could be used to separate the different groups. In addition discriminant analysis has been used to describe the separation of the different species and development class groups and to infer the contribution of the different spectral bands to the separation. The discriminant functions used was defined as the linear combination $z = a'y$, where y is a p×1 vector of the spectral variables and a' is a 1×p vector of coefficients. The NFI plots were grouped in species classes and development classes, and for each of the groupings, discriminant functions were calculated. The absolute values of the coefficients (standardised) were used to rank the contribution of the spectral band in separating the groups. The method takes into account the correlations among the spectral variables as well as the influence of each variable in the presence of the others. In addition, stepwise selection of variables was used to test whether some spectral variables were redundant in the presence of the others.

To test the effect of the sample sizes n_i for the different groups (e.g. species groups) on the accuracy, two different NFI datasets were used: (1) one with all 1075 NFI plots and (2) one random subset such that n_i was equal for all species groups. The purpose was to test how much the accuracy of predicting species groups would change when changing the relative sample sizes. To test the effect of using satellite data and site index data as ancillary data and how much these data improve the estimation above a simple estimation based on the NFI plots only, five different trials were conducted as shown in Table 2.

Table 2. Different trials used to test effect of ancillary data on accuracy. a. 'x' = used; '-' = not used.

	Ancillary data used[a]		
Trial	Image data	Site index data	# nearest neighbours
1	x	x	8
2	x	-	8
3	-	x	8
4	-	-	8
5	-	-	1

4 RESULTS AND DISCUSSION

Table 3 shows the pooled within-groups correlation matrix for species groups. The corresponding matrix for development classes is very similar and shows the same pattern. We note that band 3 is highly correlated with bands 1 and 2 ($r_{13} = 0.806$ and $r_{23} = 0.905$), and that band 5 is highly correlated with band 7 ($r_{57} = 0.940$). We also note that band 4 has the lowest correlation with all the other bands, except for band 5 where band 1 has the lowest correlation. Of the two middle infrared bands 5 and 7, the latter has the lowest correlation with band 4, i.e. $r_{47} = 0.563$ vs. $r_{45} = 0.739$. This result suggests that the dimensionality of the spectral variables is not six but four or three. Some of the bands seem redundant in the presence of the others. To further elucidate the redundancy of spectral variables, the results of a stepwise selection of variables are shown in Table 4. Wilk's Lambda shows the overall Λ of the MANOVA models. The stop criterion for entering new variables to the model was a partial F-value of 3.84. We see that TM bands 4, 7, 3, and 1 were added for species groups and only bands 4 and 7 for development groups. Thus, in the case of development classes, bands 1, 2, 3, and 5 were redundant. It may be a bit surprising that not a single band from the visible part of the spectrum was included. These results indicate already that separation of species groups will be more successful than separation of development groups.

The ANOVA test of equality of group means for species groups and development groups gave significant results for all bands (significance probabilities below 0.001). The same test was performed with subsets based on species groups. For pine dominated plots, only band 4 gave a significant difference; for deciduous dominated plots, only band 4 failed in the test ($\alpha = 0.05$). We note the results for band 4: it is the only significant band for pine-dominated plots and the only non-significant band for the deciduous plots. To further explore the separability of development classes, they were regrouped into three more general classes. Again the ANOVA results for pine-dominated plots showed a significant separation of the groups only with band 4 (F = 5.755 with 2, 240 degrees of freedom).

Table 3. Pooled within-groups correlation matrix. Groups are the four different species groups.

	TM 1	TM 2	TM 3	TM 4	TM 5	TM 7
TM 1	1.000	.786	.806	.429	.645	.697
TM 2	.786	1.000	.905	.633	.805	.813
TM 3	.806	.905	1.000	.480	.796	.858
TM 4	.429	.633	.480	1.000	.739	.563
TM 5	.645	.805	.796	.739	1.000	.940
TM 7	.697	.813	.858	.563	.940	1.000

Table 4. Stepwise selection of variables.

			Wilk's Lambda Λ			
Group	Step	Entered	Statistic	df1	df2	df3
	1	TM 4	.809	1	3	625.000
Species groups	2	TM 7	.724	2	3	625.000
	3	TM 3	.699	3	3	625.000
	4	TM 1	.683	4	3	625.000
Development groups	1	TM 4	.828	1	4	624.000
	2	TM 7	.741	2	4	624.000
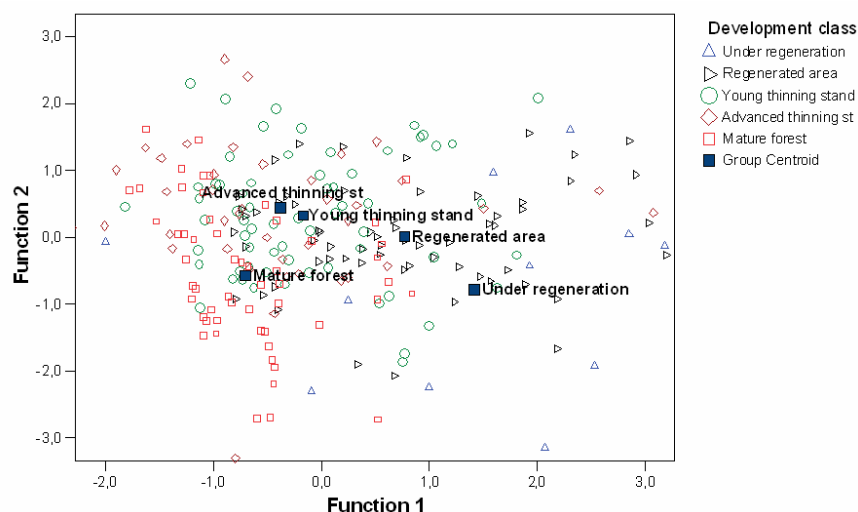
Figure 1. Scatter plot of discriminant function values for development groups. Centroids are marked with filled squares.

In order to rank the spectral bands in their usefulness to separate species and development groups, we can study the coefficients of the discriminant functions in Table 5. In addition, the corresponding eigenvalues and measure of associations are presented. The last measures how well the variables can separate the groups, and a value of 1 would mean perfect separation and 0 no separation. For species we see that bands 4, 7, and 3 are important (large absolute values of coefficients). Note that band 5 is not important, and that is because it is strongly correlated with band 7 and more correlated than band 7 with band 4 (see Table 3). For development classes, 4 and 7 are the most important bands. We also note that the level of association is lower than for species groups. In Fig. 1 a scatter plot for the first two discriminant functions for development groups is shown. We see that advanced thinning stands and young thinning stands are very close together, and the pattern of the mean vectors suggests that these groups should be combined to a general thinning stand class. We also see that the spread within the groups is large, and this will of course inflate the error rate of classification.

Table 5. Standardized discriminant function coefficients for different groupings.

	Coefficients						Eigen-	Measure of
Grouping	TM 1	TM 2	TM 3	TM 4	TM 5	TM 7	value	association
Species	.382	-.265	-.694	.971	-.220	.793	.276	.217
Dev.classes I, II, III, IV, V	-.351	.423	.085	.733	-.450	.637	.235	.190

Table 6. Accuracy (%) of classifying dominating species for two different datasets.

		Dominating Species		
Data set	Site index used	Spruce	Pine	Deciduous
1	yes	50.5	64.8	60.9
	no	48.9	63.5	60.6
2	yes	75.7	65.2	32.9
	no	68.1	60.2	29.8

The accuracy of classifying dominating species groups was tested on two different datasets. The results are presented in Table 6. In dataset # 2, n_i is unequal for the species groups, and in dataset # 1 they are equal. We note that the results for pine-dominated plots are stable; however, for deciduous dominated plots we see a large increase in accuracy, from around 30 % to around 60 %. This increase comes at a cost of a reduction in the accuracy for spruce dominated plots, from about 75 % to about 50 %. We also note that the use of the site index map as expected improves the results. It should be noted here that these results are based on a cross validation procedure and describe the accuracy at pixel level. In a recent study, an error analysis showed that the error mean (bias) were near zero for several forest parameters such as volume, age, and top height (Gjertsen *et al.*, 2004). Thus, one can expect improved estimates for large areas

summing over several pixels. In Table 7 the results from the five different trials (see Table 2) are presented. Age, top height, and volume are all strongly related to development class, and are included to further describe the trial results. Trial 5 with $k = 1$ gave as expected the highest error rate and trial 4 with $k = 8$ gave an improvement. In both these trials, the inventory method has picked the k nearest neighbours at random. In trial 1 and 2, image data have been used to pick the k nearest neighbours, and we see as expected an improvement in all the estimates compared to trials 4 and 5. We note that for spruce dominated plots, the best result is obtained in trial 3. The overall accuracy for species dominated plots increased however from 58.3 % to 63.1 % from trial 3 to trial 1 (Gjertsen *et al.*, 2004).

Table 7. Accuracy of classifying and estimating forest parameters in five different trials. a. producers accuracy.

Parameter		Trial				
		1	2	3	4	5
Spruce[a]	%	75.3	68.5	79.6	65.1	50.9
Pine[a]	%	64.2	58.3	54.6	34.4	31.7
Deciduous[a]	%	32.9	28.0	8.4	4.0	15.1
Age	RMSE (yr)	39.1	41.1	42.9	47.4	64.2
Top height	RMSE (m)	64.5	64.5	69.5	70.5	92.8
Volume	RMSE (m^3)	92.2	97.5	97.4	106.3	135.9

5 CONCLUSION

The statistical analysis showed relatively weak relationships between the spectral variables and the forest parameters, and the levels of associations are rather low. This is caused by a relative large within-group variance and overlap between the groups. This leads of course to misclassifications. The separation of species groups is better than the separation of development classes. Several of the spectral bands are redundant in the presence of the others and can thus be discarded.

The kNN method is sensitive to the sample sizes of the different groups. An experiment with equal sample sizes for the three species groups improved the accuracy for deciduous dominated plots. A relatively small sample size compared to the sample sizes for spruce and pine dominated plots, lead to a large omission error. The use of fractions instead of counts should be considered when employing the nearest neighbour classification rule.

This paper has focused on the accuracy of the kNN method at pixel level and the ability of the spectral bands of Landsat TM to separate species groups and silvicultural development classes. The multi-source forest inventory method developed, produces both maps and statistics for larger areas. For maps, the accuracy at pixel level is relevant. As for estimation for large areas (e.g. municipalities), it is important that the error mean (bias) is close to zero, and it has been shown, in another study, that it is for several forest parameters. This will allow for improved estimates when several single pixels estimates are summed up over a large area.

REFERENCES

Gjertsen, A. K. and Tomter, S. 1998. Bruk av satellittdata i kombinasjon med feltdata i Landsskogtakseringen: Utprøving av MSFI, Norsk institutt for jord- og skogkartlegging, report 19/98, Ås.

Gjertsen, A. K. and Tomppo, E. 1999. Combined use of NFI sample plots and Landsat TM data to provide forest information on municipality level, *In Conference on remote sensing and forest monitoring*, Rogow, Poland, pp. 167–174.

Gjertsen, A. K. and Eriksen, E. 2004. Test av MSFI-metoden: Nøyaktighetsanalyse på datasett fra Østfold og Hobøl, Norsk institutt for jord- og skogkartlegging, report 2/04, Ås.

COMBINING LANDSAT ETM+ WITH FIELD DATA FOR IRELAND'S NATIONAL FOREST INVENTORY
– A PILOT STUDY FOR CO. CLARE

D. McInerney [a], A. Pekkarinen [b], M. Haakana [b]

[a] Forest Research, Northern Research Station, Roslin, Midlothian, EH25 9SY, Scotland.
email: Daniel.McInerney@forestry.gsi.gov.uk
[b] Finnish Forest Research Institute, Unioninkatu 40 A, FIN-00170 Helsinki, Finland.

ABSTRACT

Forest inventory information was estimated using k-Nearest Neighbour classification for six water catchments located in the south-west of Ireland. The analysis combined field inventory data, a Landsat 7 Enhanced Thematic Mapper+ scene and ancillary spatial datasets. Estimates of the five following forest inventory variables were computed: volume per hectare, basal area per hectare, mean stem diameter, mean height and stand stocking density. It was determined that the use of three nearest neighbours provided the optimal results for the data used. At the subcompartment level, accuracies between 80 and 85% were achieved for the variables. It was concluded that accurate forest resource information could be efficiently obtained using kNN and that it be further developed as an operational tool to assist and complement the Irish national forest inventory programme.

Keywords: National Forest Inventory, kNN, Ireland.

1 INTRODUCTION

All forest landowners share one common objective, which is to ensure that their property is managed sustainably and generates a return. The formulation of successful management strategies by forestry professionals, requires accurate and timely spatial and quantitative information, which can only be obtained from forest resource inventories. While forest inventory objectives vary substantially, most foresters deal regularly with management inventories in which stand density and timber volume is assessed, forming the basis for the management plan. The scale at which management plans are implemented varies significantly, from stand level through to regional and national level for production forecasting and planning strategies (Lund, 1998, Gallagher et al., 2004).

Ireland's forest cover has increased six-fold since the beginning of the 20th century and currently represents 9.6% land cover, approximately 660,000ha. This increase is largely attributed to State and EU funded afforestation schemes (Clinch, 1990) and it is anticipated that forest cover will represent 17% by 2035. Irish forests are typically managed on commercial rotations ranging in length from thirty-five to forty-five years. Approximately 70% of Irish forests are state-owned and managed by Coillte, a semi-State forestry board. Coillte typically assess stands at the pre-thicket stage and prior to timber sale and clearfelling. Currently little information exists for private forestry and it is of critical importance that this information is acquired to provide information to private forest owners for the management of their crop.

During the mid-1990s, the Indicative Forest Strategy was launched to improve national forest resource information. This first stage was to produce the Forest Inventory and Planning System (FIPS) dataset, which was a forest map of all stands greater than 0.2ha derived from Landsat TM data and aerial photography. As a result detailed information on the extent and composition of Irish forests was available, but no attempt was made to extend this dataset with quantitative or qualitative information. A field-based national forest inventory programme was started in autumn 2004 and is expected to run until mid-2006. It is designed on a 2x2km systematic grid with the aim of providing information on the extent, health and composition of Irish forests (Farrelly, 2004). Nevertheless, it is widely acknowledged that one of the principal difficulties facing field inventories is how to accurately compute reliable estimates for small areas. This is of particular relevance to Irish forestry, where private stands have an average area of 8ha and a tendency of being spatially fragmented.

It was for these reasons that it was considered important to evaluate techniques that could complement existing methodologies. This would enhance datasets and provide more detailed, localised information of

Irish forest resources than might be derived from the sole use of field inventory data. Several forest inventory techniques exist that incorporate additional spatial datasets to acquire resource information more efficiently and at reduced costs. A traditional option has been aerial photography for stand delineation and species identification, but more recently there has been a trend to integrate space-borne satellite imagery, which cover larger areas and record more spectral information at relatively lower costs. Considerable research has demonstrated the value of remote sensing data for mapping these variables with a high degree of accuracy (Tomppo, 1996, Nilsson, 1997, Holstrom 2001, Trotter et al. 1997, Franco-Lopez et al. 2001).

The remote sensing aided forest inventories can be carried out using various methods and data, but in particular the estimation by imputation of forest variables has developed in line with increasing interest to further integrate the use of remote sensing within national forest inventory programmes. Two principal methods of imputation exist to simultaneously estimate multiple forest variables: k-Nearest Neighbour (*k*NN) (e.g. Tomppo 1996) and most similar neighbour (MSN) (Moeur et al. 1995). These algorithms compute inter-event distances and generate clusters based on a specified distance (Cressie, 1991). In *k*NN the nearest neighbours are determined in a similar way, but the neighbourhood of a given point is restricted to the number of neighbours employed i.e. *k*. The distance metrics are commonly based on absolute differences in the spectral and/or auxiliary feature space. The method is based on non-parametric regression, which is described by Altman (1992) as a collection of techniques to fit a curve when there is little a priori knowledge about its shape. *k*NN operates at the pixel level, assigning forest variables of known 'reference' pixels to the spectrally most similar unknown pixels

2 MATERIALS AND METHODS

2.1 STUDY AREA

The study area was located within six water catchments situated in the south-west of Ireland, between longitudes 8°40 and 9°30 and latitudes 52°20 and 53°40. The total area represents 188,683ha of which forest cover represents 13.5%. The majority are plantation forests, principally composed of the following coniferous species: Sitka spruce (*Picea sitchensis*), Norway spruce (*Picea abies*) and lodgepole pine (*Pinus contorta*). Broadleaf species are mainly confined to native woodlands, consisting of oak (*Quercus* spp.), birch (*Betula* spp.) and ash (*Fraxinus excelsior*). However in recent years there has been a significant increase in the afforestation of these broadleaf species throughout the study area.

The topography of the area ranges from sea-level to 531m and drumlins (low-lying, oblong hills) are widely distributed throughout the area. The Burren, a karst limestone region is located to the north-west of the study area. The main forest soils found in the study area include brown earths, wet mineral soils and blanket peatlands.

2.2 DATA

2.2.1 Field data

A systematic 1x1km grid was generated for the study with all grid intersections located within forests representing a potential sampling unit. One-hundred and thirty nine, circular 0.02ha standard forest mensuration plots were established. Plot centres were located in the field using differential global positioning system (dGPS) and within each plot the following variables were collected: diameter at breast height (DBH) of all living trees with a DBH greater than 7cm, species composition and mean top height. Plot level estimates were subsequently computed using a custom developed Java program based on the Tariff System (Hamilton, 1986), which is a standard method employed in Irish and UK forestry for computing estimates of forest parameters from field inventory data. The field ranged from recently clearfelled stands to very mature, highly productive spruce stands.

Table 8. Summary of field plot estimates

Variable	Maximum	Mean	Standard Deviation
Volume (m³ ha⁻¹)	850	311	240
Stocking (stems ha⁻¹)	2806	1402	801
DBH (cm)	52	17.72	7.5
Height (m)	26.5	14.33	4.8
Basal Area (m² ha⁻¹)	91.7	35.62	23.74

2.2.2 Satellite Imagery and Ancillary data

A Landsat 7 Enhanced Thematic Mapper + (ETM+) scene acquired during the summer of 2001 was used for the analysis. It was geo-referenced to the Irish National Grid using forty-four ground control points using a polynomial transformation, resulting in a geometric accuracy of 0.6% of a pixel. It was subset to cover the study area and bands 1-5 and 7 of the image were used in the image classification.

Additional ancillary datasets included a digital elevation model and thematic maps. The CORINE landcover 2000 and Teagasc landcover (Irish Agriculture and Food Development Authority) datasets were combined with the FIPS data to produce an up-to-date raster map of all forest parcels greater than 0.2ha. This served as a forest mask for which pixel-based estimates of target parameters were estimated.

2.3 METHODS

The estimation of forest inventory parameters was computed using field inventory data, satellite imagery and a kNN estimator. In kNN, the estimate for the pixel, p, is computed as a weighted average of the 'k'' nearest field plot pixels, pi, which are pixels with known field inventory data. The distance, d, is computed as a Euclidean distance in the feature (spectral) space. The weighted estimate of a parameter, M, for pixel, p, is defined as:

$$m_p = \sum_{j=1}^{k} w_{pi,p} . m_{pi} \qquad (1)$$

Where $w_{pi,p}$ is the weight between pixels and m_{pi} is the field plot estimate of variable m. The weight between pixels can be computed based on an inverse squared distance:

$$w_{pi,p} = \frac{1}{d_{pi}^2} \bigg/ \sum_{j=1}^{k} \frac{1}{d_{pi}^2} \qquad (2)$$

It is often necessary to be selective in the choice of neighbours that are used in the estimation process. This arises due to changes in topographic variation and vegetation zone. For instance, it is better to estimate variables from similar elevations with the same soil type. The selection can be facilitated by the use of ancillary data and by an optimised weighting of the input variables. The approach computes the distance function from the image variables and large-scale forest parameters can the weights are obtained through an optimistation process using a genetic algorithm (Tomppo, 2004). The 'new' distance function can be considered as follows, equation 3:

$$d_{pi,p}^2 = \sum_{i=1}^{n_s} (s_i, pj - s_i, p)^2 + \sum_{i=1}^{n_t} w_i, t(t_{io}, pj - t_i, p)^2 \qquad (3)$$

Where: $s_{i,p}$ = image variables – spectral bands & ratios, $t_{i,p}$ = large area forest variables, n_s & n_t = numbers of the spectral and large area forest variables, $w_{i,s}$ & $w_{i,t}$ = variable weights

The fitness function, as defined by Tomppo (2004), which is to be minimised in the genetic algorithm is denoted in Equation 4:

$$f(w, y, \hat{\delta}, \hat{\bar{e}}) = \sum_{i=1}^{n_e} y_i \hat{\delta}(w) + \sum_{i=1}^{n_e} y_{i+n_e} \hat{\bar{e}}(w) \qquad (4)$$

Where $\delta_j(w)$ is the standard error of the estimate of the forest variable i, $e_j(w)$ is the bias of the estimate of the forest variable i n_e the number of forest variables used, y_i fixed constants

Different simulations were run for the datasets and it was found that the optimal results were obtained using a value of k=3.

3 RESULTS

Thematic maps and associated statistics were produced for five variables: volume per hectare (m^3/ha), stocking density (s/ha), diameter at breast height (cm), mean top height (m) and basal area (m^2/ha). Estimates for each parameters were produced at the pixel level and figure 1 shows that there is inter-pixel variation. The information was aggregated based on the FIPS subcompartment In order to incorporate this information into exisiting, operational GIS' used by foresters, subcompartment aggregated were extended to provide subcompartment estimates using the FIPS vector boundaries and the associated sub-compartment estimates are presented in figure 2. These estimates had a high correlation when compared with a validation set of field inventory data. It was observed that the accuracies ranged from 78% for basal area per hectare to 85% for mean dbh. It was found that volume per hectare was estimated with an accuracy of 81.25%. Table 2 details the results.

Table 9. Accuracy of classification results

Variable	Stand level accuracy (%)
Volume (m^3 ha^{-1})	81.25
Stocking (stems ha^{-1})	80.00
DBH (cm)	84.75
Height (m)	87.00
Basal Area (m^2 ha^{-1})	78.00

4 DISCUSSION

The pilot study to test kNN classification in County Clare was successful. It demonstrated the advantages of this technique to provide detailed information of plantation forests. Such an approach is necessary due to the current lack of up-to-date quantitative and qualitative information of Irish forest resources. It is evident that kNN can complement the field-based inventory. The fact that estimates for small areas can be computed is highly beneficial, given the small-size and fragmented nature of private forest stands in Ireland.
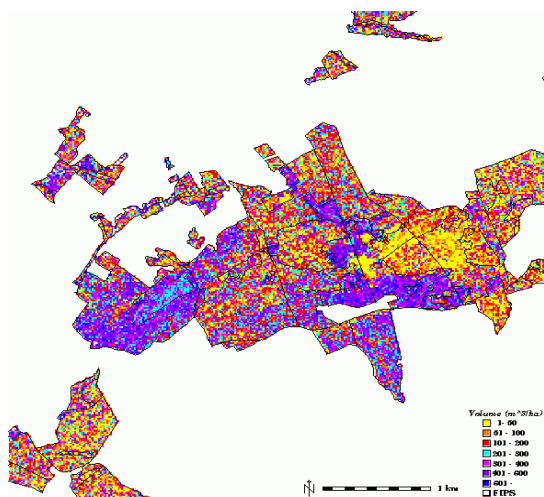
Figure 1. Volume per hectare – (k=3)
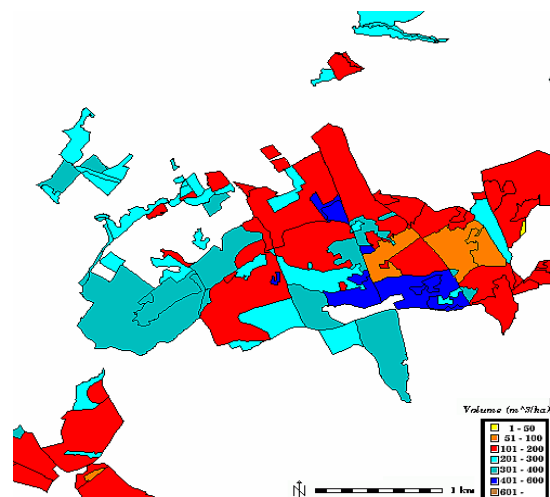
Figure 3. Volume per hectare - aggregate

15

The optimal results generated from this research were achieved using a value of *k*=3. This was due to the limited field inventory dataset that was collected during the field work. As a result, larger values of *k* produced an over-generalisation of estimates and reduction in accuracy. With a more comprehensive field inventory dataset, such as the field-based NFI, there would be greater flexibility in the choice of k. This would produce more reliable results for the entire distribution of different forest types and less generalisation of estimates.

In certain locations, the FIPS boundaries did not reflect changes that occurred in the field due to forest operations. This demonstrates the problem with outdated spatial datasets and the need for efficient methods to update them. It is conceivable that segmenting classifications of either volume per hectare or stocking density could produce updated subcompartment boundaries.

Further research has emerged from this study. In particular the development of techniques to classify areas of woodland and non-woodland as well as species composition. This provides semi-automated techniques to identify changes in woodland forest areas and species composition. This is relevant to the Irish forest sector, which has an active afforestation programme, with forests managed on short, intensive rotations. In addition, a web-enabled GIS interface was developed to deploy image datasets through the Internet and wireless networks. This is an efficient means of disseminating field inventory information to forestry professionals and can be used for basic spatial analysis.

ACKNOWLEDGEMENTS

5 REFERENCES

Altman, N.S. (1992) An introduction to kernel and nearest-neighbour non-parametric regression. *The American Statistician*. August 1992, Vol. 46. No. 43.

Clinch, P. (1999) Economics of Irish Forestry: Evaluating the Returns to Economy and Society. COFORD – National Council for Forest Research & Development, Dublin, Ireland.

Cressie, N. (1991) Statistics for Spatial Data. Wiley & Sons, New York

Farrelly, N. (2004) National Forest Inventory Ireland – Designing a sample based methodology. Irish Forest Service, Department of Agriculture, Food & Forestry

Franco-Lopez, H., Ek, A., Bauer, M. (2001) Estimation and mapping of forest stand density, volume and cover type using the k-nearest neighbours method. *Remote Sensing of Environment.* Vol. 77 251-274.

Gallagher, G., Hendrick, E., Byrne, K. (2004) Preliminary estimates of biomass carbon stock changes in managed forests in the Republic of Ireland over the period 1990-2000. *Journal of Irish Forestry* Vol. 61, No. 1.

Hamilton, G.J. (1998) Forest Mensuration – British Forestry Commission No. 39. HMSO, United Kingdom.

Holmstrom, H. (2001) Data Acquisition for Forestry Planning by Remote Sensing Based Sample Plots Imputation. Doctoral Thesis, Swedish University of Agricultural Science, Umea, Sweden.

Lund, H. (1998) The National Forest Inventory of Ireland. Retrieved from www.home.att.net/~gklund on 25th November 2003.

Moeur, M., Stage, A.R. (1995) Most similar neighbor: an improved sampling inference procedure for natural resource planning. *Forest Science* 41. 337-359

Nilsson, M. (1997) Estimation of forest variables using satellite image data and airborne lidar. PhD. Thesis, Swedish University of Agricultural Sciences, Umea, Sweden.

Tomppo, E. (1996) Application of Remote Sensing in Finnish National Forest Inventory. Proceedings of International Workshop: Application of Remote Sensing in European Forest Monitoring. Vienna, Austria 14th - 16th October 1996.

Tomppo, E., Halme, M. (2004) Using coarse scale forest variables as ancillary information and weighting of variables in k-NN estimation: a genetic algorithm approach. *Remote Sensing of Environment* 92 1-20.

Trotter, C.M., Drymond, J.R. (1997) Estimation of Timber Volume in a coniferous plantation forest using Landsat TM. *International Journal of Remote Sensing* Vol. 18 (10) 2209-2223.

THE IMPACT OF RELATIVE RADIOMETRIC CALIBRATION ON THE ACCURACY OF KNN-PREDICTIONS OF FOREST ATTRIBUTES

T. Koukal, F. Suppan, W. Schneider

University of Natural Resources and Applied Life Sciences, Vienna (BOKU),
Department of Landscape, Spatial and Infrastructure Sciences,
Institute of Surveying, Remote Sensing and Land Information,
Peter-Jordan-Strasse 82, A-1190 Vienna, Austria, email: tatjana.koukal@boku.ac.at

ABSTRACT

The kNN-algorithm is widely used for the prediction of forest attributes using remote sensing data. It requires a large amount of reference data to achieve satisfactory results. The number of available reference plots for the kNN-prediction is usually limited by the size of the area remotely sensed and covered by terrestrial reference inventory on the same date. This problem can be solved if two images are calibrated in such a way that surfaces with identical forest attributes have identical digital numbers. Two methods for radiometric scene-to-scene normalisation are tested on two adjacent Landsat TM scenes. The first, quite conventional one uses radiometric control points and the transformation parameters are determined by linear regression. The other, recently developed method exploits the kNN-cross-validation procedure. The optimal set of transformation parameters is found when the cross-validated prediction error relating to any forest attribute (e.g. forest cover type) becomes a minimum. Handling, performance, and applicability of both methods are discussed.

Keywords: scene-to-scene radiometric normalisation, k-nearest-neighbour method, forest inventory

1 INTRODUCTION

The kNN-algorithm is widely used for the prediction of forest attributes using remote sensing data (Tomppo, 1996; Koukal, 2004). It is a non-parametric approach making no assumptions on the underlying distribution. Due to this property the kNN-algorithm requires a large amount of reference data to achieve satisfactory results. This is one of the severest drawbacks of this method. The number of available reference plots for the kNN-prediction is usually limited by the size of the area remotely sensed and covered by terrestrial reference inventory on the same date.

Usually these factors cannot be influenced by the person responsible for data analysis. However, if one is able to calibrate images in such a way that surfaces with identical forest attributes have identical digital numbers, it may be possible to work with more images at a time and thereby to increase the number of available reference plots significantly.

Radiometric differences of test areas with identical forest attributes but sampled at different locations and at different times originate mainly from atmospheric effects (absorption, scattering), varying sun-target-satellite geometry (bi-directional reflectance effects), and phenology. Radiometric calibration aims at eliminating these effects except phenology. It is an important technique in studies that are based on multi-date satellite imagery, e.g. change detection studies (Du et al., 2002).

This study focuses on two empirical methods of relative radiometric calibration. They are tested on two adjacent Landsat TM scenes in the east of Austria.

2 DATA

Four Landsat TM images of two adjacent scenes (path/row) were used in the study. One of them was used as reference image (190/26-27, Aug 1994) and the others as subject images (190/27, Sept 1991; 189/27, Aug 1992; 189/27, June 1996). All of them coincide with the inventory period of the Austrian forest inventory (AFI) from 1992 to 1996.

The AFI is based on a systematic sampling grid. The grid width is 3.89 km. At each point of the grid that is within forest area, 4 permanent sample plots are established. The plots are located in the corners of a square with a side length of 200 m.

The spectral information for a sample plot was taken from the pixel closest to the sample plot. Altogether 1453 sample plots were available.

3 METHOD

3.1 CALIBRATION

It is assumed that radiometric differences between images of the same area remotely sensed at different times are linearly dependent (Schott et al., 1988). Therefore, the transformation can be accomplished by a linear function. There are two transformation parameters that have to be optimised band by band: slope and intercept. Two empirical methods for the determination of optimal transformation parameters are tested.

The first, quite conventional one is based on a number of target objects in the overlap area of the adjacent scenes (method 1). They are used as radiometric control points. The mean values of these objects are extracted from both images and the transformation equations are set up band-by-band by linear regression.

Method 2 exploits the kNN-cross-validation procedure in order to find optimal transformation parameters (holdout method; see section 3.2). A linear transformation equation is set up for each band and arbitrary initial values are assigned to the transformation parameters. The parameters are modified in such a way that the prediction error relating to any forest attribute (e.g. forest cover type) estimated by the holdout method (a simple form of cross-validation) becomes a minimum. It is obvious that this approach is a rather complex optimisation problem. For simplification, the transformation parameters are optimised band-by-band, starting with the band that is expected to show the biggest difference between the reference image and the subject image.

3.2 VALIDATION

The effect of image calibration is analysed by the holdout method, a simple train-and-test experiment with two exclusive datasets. The set of sample plots is split into a training set and a testing set. Sample plots from the reference image are assigned to the training set (1252 plots) and sample plots from the subject image are assigned to the testing set (201 plots). The kNN prediction accuracy is estimated (error matrix; Congalton and Green, 1999) and compared to the accuracy achieved without and with the calibration (Figure 1).

Moreover, the classification accuracy is estimated by leave-one-out cross-validation with the sample plots from the subject image only. It is compared to the classification accuracy achieved using two images. It is tested whether the classification accuracy can be increased by using additional sample plots from the adjacent (reference) scene.

4 RESULTS

4.1 TRANSFORMATION PARAMETERS BY LINEAR REGRESSION

The regression equations were developed with 20 target objects belonging to 4 land cover types: water and soil (regarded as being approximately constant reflectors over time) as well as deciduous forest and coniferous forest (which may change due to environmental stresses and plant phenology). The objects' mean pixel values extracted from the reference image were regressed against the mean pixel values extracted from the subject images resulting in regression equations for each band.

The relationship between the same objects found in the reference image and in the subject image makes it possible to investigate effects of phenology. If the regression equations for vegetation objects and non-vegetation objects differ significantly, one can conclude that the phenological stages were not the same at both times of acquisition. This was the case for two of three subject images: 190/27, Sept 1991 and 189/27, June 1996. In Figure 2, two examples of found relationships are given. The left graph shows phenological differences between both scenes, whereas the right one does not.

As the study focuses on vegetation, more precisely on forest cover, it may be sufficient to use the transform equations based on vegetation objects only. However, it was figured out that the relationship was not constant for all vegetation objects. Two groups of deciduous forest featuring different stages of development were found. Therefore, only the third subject image (189/27, Aug 1992) that fit well to the

reference image was used for further analysis. The transformation parameters that were used to calibrate this image are summarized in Table 1a.
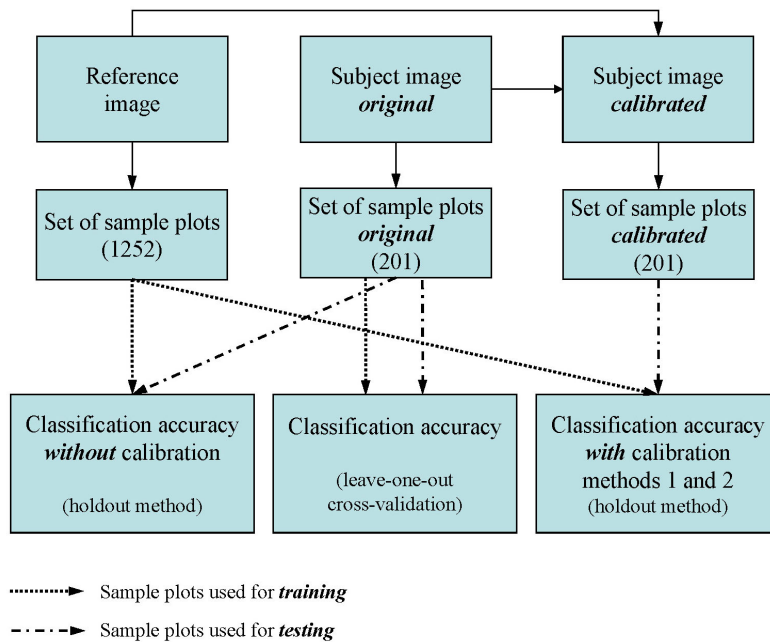
Figure 1. Validation procedure.
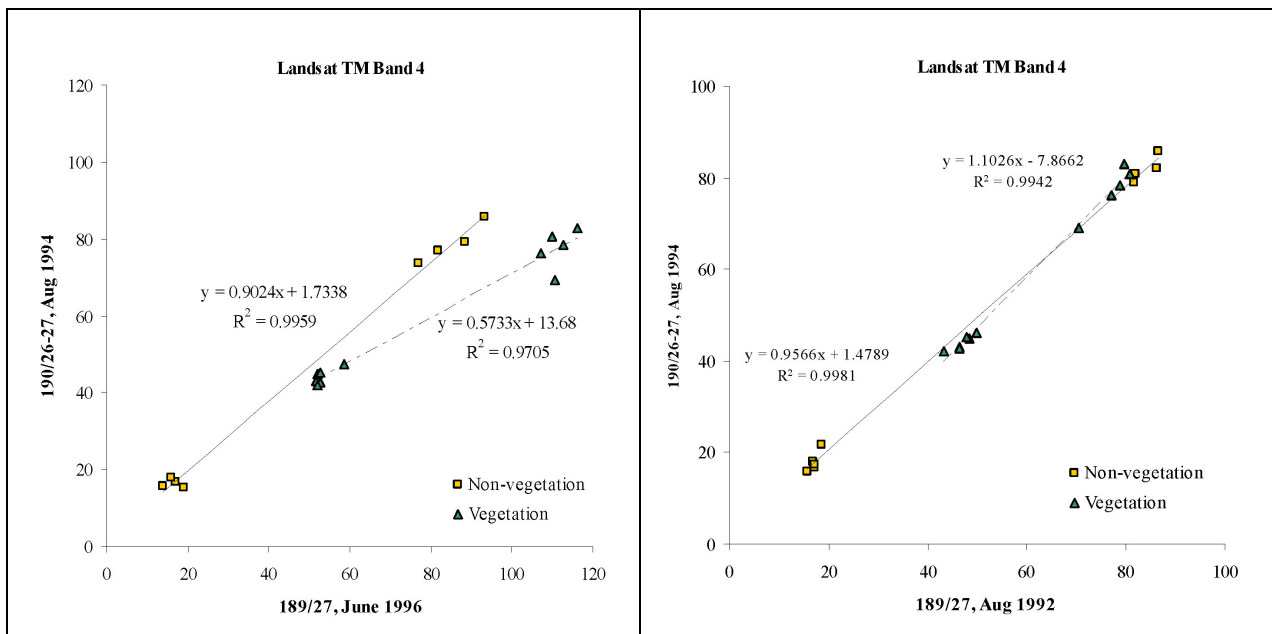
Figure 2. Relationship between the same objects (vegetation and non-vegetation) in the reference image (190/26-27, Aug 1994) and the subject images (189/27, June 1996 and 189/27, Aug 1992 respectively). Phenological differences are discernible in the left figure.

4.2 TRANSFORMATION PARAMETERS BY CROSS-VALIDATION

The optimisation procedure was started with band 1 that is most affected by atmospheric path radiance. Several combinations of slope and intercept were tested. Finally, the one that resulted in the highest classification accuracy (Section 4.3) was selected (Figure 3). This procedure was repeated for each band (except the thermal band).The transformation parameters are summarized in Table 1b. As explained in section 4.1, only the image 189/27 from Aug 1992 was calibrated.

4.3 KNN-CLASSIFICATION

The sample plots of the testing set were classified into 4 forest cover types: (1) deciduous forest, (2) mixed forest dominated by deciduous trees, (3) mixed forest dominated by coniferous trees, (4) coniferous forest. The kNN-classification was done with k=3 and with all Landsat TM bands (except the thermal band) equally weighted. The classification accuracies are given in Table 2.
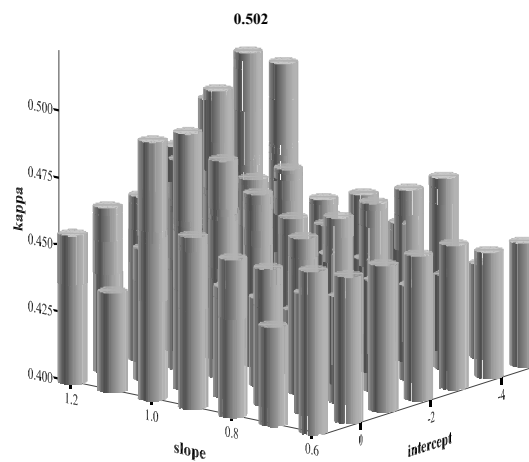
Figure 3. Variation of kappa in dependence of slope and intercept (calibration of band 3). The optimal kappa (0.502) was achieved with a slope of 1.2 and an intercept of -4.

Table 1. Transformation parameters used to calibrate the image 189/27 from Aug 1992. a) Transformation parameters derived by method 1, b) Transformation parameters derived by method 2

<table>
<tr><td>a)</td><td>Band</td><td>Slope</td><td>Intercept</td><td>R²</td><td>b)</td><td>Band</td><td>Slope</td><td>Intercept</td></tr>
<tr><td></td><td>1</td><td>0.712</td><td>+7.1</td><td>0.970</td><td></td><td>1</td><td>0.7</td><td>+8</td></tr>
<tr><td></td><td>2</td><td>0.903</td><td>-0.9</td><td>0.980</td><td></td><td>2</td><td>1.1</td><td>-3</td></tr>
<tr><td></td><td>3</td><td>0.876</td><td>-2.0</td><td>0.992</td><td></td><td>3</td><td>1.2</td><td>-4</td></tr>
<tr><td></td><td>4</td><td>1.046</td><td>-3.1</td><td>0.987</td><td></td><td>4</td><td>1.0</td><td>0</td></tr>
<tr><td></td><td>5</td><td>1.016</td><td>-4.9</td><td>0.990</td><td></td><td>5</td><td>1.1</td><td>-7</td></tr>
<tr><td></td><td>7</td><td>0.906</td><td>-1.9</td><td>0.991</td><td></td><td>7</td><td>0.9</td><td>+1</td></tr>
</table>

Table 2. Classification accuracy (producer's accuracies of class 1 to class 4 (PA1, … , PA4), overall accuracy (OA), kappa and variance of kappa) with and without calibration

	Number of images	Calibration	PA1 n=88	PA2 n=21	PA3 n=30	PA4 n=62	OA	Kappa	Var(kappa)
A	1	-	0.818	0.095	0.300	0.661	0.617	0.424	0.002
B	2	without	0.750	0.095	0.167	0.740	0.592	0.385	0.002
C	2	method 1	0.898	0.048	0.233	0.730	0.657	0.469	0.002
D	2	method 2	0.830	0.095	0.433	0.758	0.672	0.505	0.002

5 DISCUSSION

Generally, the accuracy of the forest cover type classification is quite low. This is true especially for the mixed classes (2) and (3). According to the error matrices, they are easily mixed-up with the pure classes (1) and (4) respectively. Scatter diagrams show that the mixed classes and the associated pure classes have very similar spectral signatures.

Both methods of calibration (Table 2, row C and D) increase the total classification accuracy. There is an improvement compared with the one-image-case (A) and compared with the two-image-case without calibration (B). The kNN-classification benefits from the increased number of sample plots taken from the adjacent scene due to calibration. The results achieved with method 2 are slightly better than those achieved with method 1.

Method 1 is straightforward. However, target objects from the overlap area for determining the transformation parameters have to be selected. Therefore, the method can only be applied to adjacent, overlapping scenes. Furthermore, there is often a lack of appropriate (invariant) objects, e.g. clear water, rock, which may restrict the applicability of this method.

In method 2, the images to be calibrated need not overlap, and no radiometric control points (invariant objects) have to be selected separately. Only spectral information of sample plots from the terrestrial reference inventory is needed to determine the transformation parameters. Thus, the calibration is optimised for forest and may consider phenological differences between the reference image and the subject image. The optimisation procedure (stepwise modification of slope and intercept) can be automated in such a way that the implementation of the method takes little time only.

REFERENCES

Congalton, R. G. and Green K. 1999. Assessing the accuracy of remotely sensed data: principles and practices. Boca Raton, Florida, Lewis Publishers.

Du, Y., Teillet, P. M., Cihlar, J. 2002. Radiometric normalization of multi-temporal high-resolution satellite images with quality control for land cover change detection. Remote Sens. Environ. 82: 123-134.

Koukal, T. 2004: Nonparametric assessment of forest attributes by combination of field data of the Austrian forest inventory and remote sensing data. Dissertation. University of Natural Resources and Applied Life Sciences, Vienna.

Schott, J. R., Salvaggio, C., Volchok, W. J. 1988. Radiometric scene normalization using pseudoinvariant features. Remote Sens. Environ. 26: 1-16.

Tomppo, E. 1996: Multi-source national forest inventory of Finland. In: New Thrusts in Forest Inventory - Proceedings of the Subject Group S4.02-00 'Forest Resource Inventory and Monitoring' and Subject Group S4.12-00 'Remote Sensing Technology'. Volume 1. IUFRO XX World Congress, 6-12 August 1995. R. Päivinen, J. Vanclay and S. Miina. Tampere (Finland), European Forest Institute. 7. pp. 27-41.

IMPROVED FOREST STATISTICS FROM THE SWEDISH NATIONAL FOREST INVENTORY BY COMBINING FIELD DATA AND OPTICAL SATELLITE DATA USING POST-STRATIFICATION

Mats Nilsson, Sören Holm, Heather Reese, Jörgen Wallerman, and Jonas Engberg

Department of Forest Resource Management and Geomatics
Swedish University of Agricultural Sciences
Umeå, Sweden
e-mail: Mats.Nilsson@resgeom.slu.se

ABSTRACT

There are many methods that can be used to derive estimates of forest parameters using satellite data. The accuracy of these estimates depends on different factors, such as, how well forest areas can be identified. In practice, difficulties in delineating forest areas from other land use classes might lead to biased estimates. The Swedish National Forest Inventory (NFI) has therefore decided to use a post-stratification approach to combine field data and optical satellite data to derive unbiased estimates of forest parameters over large regions. The objective of this study has been to investigate how much the estimation accuracy for different forest parameters can be improved on a county level by combining field data from the NFI and satellite data using post-stratification compared to use of field data only. Landsat ETM+ and Envisat MERIS images have been used for stratification. The results show that the standard errors for estimates of total stem volume, stem volume for pine, stem volume for spruce, and tree biomass were reduced by 10% - 30% on a county level (approximately 1 million ha forest land) by using post-stratification based on Landsat ETM+ data compared to use of field data from the NFI. For stem volume of deciduous trees and the amount of dead wood, the standard deviations were reduced by less than 10%. The stratification based on Envisat MERIS was found to produce estimates that were less accurate than the ones obtained using Landsat ETM+ for all tested forest parameters. However, all estimates based on the Envisat MERIS stratification were found to be more accurate than estimates based only on field data from the NFI.

Keywords: Landsat ETM+, Envisat MERIS, Large area estimates, post-stratification.

1 INTRODUCTION

The Swedish National Forest Inventory (NFI) is a part of the operational environmental monitoring and assessment activities carried out in Sweden. The NFI started in 1923 with the aim of giving reliable statistics describing the state of the forest and changes in the forest landscape on a county level. All estimates have been based solely on the extensive sample of field plots. The combined use of field data and optical satellite data would increase the precision for estimates of forest parameters such as stem volume. This would allow the NFI to present forest statistics for smaller areas than currently possible with the present design based on field data alone.

Methods such as *k* Nearest Neighbours (e.g., Tomppo 1993, Nilsson, 1997; McRoberts 2002a) and different types of classifiers such as maximum likelihood (e.g., Flygare, 1993; Bauer *et. al.*, 1994; Reese *et. al*., 2002) can be used to map forest parameters across large areas. There are, however, a number of problems that must be taken into consideration when combining satellite images and field data for mapping and monitoring purposes. Problems related to, for example, image geometry, positioning of field plots, mixed pixels, and atmospheric conditions will affect the possibility of deriving precise and unbiased estimates of forest variables. In theory, most of these problems can be handled, but in practice, it might be difficult to derive unbiased estimates.

Post-stratification is a straightforward approach for obtaining unbiased estimates of different forest parameters for large areas when combining satellite data and field data. It has previously been shown that post-stratification or stratified estimation based on satellite data can be used to improve the estimation accuracy for forest area estimates and estimates of forest parameters such as stem volume (McRoberts *et. al*., 2002a; McRoberts *et. al*., 2002b; Nilsson *et. al*,. 2003).

1.1 OBJECTIVE

The objective of this study was to investigate how much the precision for estimates of stem volume, stem volume per tree species, woody biomass and the amount of dead wood can be improved on a county level by combining field data from the Swedish NFI and optical satellite data using post-stratification compared to use of field data alone. An important issue has been to evaluate the potential of using satellite data from both Landsat ETM+ and Envisat MERIS for the stratification.

2 MATERIALS AND METHODS

2.1 TEST AREA

The county of Jönköping and the coastal part of the county of Västerbotten have been used as test areas. Jönköping County is located in the south of Sweden and Västerbotten is located in northern Sweden. The forests in both counties are dominated by Scots pine (*Pinus sylvestris*) and Norway spruce (*Picea abies*). A short description of the forest condition in the two test areas is given in Table 1.

Table 1. Forest data for Coastal Västerbotten and Jönköping County (Anon., 2004)

Test area	Forestland area (million ha)	Total stem volume (million m^{3}sk)	Prop. Scots pine (%)	Prop. Norway spruce (%)	Prop. Deciduous trees (%)
Västerbotten	1.3	148.0	52	31	17
Jönköping	0.7	122.1	32	55	13

2.1 FIELD DATA

In this study, field plots from the Swedish NFI were post-stratified using optical satellite data. The NFI is carried out as an annual systematic field sample across Sweden (Ranneby *et. al*., 1987). Plots are aggregated into square or rectangular clusters. In the test areas, clusters consist of either 6 or 12 temporary plots of 7 m radius or 8 permanent plots of 10 m radius. In total, about 13 000 plots are inventoried every year, and permanent plots are re-inventoried every 5-10 years. The position of each plot is recorded using GPS.

Photo interpreted data from the National Inventory of Landscapes in Sweden (NILS) was used as ground truth when classifying Envisat MERIS images. NILS is carried out through a nationwide systematic sample of 631 quadrates that are inventoried every 5 years (Esseen *et. al*., 2003). Aerial photo interpretation and field measurements are made on a 1x1 km quadrate. The photo-interpretation is made from 1:30 000 scale color infrared photos. For this study, 60 photo-interpreted quadrates were available. Due to issues of scale concerning the NILS and MERIS data, the field plots were not used in this project.

2.2 SATELLITE DATA

Six Landsat 7 ETM+ images from the European-wide Image2000 dataset were used for the stratification. The satellite data were geometrically precision-corrected by the Swedish National Land Survey to the Swedish National Grid (RT90), and re-sampled to 25x25m pixels using cubic convolution. All Landsat images used for the production were registered between June and August, from 1997- 2001.

Two Envisat MERIS full resolution scenes from the 10th of August, 2003, were also used for stratification. The images were registered using the standard MERIS band settings and the bands used were 3, 5, 7, 8, 9, 10, and 14. Both images were re-projected from WGS84 to RT90, and re-sampled to 250x250 m pixels using cubic convolution.

2.3 STRATIFICATION

For Landsat ETM+, the stratification was made using an existing raster data base with estimates of forest parameters (called *k*NN Sweden) instead of the original digital numbers. This data base was derived by combining ETM+ data and field data from the Swedish NFI using the *k* Nearest Neighbors (*k*NN) algorithm. In the *k*NN method forest parameters are calculated as weighted averages of the observed parameter values for the *k* nearest field plots (e.g., Tomppo 1993; McRoberts 2002b). In *k*NN Sweden, the nearness was measured as the Euclidean distance in the spectral space defined by bands 3, 4, 5, and 7. The weights used were proportional to the inverse squared distance and *k* was set to 15 (Reese *et. al*., 2003).

In the stratification based on *k*NN data, boundaries (y_h) between strata were selected so that $y_h = (m_h+m_{h+1})/2$, where m_h is the mean value for the *k*NN estimated variable *y* in stratum *h*, used for the stratification. All stratifications tested were either based on estimates of total stem volume or stem volume of individual tree species. Both pixel-wise estimates and different generalizations of the estimates were used for stratification. The generalization was made by first segmenting the original ETM+ images and then assigning mean values of the forest parameters in *k*NN Sweden to each segment. Four segmentations were made by running the t-ratio segmentation method (Hagner, 1990) with different minimum segment sizes (0.5, 1.0, 5.0, and 10.0 ha).

The stratification from MERIS data was made by classifying the image into coniferous forest, sparse coniferous forest, deciduous forest, mixed forest, clear felled areas, wetland, agriculture, urban and water. This was done by first running an ISODATA clustering with 40 clusters. Classes were then assigned to the clusters using photo interpreted data from NILS. Since there were not sufficient data from the photo interpretation to assign classes to all clusters, the air photos which the NILS data are interpreted from were also consulted. Different band combinations were tested and the best classification result was obtained using bands 3, 5, 9, and 14. In this combination, the class assignment was made with an overall accuracy of 76 % (Reese et. al., 2005).

2.4 ESTIMATES OF FOREST PARAMETERS

Each forest parameter in a specific stratum was estimated as a weighted average of two independent samples: one based on clusters with permanent plots and one on clusters with temporary plots. The weight given to a specific parameter estimate in each sample was inversely proportional to its variance. For both permanent and temporary clusters, each forest parameter ($\hat{Y}$) was estimated as:

$$\hat{Y} = \sum_{h=1}^{L} \hat{Y}_h = \sum_{h=1}^{L} \left(\frac{A_h}{a} \cdot \frac{\sum_{j=1}^{n} y_{jh}}{\sum_{j=1}^{n} m_{jh}} \right) = \sum_{h=1}^{L} \frac{A_h}{a} \cdot \hat{R}_h \qquad (3)$$

where:
A_h = total area in stratum *h*, *h*=1,2, .., *L*
a = the area covered by a field plot
y_{ih} = observed total value for cluster *j*, stratum *h*, *j* = 1, 2, .., *n*
m_{jh} = total number of field plots in cluster *j*, stratum *h*.

When estimating the variance for a forest parameter it was important to consider that the $\hat{R}_h$ values are correlated, which is an effect of having plots within a cluster that belong to different strata. Thus, the variance has been estimated using an extended version of the standard method used for ratio estimators (e.g., Thompson, 1992) which also takes the correlation between $\hat{R}_h$ values into account (Equation 6).

$$Var(\hat{Y}) = \sum_{h=1}^{L} \sum_{k=1}^{L} \frac{A_h A_k}{a^2} \cdot Cov(\hat{R}_h, \hat{R}_k) \qquad (4)$$

where $Cov(\hat{R}_h, \hat{R}_k)$ is estimated by

$$Cov(\hat{R}_h, \hat{R}_k) = \frac{1}{n \cdot \overline{m}_h \cdot \overline{m}_k} \cdot \frac{\sum_{j=1}^{n} (y_{jh} - \hat{R}_h \cdot m_{jh})(y_{jk} - \hat{R}_k \cdot m_{jk})}{(n-1)} \qquad (5)$$

3 RESULTS

The effect on the precision for estimated forest parameters when using different numbers of strata was evaluated using stratifications based on *k*NN data. Figure 1 shows how the standard error for total stem volume decreases as the number of strata increases. Similar results were obtained for all tested forest parameters. It was also found that the use of different minimum segment sizes (0.5 – 10.0 ha) only had a minor effect on the precision for the forest parameters tested. However, the pixel-based stratification produced estimates with slightly lower precision than the stratifications based on segments.
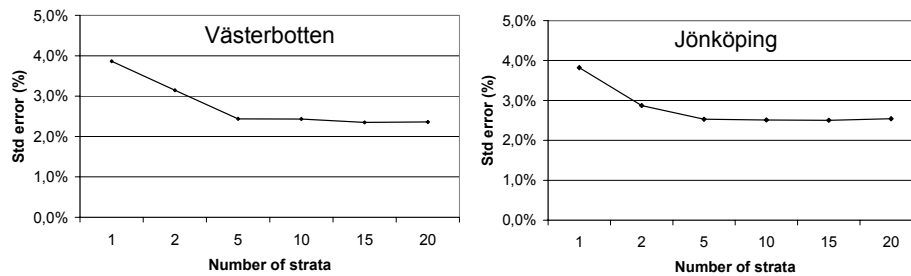
Figure 1. Standard deviation for estimates of total stem volume derived using different number of strata in Coastal Västerbotten and Jönköping County.

The use of stem volume estimates for individual tree species in the stratification did not improve the estimation precision for any parameter except stem volume for deciduous trees, which had the highest precision when the stratification was based on the *k*NN estimates of deciduous volume.

As shown in Figure 2, the standard error for the tested parameters in both counties decreased when post-stratification was used in comparison to using the field measurements alone. The largest decrease in standard deviation was obtained for estimates of total stem volume and woody biomass. It was also found that the increase in estimation accuracy was higher for all post-stratifications based on Landsat ETM+ than for post-stratifications based on MERIS data. The stratification based on Landsat ETM+ data presented in Figure 2 was made using a 0.5 ha minimum segment size and 5 strata.
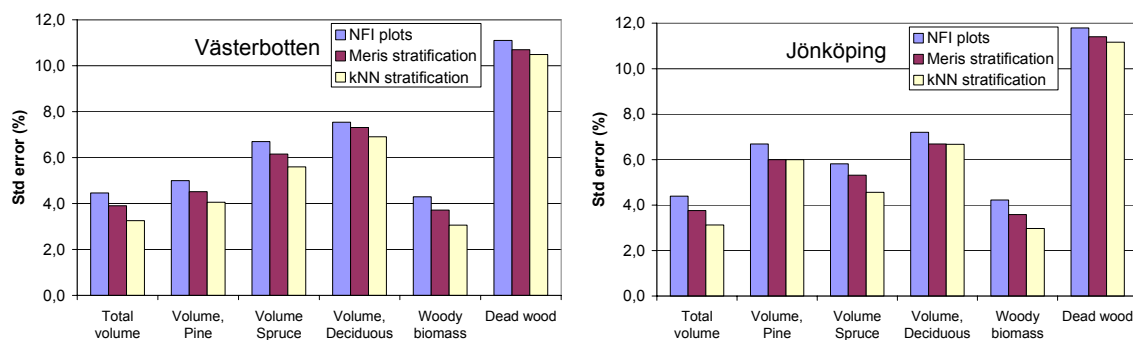
Figure 3. Standard errors for estimated forest variables derived using: 1) NFI plots only (NFI plots), 2) post-stratification based on Landsat ETM+ data (kNN stratification); and 3) post-stratification based on MERIS data (MERIS stratification) in Västerbotten and Jönköping County.

4 DISCUSSION

The major conclusion from the study is that post-stratification is a straightforward and efficient approach to derive unbiased estimates by combining remote sensing data and sample plot data from the Swedish NFI. This conclusion is also supported by results from previous studies (McRoberts *et. al.*, 2002a; McRoberts *et.al.*, 2002b; Nilsson *et. al.*, 2003). It should, however, be noted that the gain in precision when using post-stratification based on spectral data depends on the correlation between the spectral data and the target parameter, which is also reflected in the results presented here. The increase in precision is, for example, much lower for the amount of dead wood than for total stem volume.

The use of different minimum segment sizes did not have a significant impact on the precision of the estimated forest parameters. The use of large minimum segment sizes might result in a high within-segment variation, meaning that different forest types could exist within a segment. In addition, the size of the segments will affect the number of plots located on a boundary between two strata and consequently, due to geometric errors, a number of plots may be assigned to the wrong stratum. The individual effect of such problems could not be quantified in the study. However, the results indicate that the combined effect of all factors influencing the precision is nearly equal for stratifications based on segment sizes between 0.5 and 10.0 ha.

An important finding is that the precision of the estimates did not depend on the number of strata used, when using between 5 and 20 strata. This is important especially if estimates are to be derived for smaller

areas than counties, where the relatively low number of field plots available might limit the number of strata that can be used.

Based on the results from this and previous studies, the Swedish NFI has decided to use post-stratification to derive improved forest statistics for counties or smaller areas. A production system that can be used operationally in the NFI to produce post-stratified estimates based on a segmented version of kNN Sweden has been developed. However, it remains to be investigated for how small areas reliable estimates of different forest parameters can be presented with a sufficiently high precision.

ACKNOWLEDGEMENT

REFERENCES

Anon., 2004. Skogsdata 2004. Aktuella uppgifter om de svenska skogarna från Riksskogstaxeringen. Swedish University of Agricultural Sciences, Department of forest resource management and geomatics, Umeå, Sweden.

Bauer, M. E., Burk, T. E., Ek, A. R., Coppin, P. R., Lime, S. D., Walsh, T. A., Walters, D.K., Befort, W., and Heinzen, D. F. 1994. Satellite Inventory of Minnesota Forest Resources. Photogrammetric Engineering & Remote Sensing, 60:287-298.

Esseen, P.A., Glimskär, A., Ståhl, G., and Sundquist, S. 2003. Fältinstruktion för Nationell Inventering av Landskapet i Sverige (NILS). Swedish University of Agricultural Sciences, Department of forest resource management and geomatics, Umeå, Sweden.

Flygare, A-M. 1993. Contextual Classification Using Multi-temporal Landsat TM data. University of Umeå, Statistical Research Report 1993-5, Umeå, 72 p.

Hagner, O. 1990. Computer Aided Forest Stand Delineation and Inventory Based on Satellite Remote Sensing. In The Usability of Remote Sensing for Forest Inventory and Planning. In Proceedings from SNS/IUFRO workshop in Umeå, 26-28 February, pp. 94-105.

McRoberts, R.E., Nelson, M.D., and Wendt, D.G. 2002a. Stratified estimation of forest area using satellite imagery, inventory data, and the k-Nearest Neighbors technique. Remote Sensing of Environment, 82:457-468.

McRoberts, R.E., Wendt, D.G., Nelson, M.D., and Hansen, M.H. 2002b. Using a land cover classification based on satellite imagery to improve the precision of forest inventory area estimates. Remote Sensing of Environment, 81: 36-44.

Nilsson, M. 1997. Estimation of Forest Variables Using Satellite Image Data and Airborne Lidar. Doctoral thesis. Swedish University of Agricultural Sciences, Umeå.

Nilsson, M., Folving, S., Kennedy, P., Puumalainen, J., Chirici, Corona, P., Marchetti, M., Olsson, H., Ricotta, C., Ringvall, A., Ståhl, G., and Tomppo, E. 2003. Combining remote sensing and field data for deriving unbiased estimates of forest parameters over large regions. In: Corona, P., Köhl, M., and Marchetti, M (editors), Advances in Forest Inventory for Sustainable Forest Management and Biodiversity Monitoring. Kluwer Academic Publishers.

Reese, H., Lillesand, T.M., Nagel, D.E., Stewart, J.S., Goldmann, R.A., Simmons, T.E., Chipman, J.W., and Tessar, P.A. 2002. Statewide land cover derived from multiseasonal Landsat TM data – A retrospective of the WISCLAND project. Remote Sensing of Environment, 82: 224-237.

Reese, H., Nilsson, M., Granqvist Pahlén, T., Hagner, O., Joyce, S., Tingelöf, U., Egberth, M., and Olsson, H. 2003. Countrywide estimates of forest variables using satellite data and field data from the National Forest Inventory. *Ambio* 32, pp. 542-548.

Reese, H., Joyce, S., and Olsson, H. 2005. ENVISAT MERIS for country-wide estimates of forest and mountain vegetation in Sweden. *To be presented at ISRSE 2005, St Petersburg.*

Ranneby, B., Cruse, T., Hägglund, B., Jonasson, H., and Swärd, J. 1987. Designing a new national forest survey for Sweden. Studia Forestalia Suecica, No. 177.

Thompson, S.K. 1992. Sampling. John Wiley & Sons: New York. pp 59-70.

Tomppo, E. 1993. Multi-Source National Forest Inventory of Finland. In Proceedings of Ilvessalo Symposium on National Forest Inventories, pp. 52-59. August 17-21, Finland.

THE FINNISH MULTI-SOURCE INVENTORY

E.O. Tomppo

Finnish Forest research Institute
Unioninkatu 40A FIN-00170 Helsinki
email: erkki.tomppo@metla.fi

1 INTRODUCTION

To get forest resource information for smaller areas than what is possible with field data only without increasing the costs of the inventory significantly was a driving force to start the development of the multi-source forest inventory method (MS-NFI) in the connection of the Finnish national forest inventory (NFI). Furthermore, new natural resource satellites images provided new possibilities to increase the efficiency of the inventories with relatively small additional costs.

One basic requirement, set to the method, was that it should be able to provide applicable information for forestry decision making. Thus, methods that often are applied in satellite image aided approaches, and that produce only maps about forest types or land use classes, were not considered satisfactory. The methods those are able to provide area and volume estimates, possibly broken down into sub-classes, e.g., by tree species, timber assortments and stand-age classes, were sought for. In an optimal case, the method had to be able to provide all the same estimates for the small areas as the field data based method provides for national and sub-national level. Note that the number of variables measured in the field is usually high, ranging typically from 100 to 400. Estimates of additional variables are calculated from these measured variables.

One possible approach had been separate or simultaneous regression models, or logistics regression models, for variables of interest (Trotter, Daymond, & Goulding, 1997, McRoberts, 2005, Tomppo, 1987, 1992). A disadvantage had been that models had to derive separately for variables or variable groups to be predicted wherefore the dependence in predictions had not correspond the original dependence of the field variables. Furthermore, this approach is somewhat laborious in practical applications because models had to derive for each satellite image set.

These were the reasons to select k-nn approach. It had been used during several decades in image analysis and pattern recognition tasks. A somewhat similar method, a grouping method, had earlier been applied in North Finland with aerial photographs and visual interpretation to reduce errors of the estimates (Poso, 1972), and was suggested by Kilkki and Päivinen (1986) with satellite images. A further advantage of the adopted and developed method is that it simultaneously produces wall-to-wall forest resource maps.

The input data of the Finnish multi-source inventory are thus NFI field data, satellite images and digital map data of different types, e.g., basic map data, soil data for stratifying between mineral soil, spruce mires, pine mires and open bogs, as well as digital elevation model.

The k-nn estimation method is non-parametric and thus avoids the need for explicit models. However, it presumes that the total variation of all forest variables is well represented by the field sample plots. The method in which the entire field data vector are predicted simultaneously (one vector or the weighted mean of k vectors are the predictor of an un-known field data vector), also better preserves the covariance structure of field variables than the methods in which the prediction is made separately for each variable (to each element of the vector).

The k-nn method has been used or tested in forest inventories also, e.g., with the Swedish NFI (Nilsson, 1997, Reese et al., 2003), with US FIA (Franco-Lopez, Ek, & Bauer, 2001, McRoberts, Nelson, & Wendt, 2002), with Norweigian NFI to produce forest resource estimates for municipality level (Gjertsen, Tomppo, & Tomter, 1999, Gjertsen, & Eriksen, 2004), in harvest planning in radiata pine plantations in New Zealand was studied (Tomppo, Goulding, & Katila, 1999) and in multi-source inventory in Heilongjiang province in North-East China (Tomppo, Korhonen, Heikkinen, & Yli-Kojola, 2001) and in Germany (Diemer *et al*. 2000).

2 PROGRESS IN FINNISH MULTISOURCE INVENTORY

The development of the Finnish MS-NFI began in 1989. The first operative results were computed in 1990 (Tomppo, 1990, 1991, 1996). The method has been modified continuously and new features added (Katila, Heikkinen, & Tomppo, 2000, Katila, & Tomppo, 2001 and 2002). The core of the current method is presented in Tomppo, & Halme (2004).

Any digital land use map or land cover data can be used to improve the accuracy of the predictions (Tomppo, 1991, 1996). Methods to remove the effect of possible map errors from the predictions are presented by Katila, Heikkinen & Tomppo (2000) and Katila & Tomppo (2002).

The application of the k-nn estimation method presumes the selection of 'estimation parameters' for each satellite image and the other data applied with the image (Katila, & Tomppo, 2001). The operative application of the method has also shown that the predictions, particularly the predictions of volumes by tree species, may be biased if the area of interest is large and covers several different vegetation zones with different tree species compositions. The biases can be reduced if the set of potential nearest neighbors are somehow restricted. In the first operative applications of the Finnish multi-source inventory (MS-FNFI), a sub-set of field plots has been selected for potential nearest neighbours in the image space for each image pixel, usually those field plots that are within a certain geographical distance from the pixel in question. Tomppo, & Halme (2004) presented another method to guide the selection of the field plots. It has been in an operative use since early 2000s

3 INPUT DATA FOR MS-NFI

3.1 SATELLITE IMAGES

The images from Landsat 5 TM or Landsat 7 ETM+ sensors are the most suitable images for operative applications due to fairly large coverage area of one image and still a moderate spatial and spectral resolution. These images are given the priority when covering an area with satellite images. If these images are not available, e.g., due to the clouds, either Spot 2 -4 XS HRV images or IRS-1 C LISS images have been used so far.

Finland's land area is 30.4473 million hectares and together with inland waters 33.8145 million hectares. In NFI8 and its up-dating in South Finland (field data from 1990-1994), 36 Landsat 5 TM images and 2 Spot 2 XS HRV images were applied. In NFI9 (1996-2003), 40 Landsat 5 TM or Landsat 7 ETM+ images and 4 IRS-1 C LISS images were applied.

Areas corresponding to the cloud-free parts of satellite images are utilised in operative applications. Forests under clouds and cloud shadows are assumed to be similar to forests on the average on cloud-free part of the computation unit (e.g. be municipalities).

All applied images are rectified to the national coordinate system using polynomial regression models to fit the coordinates of the objects on maps. Nearest neighbor method resampling with a pixel size of 25 m × 25 m have been used. This pixel size is somewhat smaller than Landsat TM and ETM+ pixel size and a bit larger than Spot 2-4 XS HRV pixel size. The pixel of 25 m × 25 m was selected for practical reasons, more narrow objects (e.g. roads) are possible to separate than for instance with the original resolution of Landsat 5 TM.

3.2 OTHER DATA SETS

3.2.1 Field data

The core idea in employing multi-source data is to estimate new area weights for field sample plots. Furthermore, digital wall-to-wall thematic maps can be created, in principle for an arbitrary variable of the NFI. Examples of maps are spatial distributions of site fertility, mean age and diameter of stand, volumes by tree species and timber assortments and volume increment of growing stock by tree species.

The basic computation unit in image processing is a picture element, a pixel. The pixel size applied with Landsat TM images, e.g., is 25 m x 25 m. Therefore, it is more convenient to work with volumes per area unit than with volumes of tallied trees. Volumes per hectares are estimated for each sample plot by tree species and by timber assortment classes from tally tree volumes.

The tree level volumes are transformed to volumes per hectare in MS-NFI using the basal area factor and the maximum radius of the plot. Otherwise the field variables are in MS-NFI are similar to those in

NFI calculations using field data only. Field measurements based result computation does not involve increment estimates of tally trees wherefore increment estimates are not usually computed with multi-source method.

3.2.2 Digital map data

The digital map data are used to decrease the errors of the estimates. A few land use strata (forestry land, subdivided in to mineral soil and peatland soil strata, arable land, roads, built-up land, waters) are applied for stratification. The effect of possible map errors on the estimates can be reduced with statistical methods.

A digital elevation model is used in two different ways, for stratification on the basis of elevation data and to correct the spectral values by employing the angle between sun illumination and terrain normal Tomppo (1992, Katila, & Tomppo (2001).

The basic computation unit in multi-source inventory is a municipality. The number of municipalities in the entire country is about 500, and the land areas range from some 1000 hectares to some hundreds of thousands of hectares. Digital municipality boundaries are used to delineate the computation units (Tomppo, 1996).

3.2.3 Large area forest resource data

The basic k-nn method was applied in NFI8. The improved k-nn method, ik-nn method, was introduced during NFI9. It employs the coarse scale variation of the applied key forest variables in guiding the selection of the field plots from which the data are transferred to the pixel to be analyzed. The variation is presented in the form of large scale digital forest variable maps. These maps can be derived either from the current inventory data or from the data of the preceding inventory. The variables were selected in such a way that their values indicate the areas in which the covariance structure between field variables and image variables would be approximately constant (Tomppo & Halme 2004).

4 THE BASIC AND IMPROVED K-NN ESTIMATION

The basic k-nn estimation was applied in the MS-NFI calculation during NFI8 (1986-1994) since 1990, and also in the beginning of NFI9. An improved k-nn method, denoted by ik-nn was adopted in the beginning of 2000. Both methods are described and discussed in Tomppo & Halme (2004).

In the MS-NFI, new plot weights (not equal for each plot) are computed for each plot by computation units, e.g. by municipalities. The weights are computed for each field sample plot. These plot weights are sums of satellite image pixel weights by computation units. The pixel weights, in turn, are computed by a non-parametric k-nn estimation method. The method utilizes distance metric d, defined in the feature space of the satellite image data. Denote the nearest feasible field plots by $i_1(p),...,i_k(p)$. The weight $w_{i,p}$ of field plot i to pixel p is defined as

$$w_{i,p} = \left. \frac{1}{d_{p_i,p}^t} \right/ \sum_{j \in \{i_1(p), \mathrm{K}, i_k(p)\}} \frac{1}{d_{p_j,p}^t}, \text{ if and only if } i \in \{i_1(p), \mathrm{K}, i_k(p)\}$$

$$= 0 \text{ otherwise.}$$

(1)

The power t is a real number, usually $t \in (0,2]$. The distance metric d in the operative MS-NFI is

$$d_{p_j,p}^2 = \sum_{l=1}^{n_f} \omega_{l,f}^{\,2} (f_{l,p_j} - f_{l,p})^2 + \sum_{l=1}^{n_g} \omega_{l,g}^{\,2} (g_{l,p_j} - g_{l,p})^2$$

(2)

where $f_{l,p}$ is the *l*th transformed image variable, $f_{l,p_j} = f^0{}_{l,p_j} / \cos^r(\alpha)$, $f^0{}_{l,p_j}$ is the original intensity of the spectral band *l*, α the angle between terrain normal and sun illumination, *r* the applied power due to non-Lambertian surface and n_c the number of spectral, $g_{l,p}$ the large area prediction of the *l*th applied forest variable, n_f the number of image variables (or features) and n_g the number of coarse scale forest variables and ω_f and ω_g the weight vectors for image features and coarse scale forest variables respectively. A pixel size of 1 km × 1 km is used in the coarse scale forest variable predictions $g_{l,p}$.

The values of the elements of the weight vector to be estimated are derived from optimization employing a genetic algorithm. The first phase of ik-nn is to run the optimization algorithm, in the applications possibly by strata, e.g., mineral soil stratum and mire and bog stratum. The estimation after that returns to the basic k-nn estimation. The purpose of the use of coarse scale forest variables as additional elements in distance metric and optimize weights is to solve the problems how to select the sub-area and sub-set of the field plots from which the potential nearest neighbors are sought for each pixel and how to select the spectral features in the applied distance metric (2) in order to get as small as possible errors. These problems were studied in Tomppo, & Halme (2004).The problem was solved using 1) supplementary ancillary variables in addition to spectral data in selecting neighbors, 2) using 'optimal' weights for both the image features and ancillary information. These weights are sought using genetic algorithm based optimization.

A weighted sum of pixel level biases and RMSE's of the predictions was selected as the objective function. The weights are called fitness function weights and denoted by γ (3). The variables employed were: 1) total volume, 2) volume of pine, 3) volume of spruce, 4) volume of birch and 5) volume of other broad leaved tree species. These 10 variables have been used also in the operative applications of the method. The fitness (objective) function to be minimized with respect to $\boldsymbol{\omega}$ is:

$$f(\omega,\gamma,\hat{\delta},\hat{\bar{e}}) = \sum_{j=1}^{n_e} \gamma_j \hat{\sigma}_j(\omega) + \sum_{j=1}^{n_e} \gamma_{j+n_e} \hat{\bar{e}}_j(\omega) \qquad (3)$$

where $\boldsymbol{\gamma > 0}$ are user defined coefficients for pixel level standard errors $\hat{\sigma}_j$ and biases $\hat{\bar{e}}_j$ for forest variable j (applied in genetic algorithm) and $\boldsymbol{\omega}$ is the weight vector to be estimated by means of genetic algorithm.

For computing forest parameter estimates for computation units, sums of field plot weights to pixels, $w_{i,p}$ are calculated by computation units (for example, by municipalities) in the image analysis process over the pixels belonging to the unit. The weight of plot i to computation unit u is denoted

$$c_{i,u} = \sum_{p \in u} w_{i,p}. \qquad (4)$$

Reduced weight sums $c^r_{i,u}$ are obtained from the formula (4), if clouds or their shadows cover a part of the area of the computation unit u. The real weight sum for plot i is estimated by means of the formula

$$c_{i,u} = c^r_{i,u} \frac{\hat{A}_{s,u}}{\hat{A}^r_{s,u}} \quad , \qquad (5)$$

where

$\hat{A}_{s,u}$ = the estimate of the area of the forestry land of unit u, and

$\hat{A}^r_{s,u}$ = the estimate of the area of the forestry land of unit u not covered by the cloud mask.

The areas can be taken, e.g., from digital maps or estimated by means of field plot. It is thus assumed that the forestry land covered by clouds per computation units is, on average, similar to the rest of the forestry land in unit u with respect to the forest variables.

The weights (4) and (5) are computed within forestry land separately for mineral soil stratum and peatland stratum. The weights are also computed to other land use classes, arable land, built-up land, roads and waters, if stratification based map correction method is applied (Katila, & Tomppo 2002). In the other method, statistical calibration and confusion matrix are used to reduce the effect of the map errors on the estimates (Katila, Heikkinen, & Tomppo 2000).

After the final field plot weights to computation units ($c_{i,u}$) have been computed, the ratio estimation is applied to compute the estimates (e.g., Cochran 1977). In this way, the estimation is similar to that using

field plot data only. Volume estimates, e.g., are computed by computation unit u and reference unit s in the following way. Mean volumes are estimated by the formula

$$v = \frac{\sum_{i \in I_s} c_{i,u} v_{i,t}}{\sum_{i \in I_s} c_{i,u}}, \tag{6}$$

where $v_{i,t}$ is the estimated volume per hectare of timber assortment (log product) t for plot i and I_s the set of field plots belonging to stratum s. The corresponding total volumes are obtained by replacing the denominator in formula (6) by 1.

Predictions of some (optional) forest variables are written in the form of a digital map during the procedure. The land use classes outside forestry land are transferred to map form predictions directly from the digital map file. Within forestry land, the variables are predicted by the weighted averages of the k nearest neighbors (see Tomppo, 1991, 1996)

A pixel-level prediction $\hat{m}_p$, of variable M for pixel p is defined as

$$\hat{m}_p = \sum_{i \in F} w_{i,p} m_i, \tag{7}$$

where m_i is the value of the variable M on plot i. Mode or median value is used instead of the weighted average for categorical variables. The predicted variables are usually, land use class, site fertility class, stand age, mean diameter of stand, mean height of stand, and volumes by tree species (pine, spruce, birch, other broad leaved trees) and by timber assortment class. The total amount of the maps is thus somewhat over 20. These maps in which the covariance of the variables are near to that of field variables are more applicable to different forestry, ecological and environmental purposes than the maps in which the predictions have been done separately

5 THE USE OF NFI RESULTS

The output results of MS-NFI have been used mainly in three different ways: 1) for forest management planning at municipality level by regional forestry authorities and forestry planners, 2) for timber procurement planning by forest industries (by commercial basis), and 3) for different types of ecological studies by research groups. Furthermore, the output tables and maps can be and have used for different research purposes.

Some examples of estimates obtained with MS-NFI are given in Table 1. These estimates are from the 8th inventory, with field data and satellite images from year 1992, and concern the area of forestry Centre Kainuu (Tomppo, Katila, Moilanen, Mäkelä, & Peräsaari, 1998). The estimates are: Distribution of forestry land into sub-classes (Table 1a), Mean and total volume of growing stock on forest land, on forest and scrub land and on forestry land (Table 1b) and Total volume of growing stock by timber assortment classes on combined forest and scrub land (Table 1c). Forestry land (FRYL) consists in MS-NFI of forest land (FL), scrub land (SRCL) and waste land (WL). In national classification, forestry roads and depots, as well as some other minor areas belonging to forestry, are included into forestry land. Note that for the entire forestry centre, totals are given in two different ways in Table 1a) and Table 1b), based on on one hand on the MS-NFI and on the other hand on the field data based inventory only (NFI). The standard errors for forestry centre totals in Tables 1a) and 1b) are based on NFI. In addition to the previous tables, the following tables were given in MS-NFI8 for all municipalities in Finland: the areas of mineral soil and peatland soils separately on FL, SRCL and WL, tree species dominance separately on FL and on SRCL, areas of age classes on FL, mean volumes (m^3/ha) by age classes on FL, areas of development classes on FL; mean volumes (m^3/ha) by development classes on FL, mean and total volumes by tree species and timber assortment classes on FL and on combined FL and SCRL. Furthermore, some relative distributions for area and volume estimates were given.

Examples of the use of the maps in ecological studies are given in (Pakkala, Hanski, & Tomppo, 2002).

6 DISCUSSIONS AND CONCLUSIONS

The Finnish National Forest Inventory has utilized satellite image aided multi-source method since 1990 in order to be able to compute results for areas smaller than what is possible using field data only. The entire country has been covered twice with this method. Furthermore, over half of the country was covered with a satellite image based up-dating method. In that method, clear cuttings and thinning cuttings were identified on NFI plots between MFI measurement time point and image acquisition time point. Tree level growth models were applied to add volume increase of the time interval. The k-nn method was applied with new image material and up-dated NFI plots. The results became directly to the use of ministry, forestry centers and forest industries. The MS-NFI results have been used in an operative way in forestry planning, timber procurement planning and in ecological studies. The method is under continuous refinement. During the ninth inventory (1996-2003), the method was enhanced introducing a couple of new features: 1) the use of large-area forest variables for directing the selection of the nearest neighbors, 2) the use of an optimization method based on genetic algorithm to weight both large-area forest variables and satellite image variables, and further, 3) two optional methods were developed to remove the effect of the map errors on the estimates. The new ik-nn method performs noticeably better than the original k-nn method. The use of the information from large area forest variables reduces noticeably the problem of distinguishing stands with different tree species, or tree species composition, and reduces the errors of the estimates of volumes by tree species. This problem has been severe in areas where large-area tree species dominance changes, for instance, where spruce dominated forests change into pine dominated forests or vice versa: a common occurrence in the Boreal region. Note that any relevant data, like soil data or vegetation zone data, can be employed as ancillary data. The method, which has been already in operative use in the Finnish multi-source forest inventory, reduces the biases and standard errors both at pixel level and in larger areas. Comparisons with the k-nn method have been made with tens of Landsat TM and ETM+ images. The method seems to perform well, and in practice gives predictions with smaller errors than the old k-nn method. Validation has been carried out, and are always done in operative applications, at the pixel level and at the level of municipality groups for which the predictions and standard errors can be computed by means of field data only. In some cases, the regional level errors are still high and improvements are welcome.

Two methods for reducing the errors of predictions caused by the possible errors in digital base maps are in use in the operative MS-NFI, a calibration method (Katila, Heikkinen, & Tomppo 2000) and a stratification method (Katila, & Tomppo 2002). The new ik-nn method is applicable with both map correction methods. When using the stratification method, field plots outside of forestry land can be employed. Different weights can be computed for different strata, as is done within forestry land for the mineral soil stratum and peatland soil stratum.

The pixel level and stand level errors of the estimates are rather high with current satellite images. There are several reasons for this. The error sources in pixel level predictions of forest variables have been listed in many articles (e.g. Katila 2004, and Tomppo, Katila, Moilanen, Mäkelä, & Peräsaari, 1998). Examples are, 1) possible errors in field data measurements and applied models in estimating tree and plot variables, 2) errors in the geographic location of a field plot and the corresponding pixel, 3) field measurements are done from an area which does not correspond the area of a satellite image pixel, 4) very seldom all factors affecting spectral response of satellite image are measured, sometimes not all trees, and seldom ground vegetation, 5) radiometric resolution of the sensors (the sensors are not able the recognize all variation the target area, i.e., two different targets in the field may give same spectral response), 6) scattering of radiance in the atmosphere, 7) within image variation in imaging condition (different parts of an image are in different sun illumination and atmospheric conditions), 8) a possible fact that the variation of the field plots does not cover all the variation in the field, and 9) possible timing difference in field data and image data. 10) Furthermore, soil moisture variation in the target area affects the spectral properties wherefore two areas with same growing stock may have different spectral properties, or vice versa, two areas with different growing stock may have same spectral properties.

There are several methods to assess the pixel level errors. Leave-one-out cross validation has been applied in many studies. Kim, & Tomppo (2004) applied variogram modelling in the spectral space. A generally applicable error estimation method for areas larger than a pixel is a challenging task. The error of the predictor of a variable depends on the true value of the variable wherefore the errors are spatially correlated. The spatial dependencies on the image itself make the error structure even more complex. Lappi

(2001) presented a different, calibration type of approach to multi-source estimation, together with variance estimator based on variogram. Some other interesting variogram based approaches are currently under development.

The practical application of multi-source inventory is facing currently also other problems. One of the most severe one, related to optical area images in certain regions of the globe, is the availability of images, obtained in cloud-free imaging conditions. The most applicable satellite sensor, Landsat 7 ETM+, has suffered a failure of scan line corrector since 2003. Several correction methods have been introduced but the quality of the product is not the same as without the failure (see, e.g., USGS, 2005). One advantage of k-nn method is that it is applicable with all image material. The precision of the estimates depends, however, on the spectral, spatial and radiometric resolution of the sensor. Some image material may presume the use of another image material as an intermediate step between field data and the final image data (Tomppo, Nilsson, Rosengren, Aalto, & Kennedy, 2002). Furthermore, the precision of the estimation depends on how k-nn method is applied, as it has been seen above. Lot of research work has been carried out and are going on to analyse the errors and to improve the precision of the estimates.

REFERENCES

Cochran, W. G. (1977). Sampling techniques. (3rd ed.). New York: Wiley.

Diemer, C., Lucaschewski, I., Spelsberg, G., Tomppo, E., & Pekkarinen, A. (2000). Integration of terrestrial forest sample plot data, map information and satellite data. An operational multisource-inventory concept. In: Ranchin, T. & Wald, L. (Eds.), Proceedings of the Third Conference "Fusion of Earth Data: Merging Point Measurements, Raster Maps and Remotely Sensed Images" January 26-28, 2000. Sophia Antipolis, France. SEE/URISCA, Nice (pp. 143-150).

Franco-Lopez, H., Ek, A. R., & Bauer, M. E. (2001). Estimation and mapping of forest stand density, volume, and cover type using the k-nearest neighbors method. *Remote Sensing of Environment*, 77, 251-274.

Gjertsen, A.K., Tomppo, E., & Tomter, S. (1999). National forest inventory in Norway: Using sample plots, digital maps, and satellite images. In: IEEE 1999 International Geoscience and Remote Sensing Symposium, Hamburg, Germany (pp. 729-731).

Gjertsen, A. K. and R. Eriksen (2004). Test av MSFI-metoden: Nøyaktighetstest på datasett fra Østfold og Hobøl. Ås, Norsk institutt for jord- og skogkartlegging NIJOS: 52. (In Norweigian).

Halme, M., & Tomppo, E. (2001). Improving the accuracy of multisource forest inventory estimates by reducing plot location error - a multicriteria approach. *Remote Sensing of Environment*, 78, 321-327.

Katila, M., Heikkinen, J., & Tomppo, E. (2000). Calibration of small-area estimates for map errors in multisource forest inventory. *Canadian Journal of Forest Research*, 30, 1329-1339.

Katila, M., & Tomppo, E. (2001). Selecting estimation parameters for the Finnish multisource National Forest Inventory. *Remote Sensing of Environment*, 76, 16-32.

Katila, M., & Tomppo, E. (2002). Stratification by ancillary data in multisource forest inventories employing k-nearest-neighbour estimation. *Canadian Journal of Forest Research*, 32(9), 1548-1561.

Kilkki, P., & Päivinen, R. (1987). Reference sample plots to combine field measurements and satellite data in forest inventory. University of Helsinki, Department of Forest mensuration and management. Research Notes 19, 209-215.

Kim, H-J., & Tomppo, E. 2004. Model-based prediction error uncertainty estimation for k-nn method. *Submitted to Remote Sensing of Environment.*

Lappi, J. (2001). Forest inventory of small areas combining the calibration estimator and a spatial model. *Canadian Journal of Forest Research*, 3, 1551-1560.

McRoberts, R. E: (2005). Using inventory data, satellite data, and logistic regression model to estimate forest area and the precision of the estimates. *Manuscript submitted to Remote Sensing of Environment.*

McRoberts, R. E., Nelson, M. D., & Wendt, D. G. (2002). Stratified estimation of forest area using satellite imagery, inventory data, and the k-Nearest Neighbors technique. Remote Sensing of Environmetn, 82, 457-468. Mitchell, M. (1996). An Introduction to Genetic Algorithms, The MIT Press. USA. ISBN 0-262-13316-4.

Nilsson, M. (1997). Estimation of forest variables using satellite image data and airborne lidar. Ph.D. thesis, Swedish University of Agricultural Sciences, Department of Forest Resource Management and Geomatics. Acta Universitatis Agriculturae Sueciae. *Silvestria,* 17.

Pakkala, T., Hanski, I., & Tomppo, E. (2002). Spatial ecology of the three-toed woodpecker in managed forest landscapes. In: Korpilahti, E., & Kuuluvainen, T. (eds.). Disturbance dynamics in boreal forests: Defining the ecological basis of restoration and management of biodiversity. *Silva Fennica*, 36(1), 279-288.

Poso, S., 1972. A method of combining photo and field samples in forest inventory. *Commununicationes Instituti Forestalis Fenniae,* 76(1).

Reese, H., Nilsson, M., Granqvist Pahlén, T., Hagner, O. Joyce, S., Tingelöf, U., Egberth, M., and Olsson, H. 2003. Countrywide estimates of forest variables using satellite data and field data from the National Forest Inventory. Ambio 32, pp. 542-548.

Taskinen, I., & Heikkinen, J. (2004). A nonprametric Bayesian method for assessing uncertainty in thematic maps of forest variables. *Revision submitted to* Journal of Agricultural, Biological, and Environmental Statistics.

Tokola T., Pitkänen J., Partinen S., & Muinonen E. (1996). Point accuracy of a non-parametric method in estimation of forest characteristics with different satellite materials. *International Journal of Remote Sensing*, 17, 2333-2351.

Tomppo, E. 1987. Stand delineation and estimation of stand variates by means of satellite images. In: Remote Sensing-Aided Forest Inventory. *University of Helsinki, Department of Forest Mensuration and Management, Research Notes* No. 19: 60-76.

Tomppo, E. (1990). Designing a Satellite Image-Aided National Forest Survey in Finland. In: The Usability of Remote Sensing For Forest Inventory and Planning, Proceedings from SNS/IUFRO workshop in Umeå 26 - 28 February 1990. Swedish University of Agricultural Sciences, Remote Sensing Laboratory, Report 4. 43-47. Umeå, Sweden. ISBN 91-576-4208-7.

Tomppo, E. (1991). Satellite Image Based National Forest Inventory of Finland. *International Archives of Photogrammetry and Remote Sensing*, 28 (7-1), 419-424.

Tomppo, E. 1992. Satellite image aided forest site fertility estimation for forest income taxation. *Acta Forestalia Fennica*, 229. 70 p.

Tomppo, E. (1996). Multi-source National Forest Inventory of Finland. In: R. Vanclay, J. Vanclay, & S. Miina (Eds.), New Thrusts in Forest Inventory. Proceedings of the Subject Group S4.02-00 'Forest Resource Inventory and Monitoring' and Subject Group S4.12-00 'Remote Sensing Technology'. vol. 1. IUFRO XX World Congress 6-12 Aug. 1995, (pp. 27-41) Tampere, Finland. *EFI Proceedings*, 7. European Forest Institute. Joensuu. Finland.

Tomppo, E., Katila, M., Moilanen, J., Mäkelä, H. & Peräsaari, J. 1998. Kunnittaiset metsävaratiedot 1990-94. *Metsätieteen aikakauskirja - Folia Forestalia*, 4B/1998, 619-839 (in Finnish).

Tomppo E., Goulding C., & Katila M. (1999). Adapting Finnish multi-source forest inventory techniques to the New Zealand preharvest inventory. *Scandinavian Journal of Forest Research,* 14, 182-192.

Tomppo, E., Korhonen, K.T., Heikkinen, J., & Yli-Kojola, H. (2001). Multisource inventory of the forests of the Hebei Forestry Bureau, Heilongjiang, China. *Silva Fennica*, 35, 309-328.

Tomppo, E., Nilsson, M., Rosengren, M., Aalto, P. & Kennedy, P. 2002. Simultaneous use of Landsat-TM and IRS-1C WiFS data in estimating large area tree stem volume and aboveground biomass. *Remote Sensing of Environment*, 82, 156-171.

Tomppo, E. & Halme, M. 2004. Using coarse scale forest variables as ancillary information and weighting of variables in k-nn estimation: a genetic algorithm approach. *Remote Sensing of Environment*, 92, 1-20.

Topographic Database of Finland. 1998. The National Land Survey of Finland. Helsinki. Finland. http://www.nls.fi/kartta/maps/topodb.html.

Trotter, C.M., Daymond, J.R., & Goulding, C.J. (1997). Estimation of timber volume in a coniferous plantation forest using Landsat TM. *International Journal of Remote Sensing*, 18, 2209-2223.

USGS, 2005. LANDSAT PROJECT. http://landsat7.usgs.gov/slc_enhancements/.

Wallerman, J., Vencatasawmy, C.P., & Bondesson, L. (2003). Spatial simulation of forest using Bayesian state-space models and remotely sensed data. In: Wallerman, J. 2003. Remote sensing aided spatial prediction of forest stem volume. Acta Universitatis Agriculturae Sueciae, *Silvestria* 271.

Table 1a. Distribution of forestry land into sub-classes.

		Forest land		Scrub land		Waste land		Forestry land, Total	
		ha	%	ha	%	ha	%	ha	%
105	Hyrynsalmi	113370	83,7	14435	10,7	7689	5,7	135494	100,0
205	Kajaani	92850	88,8	7798	7,5	3971	3,8	104619	100,0
290	Kuhmo	388155	83,7	49706	10,7	25737	5,6	463598	100,0
578	Paltamo	73713	89,0	6429	7,8	2708	3,3	82850	100,0
620	Puolanko	191331	80,7	30259	12,8	15389	6,5	236980	100,0
697	Ristijärvi	69148	87,7	6613	8,4	3120	4,0	78881	100,0
765	Sotkamo	222928	90,0	16846	6,8	7985	3,2	247759	100,0
777	Suomussalmi	389616	77,0	65185	12,9	50876	10,1	505677	100,0
785	Vaala	88493	75,6	18862	16,1	9661	8,3	117016	100,0
940	Vuolijoki	52272	82,3	8344	13,1	2921	4,6	63536	100,0
	Total, MS-NFI	1681876	82,6	224477	11,0	130057	6,4	2036410	100,0
	Total, NFI	1659701		222675		142749		2025124	
	Standard error of NFI	13895		8969		7863		8582	

35

Table 1b. Mean and total volume of growing stock on forest land, forest and scrub land and forestry land.

		Forest land			Scrub land			Forest and scrub land			Forestry land		
		ha	m³/ha	1000 m³	ha	m³/ha	1000 m³	ha	m³/ha	1000 m³	ha	m³/ha	1000 m³
105	Hyrynsalmi	113370	67,4	7638	14435	12,0	173	127805	61,1	7812	135494	57,7	7818
205	Kajaani	92850	68,8	6386	7798	11,1	87	100648	64,3	6473	104619	61,9	6476
290	Kuhmo	388155	74,9	29083	49706	11,4	567	437861	67,7	29648	463598	64,0	29670
578	Paltamo	73713	83,2	6133	6429	12,8	82	80142	77,6	6215	82850	75,0	6214
620	Puolanko	191331	69,7	13341	30259	13,2	399	221590	62,0	13741	236980	58,0	13745
697	Ristijärvi	69148	68,7	4748	6613	11,1	73	75761	63,6	4822	78881	61,1	4820
765	Sotkamo	222928	75,7	16870	16846	11,5	194	239774	71,2	17063	247759	68,9	17071
777	Suomussalmi	389616	66,1	25747	65185	10,4	678	454801	58,1	26426	505677	52,3	26447
785	Vaala	88493	64,0	5661	18862	13,3	251	107355	55,1	5912	117016	50,5	5909
940	Vuolijoki	52272	74,6	3900	8344	10,2	85	60616	65,7	3985	63536	62,7	3984
	Total, MS-NFI	1681876	71,1	119507	224477	11,5	2589	1906353	64,0	122097	2036410	60,0	122153
	Total, NFI	1659701	70,8	117000	222675	12,6	2800	1882376	63,9	120000			
	Standard error of NFI	13895	1,4	2494	8969	0,7	198	11165	1,3	2502			

Table 1c. Total volume of growing stock by timber assortment classes on combined forest and scrub land.

	Pine			Spruce			Birch			Other broad leaved tree species			Total
	Total	Saw timber	Pulp wood	Total	Saw timber	Pulp wood	Total	Saw timber	Pulp wood	Total	Saw timber	Pulp wood	
105 Hyrynsalmi	4602	1578	2702	2132	735	1255	961	15	677	117	2	78	7812
205 Kajaani	3755	1033	2441	1527	545	867	1048	17	715	143	2	93	6473
290 Kuhmo	18163	6835	10143	7877	2727	4593	3263	138	2270	345	8	246	29648
578 Paltamo	3199	999	1987	1858	706	1040	1000	20	712	157	3	102	6215
620 Puolanko	7374	2341	4470	4410	1503	2646	1718	26	1226	238	3	169	13741
697 Ristijärvi	2549	824	1539	1446	539	815	732	14	509	94	1	63	4822
765 Sotkamo	8743	2815	5308	5115	1997	2781	2825	92	1951	380	3	266	17063
777 Suomussalmi	16264	6247	9070	6957	2252	4275	2901	71	2265	304	3	243	26426
785 Vaala	4075	1160	2541	732	222	446	984	10	657	121	4	72	5912
940 Vuolijoki	2250	554	1503	751	265	424	852	13	593	133	4	82	3985
Total, MS-NFI	70974	24386	41704	32805	11491	19142	16284	416	11575	2032	33	1414	122097

Session 1b

SINGLE TREE DETECTION IN VERY HIGH RESOLUTION REMOTE SENSING DATA

M. Hirschmugl[a], M. Franke[b], M. Ofner[a], M. Schardt[a,b] and H. Raggam[b]

[a] Technical University Graz, Institute of Photogrammetry & Remote Sensing, Steyrergasse, 8010 Graz, Austria, email: manuela.hirschmugl@joanneum.at
[b] Joanneum Research, Institute of Digital Image Processing, Wastiangasse, 8010 Graz, Austria

ABSTRACT

Tree detection is a major focus in the field of (semi-) automatic extraction of forest information from VHR data. Many existing tools require a set of seed pixels with which to start segmentation. In this study, different methods of obtaining seeds (semi-) automatically from both orthophotos and digital surface models (DSM) derived from stereo imagery are tested and compared. The evaluation is performed based on field measurements and visual aerial photo interpretation. The results for 3D seed generation using the local maximum approach (LMA) are very poor; apparently, the smoothing effect of the DSM is too strong to model single trees. Seed generation based on orthophotos performed better: for a dense, natural forest, the "morph" algorithm detected 64% of the trees visible in the aerial photos by an error of around 25% both for commission and omission. Compared to the field measurements, the results (correct 47%) are worse, as suppressed trees cannot be detected in optical data. The LMA based on orthophoto generally led to slightly lower accuracies and more multiple hits than the morph algorithm. Further studies are needed to analyze in detail the dependence of successful tree detection on different tree parameters such as height, crown diameter or tree species. Another important task is the use of the derived seed points in the region growing process in order to evaluate their applicability and accuracy concerning tree species segregation and timber volume estimation.

Keywords: single tree extraction, seed generation, LMA, digital camera data, Ikonos
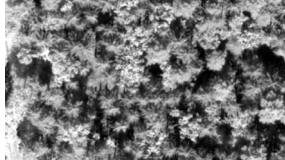
1 INTRODUCTION

The recognition of single trees is one of the main tasks when deriving forest information from VHR remote sensing data. Various image analysis methods have thus been developed in this field (Gougeon, 1995, Pitkänen, 2001, Culvenor, 2002, Erikson, 2004). Most of this work was performed based on scanned CIR imagery, while this study uses new digital airborne and spaceborne data. Furthermore, as Erikson (2002) pointed out in his paper, the integration of the 3rd dimension is an important task for further research. This paper contributes to this goal by investigating how accurate seed points for single tree detection can be extracted using methods based on orthophotos and stereoscopically derived 3D surface models.

2 DATA AND TEST SITES

In this study, the usability of stereo image data from the Ultracam$_D$ large format digital camera and Ikonos is investigated. Table 1 gives an overview of the image data and their characteristics. Additional ground truth data was obtained by extensive fieldwork. For this study, two plots with 163 terrestrially measured trees (all trees with dbh > 8 cm) and 153 trees from visual interpretation (based on Ultracam data) were used to evaluate the results of the approaches presented. Both test plots of the "Burgau" test site, which is located in south-east Austria, are characterized by heterogeneous forest mainly consisting of pine, spruce and oak trees. Test plot 64 is a dense stand with understorey, while test plot 65 is comparatively sparsely stocked with large trees, but contains dense ground vegetation. Thinning was performed on both test sites several years before the remote sensing data were acquired.

Table 1. Brief characteristics of the data used

Sensor	Acquisi-tion date	Spectral resolution	Spatial resolution	Radiometric resolution	Example (subset of plot 65: Ikonos PAN, Ultracam NIR)
Ikonos	13. 09. 2004	pan: 450 – 900 nm blue: 450 – 520 nm green: 510 – 600 nm red: 630 – 700 nm nir: 760 – 850 nm	pan: 1m multispectral: 4m	11bit	
Ultra-cam$_D$	21. 07. 2004	pan**:** 390 – 690 nm blue: 390 – 530 nm green: 470 – 660 nm red: 570 – 690 nm nir: 670 – 940 nm	pan: 15cm multispectral: approx. 55cm	12 bit	

3 GENERAL TREE DELINEATION APPROACH

A seeded region growing algorithm was used for single tree delineation (Hirschmugl *et. al.*, 2004). The bottleneck of this procedure until now has been to find the optimal seed pixels, i. e. the initial points to start the region growing process. Their location has a crucial influence on the final segmentation result. Most studies use either the brightest points of an orthophoto (Leckie *et. al.,* 1999, Culvenor, 2002, Pouliot *et. al.*, 2002) or both the brightest points of an orthophoto and the highest points of a DSM (Rawert, 2004) in a local environment as seed points. The highest point – if extractable with an adequate accuracy – would be the best alternative at least for spruce and fir trees, since it generally marks the crown center in these species. Due to illumination effects the brightest point within the orthophoto is not mandatorily the center of the visible crown, therefore seeds generated by this method tend to split crowns. Erikson (2004) presented a combination of brightness and distance to the background in order to improve the seed location. Methods working independently from seed points are e.g. the "valley following approach" (Gougeon, 1995).

4 SEED GENERATION

4.1 3D SEED GENERATION

<u>DSM from Ultracam and IKONOS data</u>: The sensor model of the Ultracam data is described by interior and exterior orientation. The Ikonos data provide no information on sensor parameters, but do give rational polynomial coefficients, which allow a point to be mapped from ground to image and vice versa. Homologous ground control points (GCPs) were measured in the stereo pairs to increase the accuracy of geometric modeling. These GCPs were used to improve the Ultracam exterior orientation parameters by least square adjustment and the Ikonos rational polynomial coefficients by additional polynomials. After optimization, a comparison with given ground coordinates leads to 3D point residuals in East, North and Height. The a-priori modeling accuracy can be expressed by the RMS error: an RMS height accuracy of 1.4 meters for Ikonos and 0.4 meters for Ultracam is achieved, while the planimetric accuracy is about 0.5 and 0.3 meters, respectively. DSMs were generated from the stereo pairs by automated image matching, calculation of ground coordinates and interpolation of a regular elevation raster. The vegetation height model (VHM) was calculated by subtracting a detailed digital terrain model (derived from Lidar data) from the DSMs derived from the Ultracam and Ikonos data. The accuracy of the VHM documented in Table 2 was assessed by the comparison of 163 tree heights measured in the field and the corresponding height values of the VHM. The comparison showed the following results: The height of suppressed trees is generally overestimated, whereas high trees at the forest border, very tall trees and trees in open forests are significantly underestimated The differences found are mainly due to smoothing effects caused by the matching procedure applied. The remaining trees, which can be regarded as "average trees", are mapped with reasonable accuracy, especially by the VHM derived from the Ultracam data.

Seed Generation: The results presented lead to the assumption that single tree extraction based on height maxima derived from the VHM might be difficult. However, seed generation was performed using a local height maximum approach with a fixed window size, the same algorithm as used to performed the 2D seed generation based on the intensity maximum (see section 4.2).

Table 2. Ikonos and Ultracam statistics for the 163 field measured trees. Overall accuracy as well as accuracy for categories of trees (categorization based on field data)

	All trees (163)	Trees at the forest border	Suppressed trees	Extraordinary tall trees	Trees in very open forest	Average trees (rest)
Ultracam						
Mean:	-0.4	11.685	-11.189	9.751	7.4	2.224
Std.Dev.:	8.36	3.779	3.941	3.911	2.5	2.399
Min:	-18.76	7.206	-18.760	5.459	3.2	-5.400
Max:	18.09	18.087	0.173	17.456	10.8	9.135
Ikonos						
Mean:	-2.2	6.068	-11.918	5.964	7.1	0.267
Std.Dev.:	7.78	4.171	4.411	5.044	5.3	2.171
Min:	-20.67	-1.799	-20.669	-0.013	0.3	-6.992
Max:	17.58	13.419	-2.223	17.584	15.0	6.010

4.2 2D SEED GENERATION

In addition to the already mentioned local maximum approach (LMA), a new method based on smoothing, thresholding and morphological operations ("morph") is presented to improve the location accuracy of the seed pixels.

LMA: As the LMA has already been thoroughly investigated (Pitkänen, 2001, Wulder *et. al.,* 2004) no further development was carried out on this topic. The only modification is the application of a threshold procedure to be carried out in the forefield of the LMA in order to eliminate non-tree crown areas, i.e. shadows and ground pixels. For threshold definition a representative tree was selected and its maximum grey value depicted from the PAN (Ikonos) or NIR band (Ultracam). The maximum grey value minus 2 times standard deviation then gives the approximate value for the shadow threshold. This threshold was used in the different methods developed to allow for better comparability. In the next step the vegetation height models (described in section 4.1.) for each image data set are used to eliminate pixels of a vegetation height lower than 10 m. Due to this step, the whole procedure can also be seen as "2.5 dimensional" seed generation. The Ultracam image was subsequently filtered with a Gauss filter kernel, while the results for Ikonos did not require filtering. Finally, the LM was calculated using a 4-neighborhood filter and a fixed minimal distance of 2m between the maxima to be found for both image types. Of course, the problem of scale always remains when using a LM filter (Daley et al. 1998).

New "morph" processing chain: The processing chain set up in this investigation is structured hierarchically and consists of the following components: 1) A threshold procedure as described above is applied to the data in order to isolate crown pixels from non-crown pixels. 2) In the next step the crown pixels are smoothed using symmetric nearest neighbor filter. 3) In the third step, morphological erosion (e.g. Gonzalez & Woods 1992) is used to reduce the visible tree crowns to their center regions. 4) After morphing, the center of gravity of each remaining region is calculated representing a seed candidate. 5) The candidates are then weighted and sorted according to their hit rate (how often and at what level one pixel was designated as the center of a region) in order to obtain tree crowns of different sizes. 6) Finally, the candidates are sorted out according to weight where they lie too closely (within 2m) together. One precondition for this procedure is that the tree crowns are tall enough and are thus represented by a sufficient number of pixels. Since most of the Ikonos imagery does not fulfil this precondition because smaller trees are represented by very few or even only one pixel, image analysis was limited to the LMA. The whole procedure is implemented in the software library called "IMPACT" developed by the Institute of Digital Image Processing of JOANNEUM RESEARCH.

5 RESULTS

The tree locations measured in the field were used for verification. A geometric preprocessing step had to be carried out before the field measurements and the detected seeds could be overlaid automatically, since there is a shift between the correct location of the treetop and the location appearing in the orthophoto due to sensor geometry. This preprocessing consists of a transformation of the field data to the geometrical properties of the corresponding orthophoto using the RSG software developed at the Institute of Digital Image Processing of JOANNEUM RESEARCH. Geometric distortions still remaining after the transformation had to be adjusted manually in a subsequent step. The adjusted ground truth points were

then buffered by one meter and intersected with the results. The quality of tree detection was then measured by counting the number of correct hits, considering both the omission and commission error (see Table 3). Double hits were avoided due to the small buffer. Additionally, the results were compared to the results of visual, monoscopic delineation of all visible tree crowns in the Ultracam data, which was carried out by an independent expert from the Finnish Geodetic Institute. All seeds detected automatically were then intersected with these visually interpreted segments and the number of correct and multiple hits, as well as the omission and commission errors evaluated (see Table 3). The first verification thus shows how many of the trees measured in the field can be detected automatically, whereas the second procedure only refers to the trees visible in the aerial photos.

5.1 RESULTS FOR 3D SEED GENERATION

As already demonstrated, "treetops" are not clearly defined in the derived DSMs (see Table 2). Several reasons for this can be identified: First, as a result of different viewing angles, different shadow distributions in the corresponding stereo images lead to data gaps that must be interpolated in the matching process, which may cause a smoothing of the surface. Second, the radiometric properties of the stereo images differ slightly, which complicates the definition of homologous points. Third, forest structure is very fuzzy and various image subsets have many similar characteristics, which further complicate the matching process. The difficulties mentioned above, the coarse spatial resolution of Ikonos and the small and partly overlapping tree crowns of the test site lead to a very smooth VHM derivable from Ikonos data. Thus, it is likely that more adjacent pixels have the same value, which leads to the fact that only a few maxima can be detected (only 19/14 maxima for 75/88 trees measured). It can therefore be stated that the Ikonos DSM is not suitable for single tree detection in this kind of forest. Similar problems were observed for the Ultracam DSM, although the results are better due to more variability within the DSM, but the commission error is also far higher, especially for the sparsely stocked stand. The number of correctly identified trees from the Ultracam DSM compared to field measurements was between 29 and 48% for both plots (depending on the value of sigma for the gauss filter), but always with a high commission error (80-340%). Both the commission error and the number of correct trees generally decrease with increasing sigma. Other procedures are obviously needed to process this kind of data. A more promising alternative to be tested in the future is the use of Ikonos and Ultracam DSMs for stand-wise estimation of tree heights.

5.2 RESULTS FOR 2D SEED GENERATION

The verification of 2D seed generation has shown that the accuracy is lower than expected. The reasons for this are: 1. All ground reference trees were used, including sub-dominant and suppressed trees, which are not visible in the image. This fact should generally lead to an underestimation of tree number. 2. The test sites include oak trees, which are characterized by rather large and heterogeneous crowns. This results in an overestimation, as one oak crown may well be regarded as several trees (multiple hits). 3. Visible ground vegetation can also be regarded as tree crowns (especially in the sparsely stocked test plot 65). The accuracy of the Ikonos results is quite poor in comparison to literature (Wulder et al, 2004). Aside from the reasons mentioned above, this is probably due to the relatively small average tree crown size and the natural state of the forest in the test site. In the above study, 75% of the trees were plantation trees and the rest were major trees with heights up to 70m and accordingly large crowns, both factors facilitating tree detection from Ikonos imagery. The results in comparison to visual interpretation are better: the omission and commission errors of both methods based on Ultracam data are about the same, but the percentage of correctly identified trees of the morph algorithm is slightly higher (morph: 59/64%; LMA 57/54%). In general, the accuracies are better for the dense than for the sparsely stocked test plot, mainly because of the disturbing ground vegetation in plot 65.

Table 3. Results for 2D seed generation

PLOT 65 – sparse stand		Field trees (75 trees, buffer: 1m)			Visual interpretation (81 segments)			
		Correct no|%	Omission no|%	Commission no|%	Correct no|%	Multiple hits (seg.)	Omission no|%	Commission no|%
LMA	Ultracam (120)	29|39%	46|61%	91|121%	46|57%	37 (15)	20|25%	37|46%
	Ikonos (125)	25|33%	50|67%	100|133%	27|33%	15(6)	48|59%	83|103%
Morph	Ultracam (125)	46|61%	29|39%	79|105%	48|59%	39 (16)	17|21%	38|47%
PLOT 64 – dense stand		Field trees (88 trees, buffer: 1m)			Visual interpretation (72 segments)			
		Correct no|%	Omission no|%	Commission no|%	Correct no|%	Multiple hits (seg.)	Omission no|%	Commission no|%
LMA	Ultracam (98)	38|43%	50|57%	58|66%	39|54%	42(18)	15|21%	15|21%
	Ikonos (55)	23|26%	65|74%	32|36%	20|28%	4(2)	50|69%	31|43%
Morph	Ultracam (84)	41|47%	47|53%	43|49%	46|64%	20(9)	16|22%	19|26%

6 CONCLUSIONS AND OUTLOOK

The investigation has shown that it is difficult to compare the results derivable from aerial photos to field measurements, as suppressed trees cannot be seen in optical data. Field measurements will be used in further investigations, however, to analyze in detail the dependence of successful tree detection on different tree parameters such as height, crown diameter, tree species, vertical crown or crown density. Obtaining seed points only from the 3D surface proved to be unsatisfactory with LM filters, as the canopy surface is not detailed enough to model single treetops, or alternative methods need to be developed first to derive more precise DSMs from stereo data or for seed generation. An integration of the vegetation height in 2D approaches, however, is very useful and should be extended. Of the 2D methods tested, the morph algorithm performed slightly better than the LM approach. However, both methods need further development to improve the accuracy for these heterogeneous and structured stands. In general, a large accuracy variation was observed based on the plot characteristics such as density, tree types and structure, which might also be one of the reasons for varying accuracy reports of different studies. More plots must be included in further testing to confirm the preliminary results of this study. The development of an improved shadow and ground threshold generation procedure could be another interesting research topic. However, the most important task coming up is the use of the derived seed points in the region growing process in order to evaluate their applicability and accuracy for further investigations concerning tree species segregation and timber volume estimation. It can be expected that the error in timber volume will be much less, as suppressed trees do not account for a significant part of the timber volume.

REFERENCES

Culvenor, D. S. 2002. TIDA: an Algorithm for the Delineation of Tree Crowns in High Spatial Resolution Remotely Sensed Imagery. *Computers & Geosciences, Vol. 28, Issue 1*, pp. 33 – 44.

Daley, N. M. A., Charles N. Burnett, Mike Wulder, K. Olaf Niemann, and David G. Goodenough 1998. Comparison of Fixed-size and Variable-sized Windows for the Estimation of Tree Crown Position. *Proc. IGARSS'98*, 3, Seattle, WA, pp. 1323-1325.

Erikson, M. 2004. Segmentation and Classification of Individual Tree Crowns in High Spatial Resolution Aerial Images. Doctoral Thesis, Swedish University of Agricultural Sciences, Uppsala, 110 p.

Gonzalez, R. C. and Woods, R. E. 1992. Digital Image Processing. – Addison-Wesley Publishing Company, Tennessee, 716 S.

Gougeon, F. A. 1995. A Crown-Following Approach to the Automatic Delineation of Individual Tree Crowns in High Spatial Resolution Aerial Images. *Canadian Journal of Remote Sensing 21, Special Issue on Aerial Optical Remote Sensing*. S. 274 – 282.

Hirschmugl, M. and Schardt, M. 2004. Methods for the Automatic Estimation of Forest Attributes from Aerial Imagery. Proceedings of 1st Göttingen GIS & Remote Sensing Days 7-8 Oct. 2004, Göttingen. In: Kleinn, C., Nieschulze, J., Sloboda, B. (Eds.) (2005): Remote Sensing & GIS for Environmental Studies: Applications in

Forestry. Schriften aus der Forstl. Fakultät der Univ. Göttingen und der Nieders. Versuchsanstalt, Vol. 137, Sauerländer Verlag, Frankfurt, Main (in print).

Leckie, D., Burnett, C., Nelson, T., Jay, C., Walsworth, N., Gougeon, F. and Cloney, E. 1999. Forest parameter extraction through computer-based analysis of high resolution imagery. *In Proc. Fourth Int. Airborne Rem. Sens. Conf. and Exh. / 21st 1Can. Symp. Rem. Sens, Vol. II.* Ottawa, Canada, June 21-24, 1999, pp. 205-213.

Pitkänen, J. 2001. Individual tree detection in digital aerial images by combining locally adaptive binarization and local maxima methods. Canadian Journal of Forest Research 31(5): 832-844.

Pouliot D. A., King D. J., Bell F. W. and Pitt D. G. 2002. Automated Tree Crown Detection and Delineation in High-Resolution Digital Camera Imagery of Coniferous Forest Regeneration. *Remote Sensing of Environment Vol. 82, Issues 2 - 3*, S. 322 - 334.

RAWERT, B. (2004): Automatic Tree-Crown Segmentation Using LM Filters and Balloons. Unpublished Master's Project, University of Massachusetts, available at:
http://vis-www.cs.umass.edu/~rawert/treeseg/masters/masters.pdf

Wulder, M.A., White, J.C., Niemann, K.O. and Nelson, T. 2004. Comparison of airborne and satellite high spatial resolution data for the identification of individual trees with local maxima filtering. *International Journal of Remote Sensing Vol. 25, No. 11*, p. 2225 – 2232.

SINGLE TREE SPECIES CLASSIFICATION WITH A HYPOTHETICAL MULTISPECTRAL SATELLITE

Morten Larsen

Department of Natural Sciences, Royal Veterinary and Agricultural University
Thorvaldsensvej 40, 1871 Frederiksberg C, Denmark
email: `ml@dina.kvl.dk`

ABSTRACT

The requirements for high resolution multispectral satellite images to be used in single tree species classification for forest inventories are investigated, especially with respect to spatial resolution, sensor noise and geo-registration. In the hypothetical setup, a tree crown map is first obtained from very high resolution panchromatic aerial imagery and subsequently each crown is classified into one of a set of known tree species such that the difference between a synthetic multispectral image generated from the crown map and a multispectral satellite image of the forested area is minimized. The investigation is conducted partly by generating synthetic data from a 3D crown map from a real mixed forest stand and partly on hypothetical high resolution multispectral satellite images obtained from very high resolution colour infrared aerial photographs, allowing different hypothetical spatial resolutions. Conclusions are that until a new generation of even higher resolution satellites becomes available, the most feasible source of remote sensing data for single tree classification will be aerial platforms.

Keywords: Single trees, high resolution satellites

1   INTRODUCTION

Individual tree crowns in aerial photographs may be found by delineation based on light/shadow contrasts (Gougeon, 1995; Brandtberg and Walter, 1998) or by fitting three dimensional optical tree crown models rendered in accordance with the geometry and lighting at image acquisition (Larsen and Rudemo, 1998). With the latter approach one may obtain a 3D tree crown map from multiple images by fitting the crown shape parameters to maximize the correspondence of the rendered crows within all images. See Larsen and Rudemo (2004) for first steps in this direction: a Bayesian framework for reconstructing the 3D tree top positions. One could also use laser scanning data to obtain the 3D tree crown map (Brandtberg et al., 2003), alone or in conjunction with aerial photography. However, the high resolution data sources enabling the generation of a 3D tree crown map do not necessarily carry the spectral information needed for species classification. Specifically, traditionally aerial photography used for survey purposes in Denmark is panchromatic and earlier Danish research into high resolution remote sensing for forest inventory has been based on digitized fine scale panchromatic images (Dralle and Rudemo, 1997; Larsen and Rudemo, 1998; Tarp-Johansen, 2002). The advent of commercially available high resolution multispectral satellite imagery (i.e. IKONOS in September 1999) motivated experiments with a framework for single tree forest inventories where crown mapping would be done from very high resolution panchromatic aerial photography followed by species classification from multispectral high resolution satellite imagery.

Since then, airborne high resolution multispectral systems have become an economically more viable source for forest inventory data (at least in Denmark). An airborne system is more flexible in deployment than a satellite system and this is an advantage when images have to be acquired within a narrow timeframe, e.g. as dictated by the desire for capturing data when the trees are in a certain stage of their annual cyclus. Furthermore there is great promise in combining optical with laser scanning data from the same flight when mapping the 3D canopy structure (Næsset and Bjerknes, 2001). Thus technological and commercial developments in aerial imaging mean that today the combination of aerial photography and satellite imaging is not economically sound for forest inventories. However, future development of imaging platforms could make the multiresolution approach with fine scale panchromatic and coarser scale multispectral data attractive again.

2 THE PROPOSED METHOD

A method for tree species classification from a multispectral high resolution satellite image is proposed in the following. It is assumed that a very accurate 3D tree crown map is available for the area of interest and that there is a limited set of candidate tree species (classes) for which spectral properties are known, both for crown segments illuminated directly by the sun and for segments that are shaded. If the ground is visible through the canopy from above, spectral information for sunlit and shaded ground must also be known.

A high resolution multispectral satellite image of the area is acquired. The crowns of the crown map are classified by minimising the difference between this image and a *model image*.

The model image I is generated from the 3D tree crown map, T, with the spectral properties of each tree crown $t \in T$ determined by its proposed species $\phi(t)$, where the function ϕ assigns a species label to each tree. Each species s in the set of possible species' S has associated *sunlit* spectral vector $\boldsymbol{\alpha}_s$ and *shaded* spectral vector $\boldsymbol{\beta}_s$. The ground has associated sunlit and shaded spectral vectors $\boldsymbol{\alpha}_G$ and $\boldsymbol{\beta}_G$. Let T_i be the trees in T which are visible in image pixel $i \in I$. The spectral vector $\boldsymbol{\gamma}_i$ of pixel i is then:

$$\boldsymbol{\gamma}_i = \sum_{t \in T_i} \left(\boldsymbol{\alpha}_{\phi(t)} A_{\alpha t, i} + \boldsymbol{\beta}_{\phi(t)} A_{\beta_{t,i}} \right) + \boldsymbol{\alpha}_G G_{\alpha i} + \boldsymbol{\beta}_G G_{\beta_i}, \tag{1}$$

where $A_{\alpha t, i}$ is the fraction of the area of pixel i covered by the sunlit portion of the crown of tree t, and similarly $A_{\beta_{t,i}}$ is the fraction covered by the shaded portion of the crown of t, $G_{\alpha i}$ is the fraction showing sunlit ground and G_{β_i} is the fraction showing shaded ground.

In order that $\boldsymbol{\gamma}_i$ can be computed efficiently, the $A_{\cdot t, i}$ and $G_{\cdot i}$ must be precomputed. This is however difficult to do exactly for any nontrivial 3D tree crown map and optical crown model. The difficulty lies in the partially self-shading nature of the tree crowns, i.e. that sunlight penetrates to and illuminates some parts of the "back" of the crown while other parts are shaded (see Larsen and Rudemo (1998) for an optical model). With trees close together and partially shading each other, the situation is even more complex. Therefore an approximating approach is adopted in which the 3D crown map, the image formation geometry and the sun position are used to ray-trace a *lighting map image* at very high resolution (5 cm in the experiments reported here). Each pixel of the lighting map image is classified as showing either sunlit tree crown, shaded tree crown, sunlit ground or shaded ground. To determine values for $A_{\cdot t, i}$ and $G_{\cdot i}$ the lighting map image is superimposed on the model image and each lighting map pixel contribute to one of the $A_{\cdot t, i}$ or $G_{\cdot i}$ according to its lighting class and position in the crown map.

To classify the trees in T, we find the ϕ which minimizes the function

$$\Delta(\mathbf{O}, T, \phi) = \sum_{i \in I} ||\boldsymbol{\gamma}_i - \mathbf{O}_i||, \tag{2}$$

where $\mathbf{O}_i$ is the spectral vector for pixel i in the observed image $\mathbf{O}$ and $|| \cdot ||$ is the Euclidian norm. In this work minimisation was performed by a greedy algorithm with a stochastic element in the vein of simulated annealing; space does not permit a detailed description here.

3 EXPERIMENTS

For the application of the algorithm one needs a mixed forest stand for which multispectral imagery is available, along with spectral signatures under the conditions of image acquisition for the tree species present and an accurate 3D crown map of the visible tree crowns. Spectral signatures will likely have to be obtained from the imagery itself and this may require some field work to verify the species of selected specimen trees. The crown map must be obtainable from other, higher resolution data and the accuracy of the map and its exact registration to the imagery are paramount. In the experiments reported here, neither multispectral imagery nor crown map were obtained in the manner they would be in a real application.

For evaluating performance the true species of each tree must be known. The cost of the field work involved in obtaining the required ground truth data necessitated the choice of a forest stand for which
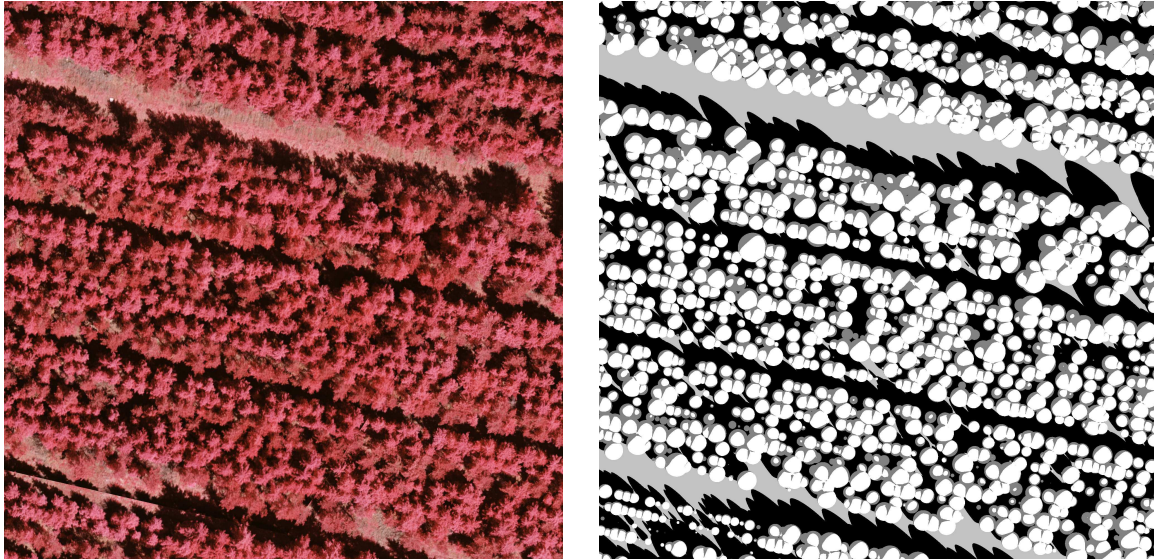
Figure 1: Part of the study area, 100 m × 100 m on the ground. **Left:** false colour infrared orthoimage, 5 cm resolution. Note that the seams between original images are obvious at ground level but harder to detect at canopy level. **Right:** Lighting map for the same area. Grey value indicates class of pixel: sunlit crown is white, shaded crown dark grey, sunlit ground light grey and shaded ground black.

a reasonable recent single tree stem map already existed. Fortunately the Danish Forest and Landscape Institute were able to supply a 1998 stem map of a regeneration trial experimental plot located in Gludsted Plantation Forest in Jutland. The stem map consists of 2D stem positions in a local coordinate system, as well as the diameter at breast height (dbh) and species of each tree. The tree species are Norway spruce (*Picea abies* (L.) Karst.), Scots pine (*Pinus sylvéstris* L.), Silver fir (*Abies alba* Mill.) and Japanese larch (*Larix leptólepis* (Sieb. & Succ.) Gord.). The total basal area (cross sectional area of the stems at breast height) of the 5321 trees in the experimental area was $48.77\,\text{m}^2$; $\approx 90\%$ spruce and pine.

No actual satellite imagery was used. Instead, "satellite images" of three spectral channels were obtained from colour infra red (CIR) aerial photos obtained in July 2001 from an altitude of about 500 m above ground level. Multiple CIR images were combined to produce a digital orthoimage of the trial area at 5 cm resolution. No good terrain model was available, but the area is reasonably flat and a plane fitted to ground control points was deemed usable as terrain model. Elevations were increased by 10 m to produce a "crown level" orthoimage corresponding to field measured tree heights. This gave an image with only barely discernible seams at the canopy level. No attempt was made at radiometric correction. Part of the orthoimage is shown in figure 1.

A 3D crown map of 3735 potentially visible tree crowns was constructed from the stem map; tree heights and crown sizes were found by regression on the measured breast height diameters (the height regression coefficients per species being based on field measurements in the trial and the crown widths on visual fitting in the orthoimage). Trees lower than breast height were left out, as were understory trees which according to the crown map would not be visible from above. For a crown shape model, the truncated generalized ellipsoid also employed in Larsen and Rudemo (1998) was used, with shape parameter $n = 1.6$ for all trees regardless of species; inspection of the available imagery from off-nadir angles and the shape of the shadows cast by the crowns suggested that this would fit most medium and large crowns fairly well. Figure 1 shows part of the lighting map image generated from the crown map.

The crown map had to be transformed from its local coordinate system to UTM in order to be registered with the orthoimage. Unfortunately, no points had been measured in both systems. The registration was thus performed by visually aligning the crown map with the orthoimage, with crowns drawn as circles and colour coded to indicate tree species. Completely satisfactory results could not be obtained however.

Spectral vectors $\boldsymbol{\alpha}_s$ and $\boldsymbol{\beta}_s$ for model image generation were obtained by selecting ten medium to large sized crowns for each tree species and manually delineating sunlit respectively shaded portions of the crowns and then taking a simple average of the pixel spectral vectors. Similarly, sunlit and shaded patches of ground were sampled for the ground spectral vectors $\boldsymbol{\alpha}_G$ and $\boldsymbol{\beta}_G$.

In spite of the unsatisfactory crown map, an experiment was performed where the algorithm was applied to "satellite imagery" obtained by subsampling the orthophoto at resolutions 2 m, 1 m, 50 cm and 25 cm. Results were not encouraging, with the proportion of accurately classified basal area varying from 22.6% for 2 m resolution to 29.7% for 50 cm and 25 cm resolution. Examination of the results showed that most errors were spruce being misclassified as larch and pine being misclassified as fir. This was not surprising as the spectral vectors for the bright spruce and larch were very close, as were the vectors for the darker pine and fir. Reducing the classes to a "bright" class of spruce/larch and a "dark" class of pine/fir improved results; now 65.9% were correctly classified at the high resolutions. Still, performance is not good enough for practical application and the experiment illustrates the need for an accurate crown map.

Experiments were performed on synthetic images to gauge the impact of image resolution and observation and model noise on classification performance. Synthetic images were generated from the crown map and spectral signatures of the tree species so that each pixel $\mathbf{I}'_i$ of synthetic image $\mathbf{I}'$ was computed by a modified equation (1):

$$
\begin{aligned}
\mathbf{I}'_i \;=\; [\quad & \textstyle\sum_{t \in T_i} \left((\boldsymbol{\alpha}_{\phi(t)} + \boldsymbol{\epsilon}_{\mathrm{tree}t}) A_{\alpha t,i} + (\boldsymbol{\beta}_{\phi(t)} + \tfrac{1}{2}\boldsymbol{\epsilon}_{\mathrm{tree}t}) A_{\beta t,i} \right) \\
& + (\boldsymbol{\alpha}_G + \boldsymbol{\epsilon}_{\mathrm{gnd}_i}) G_{\alpha i} + (\boldsymbol{\beta}_G + \tfrac{1}{2}\boldsymbol{\epsilon}_{\mathrm{gnd}_i}) G_{\beta_i} \;\;] \; (1 + \boldsymbol{\epsilon}_{\mathrm{pix}_i}) ,
\end{aligned}
\tag{3}
$$

where $\boldsymbol{\epsilon}_{\mathrm{tree}t}$, $\boldsymbol{\epsilon}_{\mathrm{gnd}_i}$ and $\boldsymbol{\epsilon}_{\mathrm{pix}_i}$ are random spectral noise vectors. The $\boldsymbol{\epsilon}_{\mathrm{tree}t}$ is the "biological noise" for tree t, i.e. the deviation from the ideal spectral signature for the tree species. The $\boldsymbol{\epsilon}_{\mathrm{gnd}_i}$ is "ground patch noise", i.e. the deviation from the ground spectral signature in the ground patch of pixel i. Finally, $\boldsymbol{\epsilon}_{\mathrm{pix}_i}$ is multiplicative pixel level "sensor noise". All components of the $\boldsymbol{\epsilon}_{\cdot}$ error vectors are independent and drawn from zero mean normal distributions. To gauge the effect of each type of noise, experiments were performed in which images were generated with only one type of noise at different variances. The results are shown in figure 2 (a)–(c). The effect of a misregistered crown map was examined by using a noise free synthetic image and shifting the crown map horizontally. The results are shown in figure 2 (d).

4 CONCLUSIONS

In order for satellite imagery from a future hypothetical 1 m multispectral satellite to be attractive for single tree species classification, either the panchromatic resolution must be extremely high, on the order of 20 cm, so that an accurate crown map may be obtained directly from the satellite without the need for aerial photography, or the cost of satellite imagery must be much lower than with the commercial high resolution satellites of today and time frames for image acquisition must be more flexible (i.e. there must be more satellites so that image acquisition becomes almost "on demand"). For the foreseeable future, multispectral sensors on aerial platforms is the realistic data source for single tree species classification.

The experiments on synthetic images suggest that given a near perfect crown map and imagery from a hypothetical 1 m resolution multispectral satellite, about 90% of the basal area can be expected to be correctly classified on the single tree level. However, the experiments on actual 1 m images with an imperfect crown map yield classification results which at less than 30% are unusable for forest inventory purposes. Accurately establishing the positions, shapes and extents of every tree crown is thus the main challenge in a remote sensing approach for single tree forest inventories. Given an accurate crown map and multispectral imagery of sufficient resolution, single tree species classification will be a comparatively straightforward next step, either with a method like the one proposed or by a more elaborate Bayesian scheme when informative priors can be obtained.
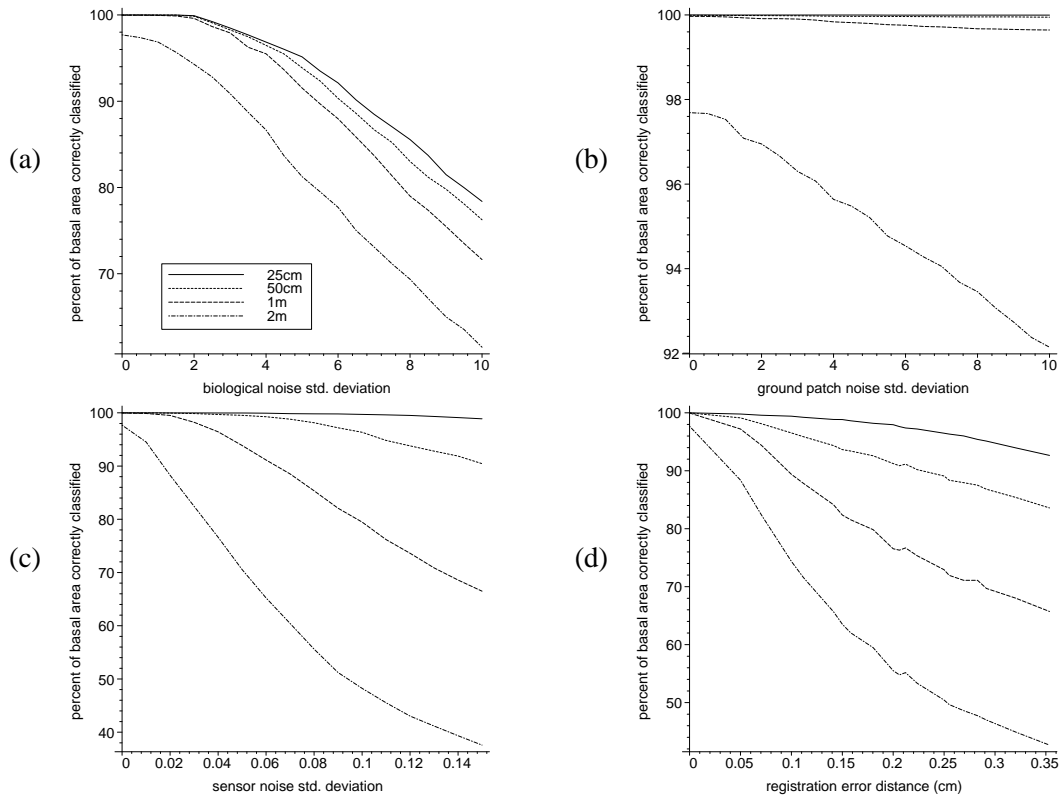
Figure 2: Experiments on synthetic data for different image resolutions. (a) Effects of "biological noise". (b) Effects of "ground patch noise". (c) Effects of multiplicative "sensor noise". (d) Effects of crown map misregistration.

ACKNOWLEDGEMENTS

REFERENCES

Brandtberg, T. and Walter, F. 1998. Automated delineation of individual tree crowns in high spatial resolution aerial images by multiple-scale analysis. *Machine Vision and Applications*, 11:64–73.

Brandtberg, T., Warner, T. A., Landenberger, R. E., and McGraw, J. B. 2003. Detection and analysis of individual leaf-off tree crowns in small footprint, high sampling density lidar data from the eastern deciduous forest in north america. *Remote Sensing of Environment*, 85(3):290–303.

Dralle, K. and Rudemo, M. 1997. Automatic estimation of individual tree positions from aerial photos. *Canadian Journal of Forest Research*, 27:1728–1736.

Gougeon, F. A. 1995. A crown–following approach to the automatic delineation of individual tree crowns in high spatial resolution aerial images. *Canadian Journal of Remote Sensing*, 21(3):274–284.

Larsen, M. and Rudemo, M. 1998. Optimizing templates for finding trees in aerial photographs. *Pattern Recognition Letters*, 19(12):1153–1162.

Larsen, M. and Rudemo, M. 2004. Approximate bayesian estimation of a 3d point pattern from multiple views. *Pattern Recognition Letters*, 25(12):1359–1368.

Næsset, E. and Bjerknes, K.-O. 2001. Estimating tree heights and number of stems in young forest stands using airborne laser scanner data. *Remote Sensing of Environment*, 78(3):328–340.

Tarp-Johansen, M. J. 2002. Stem diameter estimation from aerial photographs. *Scandinavian Journal of Forest Research*, 17:369–376.

A DIRECTIONAL VARIANT OF THE LOCAL MAXIMUM FILTER FOR STAND DENSITY ESTIMATION FROM IKONOS IMAGERY

Lieven P.C. Verbeke[a], Frieke M. B. Van Coillie[a] and Robert R. De Wulf[a]

[a] Laboratory of Forest Management and Spatial Information Techniques,
Coupure Links 653, 9000 Gent, Belgium. email: Lieven.Verbeke@Ugent.be

ABSTRACT

A new technique for deriving stand density from remotely sensed imagery is presented. First, an artificial stand generation model was developed in order to illustrate the importance of viewing direction. Then, artificially generated stands were used to develop a new directional filter technique for identifying local brightness minima and maxima. Statistics derived from the distances between consecutive maxima embracing a minimum were then investigated to establish a relationship with stand density. Once this relationship was established for artificial imagery, the new method was tested on selected study sites in Flanders, Belgium. Both IKONOS imagery and a scanned aerial photograph with a 1m spatial resolution, together with manually digitized and field inventory data were used to evaluate the new technique. It was found that the relationship derived from artificial imagery holds for real images. Also, a directional local filter yielded higher coefficients of determination (0.752 and 0.886 for the IKONOS image and the aerial photograph respectively) when compared to the results obtained from the local maximum filter method (0.625 and 0.833 respectively).

Keywords: Stand density, artificial stands, local maximum, IKONOS, forest inventory

1 INTRODUCTION

Stand density, expressed as the number of trees per unit area, is an important forest management statistic. Most often it is assessed with large scale forest inventories in the field. Given the cost (in terms of human resources and time) of field excursions, remote sensing has always been regarded an attractive alternative tool for automating or facilitating forest inventories. The problem of stand density estimation is closely related to tree crown delineation or individual tree identification (location). The latter aim at locating and describing individual trees whereas the former breaks down to estimating an area property. Individual tree detection and crown delineation has been performed using a variety of techniques of which local maximum filtering (Wulder *et al.*, 2000) and valley following (Gougeon, 1995, Leckie *et al.*, 2003) are typical examples. Yet these methods assume that tree tops show maximum local reflectance, or that individual trees are surrounded by shadow valleys. As is demonstrated below using cross profiles, this is not always the case. A new variant of the local maximum filtering technique is therefore developed, producing stand density estimates without having to locate individual tree tops. The method presented is similar to assessing stand density using directional variograms, as introduced by St-Onge and Cavayas (1997).

2 METHOD

The derivation of the new method is largely based on the use of artificially generated stands and therefore this issue is introduced first. Secondly, it will be motivated and demonstrated why viewing geometry is important for tree identification, followed by a discussion of a method to find directional local minima and maxima. Then, the statistics of the distances between consecutive maxima (or minima) are discussed. Finally, the local maximum filter is presented as a means of comparing the algorithm's performance with a more conventional method.

2.1 ARTIFICIAL STAND GENERATION

Artificial stands contain artificial trees with properties drawn from probability distributions. Tree crowns are assumed dilated spheres that can intersect with each other. An overview of the parameters used and the associated distributions can be found in Table 1. The parameters of the distributions are set according to the type of stand to be generated. Depending on the parameter, minimum and maximum thresholds are set to avoid the generation of unrealistic trees.

Table 1. . Parameters, distribution and values used for artificial stand generation

Parameter	Distribution / value
(positionX,positionY)	Uniform
Crown diameter	Normal
Allowed overlap between two crowns (in terms of diameter)	Uniform
Crown height	Normal
Stem height	Normal
Sun azimuth	180° (South)
Sun elevation	26.5°
Viewing azimuth	180°

Stand generation is a two stage process. First of all, a sequence of trees is generated. It is checked if each tree can be added to the artificial stand without violating the overlap conditions. Once a fixed number of consecutive invalid (i.e. violating overlap conditions) trees are found, the stand is assumed to be completely filled with trees. The second step consists of rendering the artificial stand using ray-tracing software. Here the freely available package POV-Ray version 3.6 (Persistence of Vision Pty. Ltd., 2004) was used. Illumination and viewing geometry are shown in Table 1.

The use of simulated remotely sensed imagery derived from artificially generated tree stands offers several advantages. Firstly, the resulting images are not disturbed by atmospheric or sensor noise. Secondly, the need for validation data is alleviated since stand parameters are known in advance. Finally, there is total control over illumination conditions and image resolution. There is ample room for improvement on the stand generation and rendering algorithm. It is assumed however that the stand model presented here shares basic geometrical properties with real life forest stands. If an algorithm would perform poorly on images produced with the simplest of models, it will almost certainly fail to work on images derived from more realistic yet complicated models.
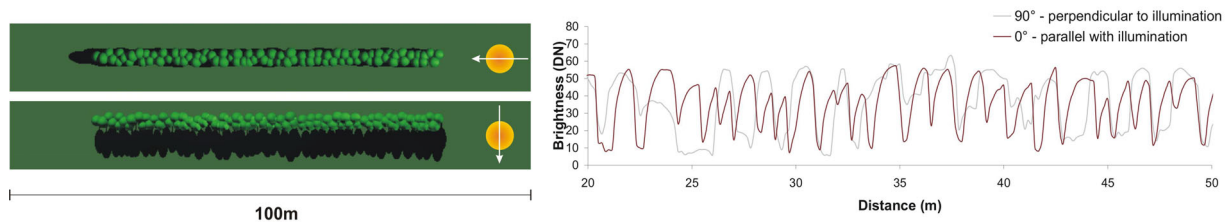
Figure 1. Artificially generated tree lanes under different illumination conditions (parallel / perpendicular) and part of the corresponding cross profiles

2.2 RATIONALE FOR LOOKING IN A SINGLE DIRECTION

In order to assess the importance of viewing geometry, two identical artificial tree lanes were rendered under different illumination conditions (Figure 1). Then, cross profiles respectively parallel with and perpendicular to the illumination angle were constructed. For the sake of clarity, only part of these cross profiles is shown in Figure 1. From the profiles it can be seen that looking parallel to the illumination azimuth allows for individual tree identification, whereas looking perpendicular to the illumination azimuth results in a cross profile with reduced brightness dynamics, even including the 'loss' of trees in the profile.

The rationale of this study is that especially when both spatial and radiometric resolutions are limited and the suns elevation is low, looking perpendicular to the illumination azimuth may disturb further analysis. On the other hand, when spatial and radiometric resolutions are sufficiently high and with higher sun elevations, one might actually benefit from including both viewing directions in the analysis, since these two viewing directions then produce profiles with the largest amount of uncorrelated information possible.

2.3 FINDING DIRECTIONAL LOCAL MINIMA AND MAXIMA

Analogous to the local maximum filter (LMF), a directional local filtering (DLF) technique is presented. Following the argumentation of the previous section, filtering only takes place in one-dimensional

windows (lines) of fixed length. Both local minima and maxima are identified. Two examples of this type of filtering are shown in Figure 2. The DLF and the LMF techniques are compared for an artificially generated stand and part of a 50cm resolution scanned aerial photograph respectively, with the filter direction parallel with the illumination azimuth.
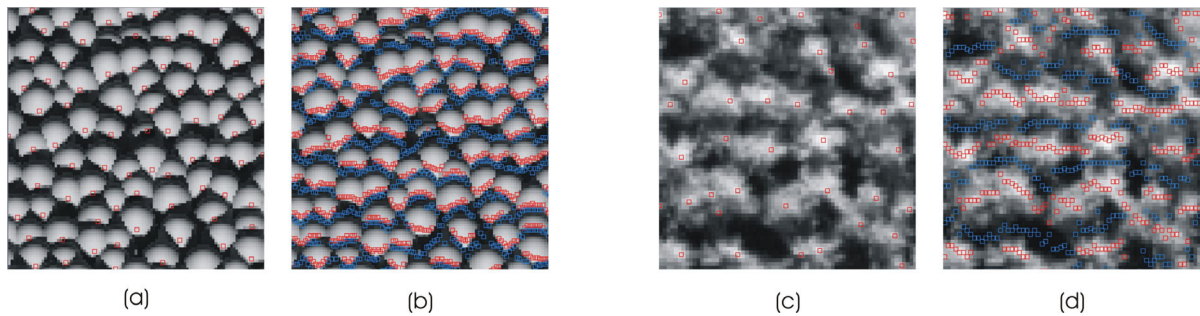

(a)   (b)   (c)   (d)

Figure 2. Comparison between local maximum and directional local filtering (maxima: red, minima: blue). (a) LMF artificial stand (b) DLF artificial stand (c) LMF aerial photograph (d) DLF aerial photograph

2.4 STATISTICS DERIVED FROM DIRECTIONAL LOCAL MINIMA AND MAXIMA

Once the minima and maxima are identified, the distances between all two consecutive maxima embracing a single minimum are collected. To demonstrate how the statistics and distribution of the collected distances relate to stand density, the histograms of the distances and the relation between stand density and average distance are given in Figure 3. To construct this figure, respectively three and seven artificially stands were generated according to the procedure described before. As can be clearly seen from the left part of Figure 3, stand density strongly influences the shape and size of the histograms. Stands with more trees per hectare tend to have sharper and narrower histograms with a higher maximal frequency situated closer to zero. The right part of Figure 3 demonstrates that there exists an almost perfectly linear relationship ($R^2 = 0.966$) between the average of the collected distances and the natural logarithm of the stand density. Thus, the mean distance between two maxima embracing a minimum could be used as an explanatory variable for stand density estimation.

Although the relationship between average distance and stand density here is almost perfect, the regression line in Figure 3 will probably not be useful for real life density estimates. The average distances and the histograms also depend on the crown closure of the stands under investigation. Future research will focus, as in St-Onge and Cavayas (1997), on generating artificial stands as a function of both stand density and crown closure, and on how the derived statistics can be linked to real life stand properties. As for now, it is assumed that, the relationship between stand density and the mean distance is approximately logarithmic.
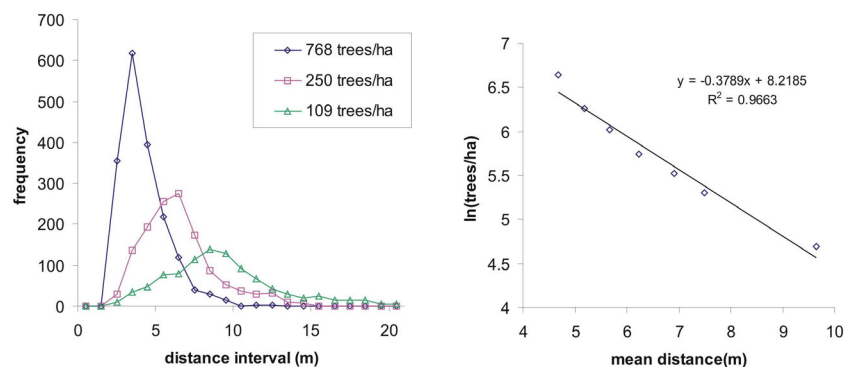
Figure 3. Histograms and relation between stand density and mean distance between consecutive maxima for respectively three and seven artificially generated stands with different tree densities

2.5 ACCURACY ASSESSMENT

In order to assess the performance of the newly derived method, a comparison with a non-directional method is needed. We used the local maximum filter for this purpose. The window size of the MLF is fixed to the size yielding the best possible overall performance after an extensive trial and error process. Also, we did not use the number of local maxima per hectare as an estimate for stand density, but rather investigated how strong this number is related with true stand density. Finally, in order to reach the best possible MLF results, logarithmic transformations were used for both the true stand density and the number of maxima per hectare. The method yielding the strongest relationship between the explanatory variable and the true stand density (in terms of R^2) can then be considered the best performing method.

3 MATERIALS

The panchromatic 1m resolution IKONOS image used in this study is part of the global very high resolution coverage of the Flemish territory. All image data were geo-radiometrically corrected and mosaiced by the image supplier. The extract from the global coverage used here consists of a mosaic of three images, recorded in the course of summer 2002. Unfortunately, some problems are associated with the image data. Firstly, in the process of creating the mosaic, image histograms were matched. An unwelcome consequence of histogram matching is the reduction of brightness dynamics due to the presence of clouds. A smaller dynamic range will render the tree detection / counting a more difficult task, although in this case, it may help demonstrating the added value of the new method. Secondly, the image contains severe artifacts under the form of the image being systematically unsharp on a grid with a period of approximately 50m. Because of the problems discovered in the IKONOS imagery, a very high resolution aerial photograph (scale 1:5000, October 1987, Heverlee, Belgium) was scanned, georeferenced and resampled to obtain a high quality, very high resolution (25cm) grey-scaled image. Then the scanned image was degraded to the same spatial resolution as the IKONOS panchromatic band, producing a high quality, 1m resolution image.

To assess the performance of the newly developed method, reference data was collected in two ways. Firstly, a database containing the field data recorded during the latest extensive Flemish Forest Inventory (Afdeling Bos en Groen, 2001) provided information on tree species, stand density and numerous other variables for a systematic grid of circular plots located in the whole of Flanders, Belgium. The database was used to evaluate algorithm performance on IKONOS imagery. In total, 16 sample plots embedded in a sufficiently large forest stand and contained in the available IKONOS imagery could be selected. Since only trees in the upper story can be identified by the algorithms under study, the stand density derived from the database was adjusted to exclude lower story trees. This was possible because the forest inventory database keeps track of the story individual trees in a sample plot belong to. Secondly, to evaluate algorithm performance on an older scanned aerial photograph, tree tops were manually digitized in 20 selected polygons spanning a range of tree densities. This was done on the 25cm resolution scan, on which individual trees could be easily identified. In total, 3161 tree tops were digitized.

4 RESULTS AND DISCUSSION

For the IKONOS and the aerial photographs, a filter length of 7 pixels was used for the DLF technique. For the LMF method, the window size yielding the best relationship was found to be 5 pixels by 5 pixels. As explanatory variables, the natural logarithm of the number of maxima per hectare and the average distance between maxima embracing a minimum were used for LMF and DLF respectively. For the IKONOS image, distances were collected parallel with the illumination azimuth whereas for the scanned aerial photograph, distances were collected both parallel with and perpendicular to the illumination azimuth. The latter is motivated by the high radiometric quality of the image; perpendicular measurements here are assumed to yield additional information on the true distance distribution. The resulting relationships between the explanatory variables and the number of trees per hectare are displayed in Figure 4.

Several observations can be made from Figure 4. For both the IKONOS image and the aerial photograph, the DLF technique outperforms the LMF technique. Coefficients of determination are, for the IKONOS image and the aerial photographs respectively, 0.625 and 0.833 for LMF and 0.752 and 0.886 for DLF. Also, it can be seen that the approximately linear relationship between the average distance and ln(trees/ha) derived on artificial imagery is confirmed. Finally, the results from the IKONOS image are worse then those from the aerial photograph. This could be explained by (1) image quality, (2) violations

of the assumptions that the sample plots used as reference data are representative for their immediate surroundings, (3) the fact that the ground truth digitized on the scanned aerial photograph is truly representative for the number of upper story trees, whereas for the ground truth derived from the inventory database, this can not be guaranteed and (4) species composition: the IKONOS scene contains a mix of primarily conifers and some broadleaves, whereas the aerial photograph contains solely conifers.
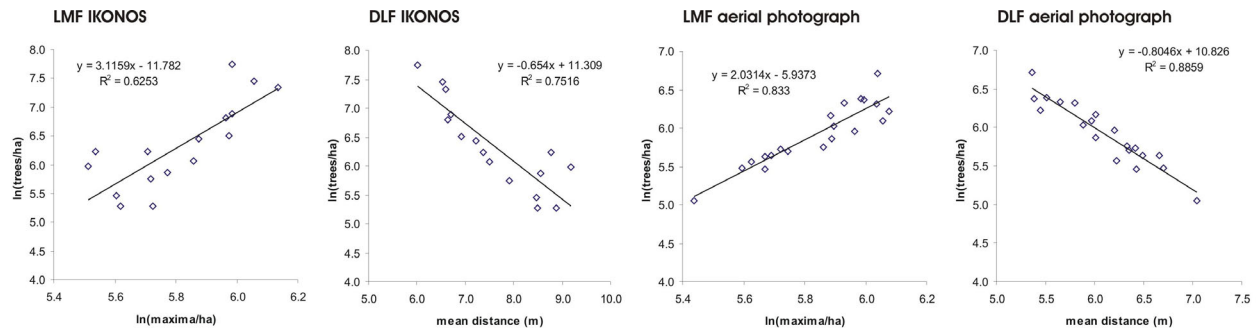

Figure 4. Resulting relations between the explanatory variable and ln(trees/ha) for the LMF and DLF methods and two image types (1m resolution)

5 CONCLUSIONS

The aim of this study was to develop a new method that allows for stand density estimation. To achieve this goal, a simple artificial stand model was first developed. Generation of artificial stands proved useful for demonstrating the basic ideas of this work, as well as for deriving the empirical relationship between stand density and an explanatory variable. After generating a series of artificial stands with different stand density, the latter was chosen to be the mean distance between local directional maxima embracing a minimum. Two types of images, IKONOS data and a scanned aerial photograph, were used to evaluate the new method. It was found that the directional local filtering technique yielded better relationships (in terms of coefficients of determination) when compared with the local maximum filter. Also, it was observed that with a better image quality, a stronger the relationship is found.

The method presented could be implemented for real life stand density estimation by first constructing the relationship between average distances and stand density for a number of representative stands with known stand density, and than processing a large number of stands with unknown tree densities. Future research will focus on improving stand density estimates using additional statistics, improving the artificial stand model, relating natural stand properties to artificial stand properties and the estimation of stand parameters other than stand density. Also, the importance of image resolution will be assessed.

ACKNOWLEDGMENTS

REFERENCES

Afdeling Bos en Groen 2001. De Bosinventarisatie Van Het Vlaamse Gewest. Resultaten Van de Eerste Inventarisatie 1997–1999. Ministerie van de Vlaamse Gemeenschap.

Gougeon, F.A. 1995. A crown-following approach to the automatic delineation of individual tree crowns in high spatial resolution aerial images. *Canadian Journal of Remote Sensing*, 21:274-284.

Leckie, D. G., Gougeon, F. A., Walsworth, N. and Paradine, D. 2003. Stand delineation and composition estimation using semi-automated individual tree crown analysis. *Remote Sensing of Environment*, 85:355-369.

Persistence of Vision Pty. Ltd. 2004. Persistence of Vision (TM) Raytracer. Persistence of Vision Pty. Ltd., Williamstown, Victoria, Australia. http://www.povray.org

St-Onge, B. and Cavayas, F. 1997. Automated forest structure mapping from high resolution imagery based on directional semivariogram estimates. *Remote Sensing of Environment*, 61: 82-95

Wulder, M., Niemann, K. O. And Goodenough, G. D. 2000. Local maximum filtering for the extraction of tree locations and basal area from high spatial resolution imagery. *Remote Sensing of Environment*, 73:103-114.

MEASUREMENTS AT TREE LEVEL USING CARABAS-II

B. Hallberg[a], G. Smith-Jonforsen[a] and L. M. H. Ulander[b]

[a] Chalmers University of Technology, Dept. of Radio and Space Science, Göteborg, Sweden,
email: hallberg@rss.chalmers.se
[b] Swedish Defence Research Agency, Dept. of Radar Systems, Linköping, Sweden

ABSTRACT

In this study, multiple synthetic-aperture radar images acquired with the airborne CARABAS-II VHF system have been used in order to study the possibilities to make measurements on individual trees in coniferous forests. Images over the same area from eight different flight tracks were available. The flight tracks were laid our in a star shaped pattern round the image centre with 45° separation between adjacent tracks. In this way it is possible to extend the aperture angle of the synthetic array by means of a coherent combination of the images. Thereby the spatial resolution of the system is expected to improve to a level where single trees can be resolved. Signal-to-noise ratio is also expected to increase when images are combined, which would improve the possibilities to identify single trees. In a previous and similar study, high correlation between coherently combined CARABAS images and ground-measured stem size of individual trees has been found when trees are standing on relatively flat ground. In this study however images over a more sloping ground was analysed. The results presented in this study do not show as good results as in the case of flat ground, indicating that the combination CARABAS images is more complicated in topographic areas.

Keywords: Synthetic-aperture radar, VHF, forestry, individual trees.

1 INTRODUCTION

Synthetic-aperture radar (SAR) is an active remote-sensing technique capable of providing high-resolution radar images independent of sunlight and weather conditions. During the last decades, several studies have investigated the possibilities to use SAR for estimation of forest parameters such as stem volume, which is an important parameter for the forest industry and their planning of e.g. thinning and harvesting. Traditionally, these measurements have been carried out by highly costly and labour intensive field inventories. SAR can assist these inventories in a cost-effective way due to its capability to cover large areas at low cost.

In addition to stem volume estimation, the possibility to use different remote sensing techniques to resolve and make measurements on individual stems has recently been studied. Data at individual tree level is important in cost-benefit calculations that are done prior to harvest. The techniques that have been studied are e.g. airborne laser-scanning (Persson *et al.*, 2002) and automatic interpretation of high-resolution aerial photos (Pouliot *et al.*, 2002). Promising results have been shown, yet drawbacks exist such as the relative high cost per area for laser-scanning and problems with low contrast between tree crown and understorey in optical images.

CARABAS is an airborne VHF SAR system that has shown to be able to measure stem volume with high precision and with no signs of saturation of backscattered signal up to the highest stem volume measured which is 900 m³/ha (Melon *et al.* 2001). The relatively low frequencies (20–90 MHz) used by CARABAS implies very low attenuation through the canopy and that the main backscattering from forested areas comes from a dihedral ground-stem scattering mechanism (Smith and Ulander, 2000) even on a moderately sloping ground (Smith-Jonforsen *et al.*, 2005). This mechanism has a scattering centre located near the ground stem junction and therefore resolved trees in CARABAS images can be seen as point-objects. However, the spatial resolution of CARABAS is approx. 3×3 m², i.e. in the same order as stem separation in mature forests, and therefore individual stems are not always resolved in the radar image. In addition, noise in the radar images obstructs the possibilities to identify individual trees. By moderate improvements of spatial and radiometric resolution, however, it is expected that more trees would become resolved. These improvements can be done by combining different CARABAS images acquired over the same area.

In a previous study (Hallberg *et al.*, 2003), (Hallberg, 2004), (Hallberg, *et al.*, 2005), multiple CARABAS images were used in order to study the possibilities to resolve single trees in boreal forests. It was found that both spatial and radiometric resolution could be improved by a coherent combination of radar images acquired with different look directions to the imaged area. It was also found that larger trees were easily detected visually in the combined images and that there was a good correlation between stem volume of individual trees and radar-image amplitude for stems with a diameter larger than approximately 200 mm. The forested area was, however, relatively flat and it was not studied how topography may affect the possibilities to improve image quality by a combination of images.

In this study, CARABAS images acquired over a more topographic area are combined and compared with ground measurements of stem sizes of individual trees in order to study the effects of topography on image quality.

2 EXPERIMENTAL DATA

2.1 TEST-SITE CHARACTERISATION

The forested area studied here is located close to the small lake Ämten (lat. 58° 37' N, long. 15° 33' E) near Linköping, southern Sweden. The forest is dominated by Scots pine (*Pinus sylvestris*) and Norway spruce (*Picea abies*). The area is relatively topographic with height variations of approximately 5 m over a length-scale of 100 m. Large boulders also exist in the area

2.2 GROUND MEASUREMENTS

Ground measurements were done in February 2004. In the area, 40 sample plots where laid out in harvest-ready stands. At each sample plot, the diameter at breast height (dbh), i.e. 1.3 m above ground, was measured for every tree within a radius of 10 m from the sample-plot centre. The position of each tree was measured relative to respective plot centre by means of measuring tape and angle decoder. Also, the tree species was recorded. Furthermore, for a limited number of trees (approx. 10%), the height was measured. The total number of measured trees was 645.

The position of every plot centre was measured by means of differential GPS. In this way, a position estimate of every tree could be derived. The GPS measurements were first done before the harvest. However, it was later believed that the quality of the position estimate was affected by the fact that the GPS signal had to travel through the canopy. Therefore, new measurements were performed in September 2004 after harvesting of the stands in question.

2.3 SAR DATA

CARABAS-II is the second generation ultra-wideband low frequency SAR (Hellsten *et al.*, 1996), (Hellsten *et al.*, 2000). It has been developed by the Swedish Defence Research Agency (FOI) and is mounted in a Sabreliner small business jet. It uses essentially horizontal polarisation on both transceiver and receive (HH) in the frequency range 20–90 MHz. Typical resolution achieved in the slant-range plane is 3 m in both the range and azimuth direction. The high azimuth resolution is achieved by employing a wide Doppler cone angle of typical ±35°.

Radar data was collected in November 2003. Images from eight different flight tracks were available. The flight tracks were planned around an aim-point in the centre of the area in such a way that the aspect angle towards the aim-point was shifted 45° degrees between adjacent tracks. Transmitted bandwidth was 22–82 MHz and the processed Doppler cone angle was 60° for all images expect one where the Doppler cone angle was limited to 40° due to accidental loss of data. Incidence angle to the study area was typically 65° for all tracks. The SAR data were focused by a global back-projection scheme and consequently projected onto a coarse digital elevation model (DEM) (50×50 m^2 resolution) using a phase preserving interpolation algorithm.

3 THEORY

In this section it is shown how the spatial resolution can be improved by a coherent combination of CARABAS images acquired with different look-directions to the imaged area.

Unlike narrow beam-width SAR systems, the resolution of CARABAS can not be separated in azimuth and range directions. Therefore, a resolution area ΔA has been proposed as an adequate measure of resolution (Ulander and Hellsten, 1996) which is defined as

$$\Delta A = \frac{\int |a(x,y)|^2 \, dx \, dy}{|a(0,0)|^2} \, ,$$

(1)

where $a(x,y)$ is the system impulse response with its assumed peak located at (0,0). The best possible resolution was derived as

$$\Delta A_{min} = \frac{\lambda_c}{2\Delta\vartheta} \frac{c}{2B} \, ,$$

(2)

where λ_c is the wavelength at the centre frequency, $\Delta\vartheta$ is the aperture angle, c is the speed of propagation and B is the bandwidth of the transmitted pulse. As seen, the resolution area is inversely dependent on aperture angle. By a coherent combination of images with different look directions to the imaged area, the aperture angle can be extended to a maximum of 360°. For the images used here, it would mean that the best theoretical ground-range resolution-area would improve from approx. 8 m^2 to 1.3 m^2. The spatial resolution in an incoherent combination would, however, be unaffected.

In order to improve the resolution of imaged trees, the phase characteristics of the scattering mechanism must be azimuthally isotropic. The scattering has been modeled as dielectric cylinders on a flat sloping ground (Smith- Jonforsen, *et al.*, 2005). Then it can be shown that the main backscattering comes from a ground-trunk dihedral bounce and as long as the wavelength is much longer than the diameter of the trunk, the phase scattering of this mechanism is located near the ground-stem junction. Thus, the phase characteristic is constant over different look-angles. The characteristics of a stem standing on topographic ground are more complicated and further investigations into this topic is on-going.

4 METHOD

Due to small errors in the DEM used in the ground-range projection scheme, the images had to be spatially co-registered before they could be combined. The spatial co-registration was done by maximising the contrast of an incoherent combination of the images. The contrast measure used was the normalised standard deviation of the image intensity (Berizzi and Corsini, 1996). The scheme resulted in offset compensations of approx. 1–3 m. Secondly; an unknown phase offset between the images had to be compensated. The compensation phase was estimated by maximising the contrast of a coherent combination of the images. The method is described in more detail in (Hallberg, *et al.*, 2005).

From the co-registered images both an incoherent and coherent combination can be formed. The incoherent combination was formed in a similar way as multi-looking i.e. pixel-wise mean value of image intensity (Oliver and Queagan, 1998), while the coherent combination was formed as the pixel-wise complex mean value.

5 RESULTS

The eight images were co-registered and combined using the method described in the previous section. The combined images were subsequently oversampled to 6 × 6 pixels/m^2. Since it was believed that the centre position of plots had some residual error, the position of the ground measurements where spatially co-registered to the radar data. The co-registration was done by maximizing the cross-correlation between the radar amplitude-image in the incoherent combination and the square of ground measured dbh. In this way each plot-sample centre was moved with a constrained maximum length of ±5 m in each direction.

After co-registration, the combined images were compared with the ground measured tree positions. Fig. 1 shows both incoherent and coherent image examples from two plots which were randomly chosen from the 40 plots. From all plots inspected, it can generally be said that the incoherent combination shows some (väldigt vagt– kan du skärpa formuleringen? Igår nämndes siffran 50% av plottarna visade på dålig correlation?) correlation between radar data and ground measurements. That also holds for the coherent combination, although high sidelobes are visible.
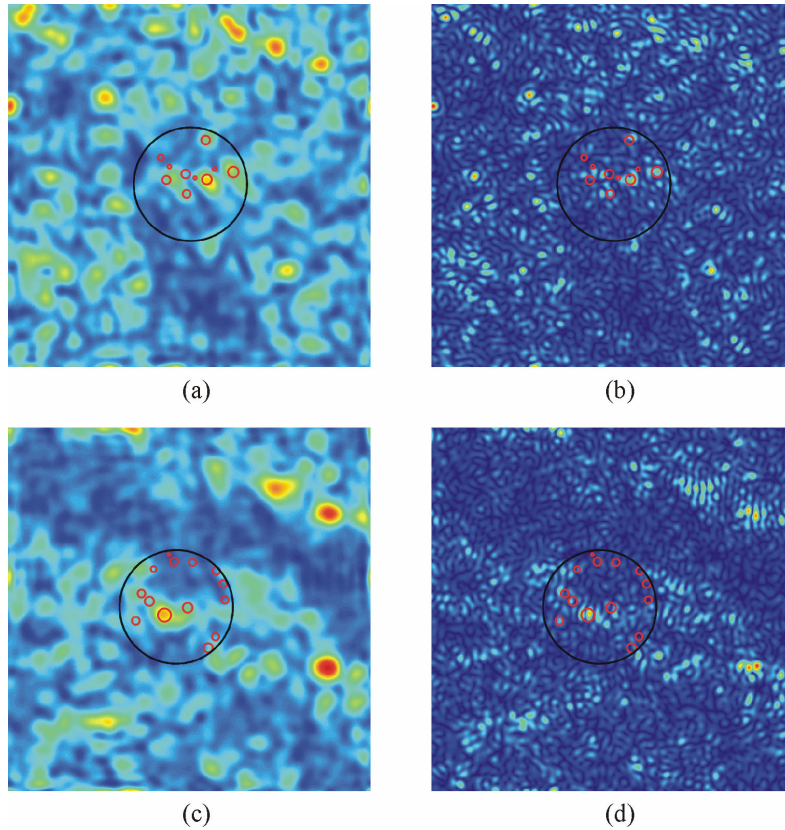
Figure 1. Examples of combined CARABAS amplitude-images. Panel **a** and **c** is an incoherent combination from two different plots. Panel **c** and **d** is corresponding images from a coherent combination. The black circles indicate the 10 m radius sample plot and red circles indicate position and size of ground measured trees. Image sizes are 64×64 m^2.

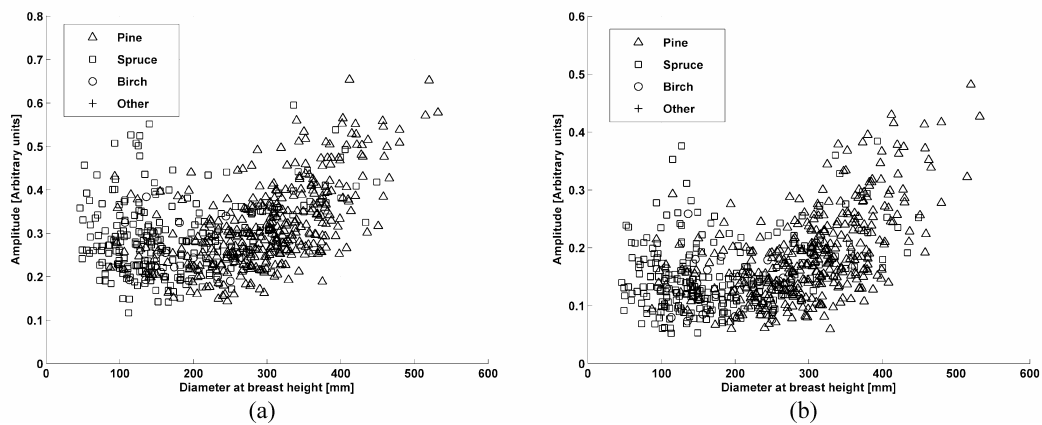**Figure 2.** Scattering amplitude plotted against ground measured stem diameters for 645 trees. Panel **a** shows the results from an incoherent combination whilst panel **b** is from a coherent combination. In both cases, correlation is visible for stem diameter > 200 mm.

The analysis was continued by extracting the pixel amplitude corresponding to the ground measured tree position. The extraction was done by picking out the maximum amplitude value within a 7×7 pixel box (approximately 1×1 m^2) centred at the ground measured position. Fig. 2 shows the stem diameter of individual trees plotted against extracted CARABAS image amplitude from a coherent and incoherent combination respectively. In both cases, some correlation exists for stems with a diameter greater than approximately 200 mm.

To examine whether the matching scheme resulted in an over-fitting of the data, a simple test was performed. In this test, each sample-plot centre was moved 20 m in some direction before it was automatically matched to the image data (with a maximum constrained shift of ±5 m in each direction). In

this case, no or very little correlation was found between image amplitude and stem diameter. It is therefore likely that the correlation seen in Fig. 2, is not a result of over-fitting.

6 DISCUSSION AND CONCLUSIONS

In (Hallberg, 2004), eight CARABAS images over forested areas with relatively little topography were successfully combined, both incoherently and coherently. In this study however, the coherent combination shows quite irresolute results with high sidelobes visible in the images. Also the incoherent combination in this study show less contrast compared to the previous study. It is believed that this is due to the topography of the area studied here. Height variations can affect the quality of combined images in two ways. First, large-scale topography, together with DEM inaccuracies, can complicate the image co-registration scheme, implying that a spatial image shift must be estimated over smaller spatial subsets. Secondly, small scale topography (within the first Fresnel zone of the ground reflection point) deteriorates the azimuthal isotropy of the scattering mechanisms causing the quality of the combined images to decrease. It is however still unclear to what extent height variations affect the image quality and to fully understand these mechanisms may require rigorous electromagnetic modelling.

Despite these problems, correlation between stem diameter and image amplitude was found for larger trees. The sensitivity threshold for stem diameters as estimated from Fig. 2 is approximately 200 mm. This agrees quite well with other studies (Hallberg, *et al.*, 2005), though the number of images used there was fifteen in a coherent combination instead of, in this case, eight in an incoherent combination.

ACKNOWLEDGMENTS

REFERENCES

Berizzi, F. and Corsini, G. 1996. Autofocusing of inverse synthetic aperture radar images using contrast optimization. *IEEE Trans. Aerospace and Electronoc Systems*, Vol. 32, No. 3, pp. 1185–1191.

Fransson, J. E. S., Walter, F. and Ulander, L. M. H. 2000. Estimation of forest parameters using CARABAS-II VHF SAR data. *IEEE Trans. Geosci. Remote Sensing*, Vol. 38, No. 2, pp. 720–727.

Hallberg, B., Smith-Jonforsen, G. and Ulander, L. M. H. 2005. Measurements on individual trees using multiple VHF SAR images. Submitted to *IEEE Trans. Geosci. Remote Sensing*.

Hallberg, B. Smith, G. Ulander L. M. H. and Frölind P.-O. 2003. Individual tree detection using CARABAS-II. In *Proc. IGARSS'03*, Toulouse, France, Jul. 21–25, Vol. 3, pp. 1639–1641.

Hallberg, B. 2004. Forest imaging using synthetic-aperture radar in VHF and P band. Technical report No. 501L, Department of Radio and Space Science, Chalmers University of Technology, Sweden.

Hellsten, H., Ulander, L . M. H., Gustavsson, A. and Larsson, B. 1996. Development of VHF CARABAS II SAR. In *Proc. Radar Sensor Technology*, *SPIE*, Vol. 2747, Orlando, FL, USA, Apr. 8–9, pp. 48–60.

Hellsten, H., Ulander, L. and Taylor, J. D. 2000. The CARABAS II VHF synthetic aperture radar. In *Ultra-wideband radar technology*, Taylor, E. D. Ed. London, USA: CRC Press, pp. 329–343.

Melon, P., Martinez, J. M., Le Toan, T., Ulander, L. M. H., Beaudoin, A. 2001. On the retrieving of forest stem volume from VHF SAR data: observation and modelling. *IEEE Trans. Geosci. Remote Sensing*, Vol. 39, No 11, pp. 2364–2372.

Oliver, C. and Quegan, S. 1998. Understanding synthetic aperture radar images. Artech House Publishers, pp. 93–96.

Persson, Å., Holmgen, J. and Söderman U. 2002. Detecting and measuring individual trees using an airborne laser scanner. *Photogrammetric Engineering and Remote Sensing*, Vol. 68, No. 9, pp. 925–932.

Pouliot, D. A., King, D. J., Bell, F. W. and Pitt, D. G. 2002. Automated tree crown detection and delineation in high-resolution digital camera imagery of coniferous forest regeneration. *Remote Sensing of Environment*, Vol. 82, No. 2–3, pp. 322–334.

Smith, G., Ulander, L. M. H. 2000. A model relating VHF-band backscatter to stem volume of coniferous boreal forest. *IEEE Trans. Geosci. Remote Sensing*, Vol. 38, No, pp. 728–740.

Smith-Jonforsen, G., Ulander, L. M. H. and Luo, X. 2005. Low frequency scattering of coniferous forests on sloping terrain. Submitted to *IEEE Trans. Geosci. Remote Sensing*.

Ulander, L. M. H. and Hellsten, H. 1996. A new formula for SAR spatial resolution. *AEÜ Int. J. Electron. Commun.*, Vol. 50, No. 2, pp. 117–121.

SIBERIA-II: MULTI-SENSOR LAND COVER PRODUCTS FOR GREENHOUSE GAS ACCOUNTING OF NORTHERN EURASIA

C. Schmullius[a], C. Beer[a], R. Gerlach[a], S. Hese[a], D. Knorr[a], M. Santoro[a], L. Skinner[b] and A. Luckman[b]

[a] Department for Geoinformatics and Earth Observation, Friedrich-Schiller-University, 07743 Jena, Germany, email: c.schmullius@uni-jena.de
[b] University of Wales, Swansea, U.K.

ABSTRACT

In the SIBERIA-II Project the synergy between multi-sensor Earth Observation products and ecological regional models is investigated to assess the impact of terrestrial biota on the budget of major greenhouse gases (GHGs) in a 3 Million km^2 area in Central Siberia. EO-products not only represent the input to the ecological models but also serve to improve knowledge on several indicators. In this sense two fundamental products obtained in SIBERIA-II are land cover and land cover change in form of Af-,Re-,Deforestation (ARD). By using MODIS data acquired between 2001 and 2004, yearly land cover maps have been obtained with an automatic chain. A comparison with the GLC2000 map showed a good agreement. This product together with a MODIS Vegetation Continuous Fields (VCF) product also represents a significant driver of the GHG calculations through the Dynamic Vegetation Model LPJ. ARD activities are detected using multi-temporal classification of high resolution Landsat TM 5 and ETM data at four test territories comparing the 1989 Kyoto Protocol baseline with the 2000 status. With an object oriented change detection approach based on a primary segmentation it has been possible to detect forest cover changes.

Keywords: SIBERIA-II, land cover, GLC2000, MODIS, VCF, LPJ, DVM, Landsat, ARD.

1 INTRODUCTION

The SIBERIA-II project (http://www.siberia2.uni-jena.de/) has as overall objective to demonstrate the viability of full carbon accounting, including all greenhouse gases, on a regional basis using Earth Observation (EO) products as data source. GHGs predictions are provided by two Dynamic Vegetation Models (DVMs) – the Lund-Potsdam-Jena (LPJ) Model and the Sheffield Dynamic Vegetation Model (SDVM) - and a GIS-based landscape approach developed at the International Institute of Applied Systems Analysis (IIASA). As study area a 3.2 Million km^2 area in Central Siberia (85°-110° E and 55°-75° N) has been chosen, for which a multi-layer GIS (i.e. a ground data information system) at a scale 1:1 Mio has been available. This region is to a high degree isolated from oceanic climate influences and represents a significant part of the Earth's boreal biome, which plays a critical role in global climate. The set of EO-products, which have been obtained by means of a multi-sensor approach, has been defined based on the needs of the accounting schemes and includes among others land cover and land cover change Afforestation/Reforestation/Deforestation (ARD) maps. In this paper we present a summary of the characteristics of the land cover and the ARD products, and describe the impact of land cover on the GHG accounting with particular regard to the LPJ model and the GIS-based landscape approach.

2 LAND COVER

2.1 LAND COVER PRODUCT

The generation of the land cover product is based on an operational, fully automated method. The method has been developed based on MODIS data, but allows the explicit use of additional remote sensing data and ancillary information. For each year between 2001 and 2004 MODIS 8-day temporal composites (MOD09A2, surface reflectance in 7 bands, visible, NIR and SWIR at 500m spatial resolution) were independently classified using imagery from May to October within a C5.0 decision tree classifier. The independent thematic results were then combined using a Bayesian addition (McIver *et al.*, 2001) to create a single land cover map for each year. No further spatial or temporal filtering has been applied.

To meet the requirements of the DVMs users the final choice of the land cover classification scheme was driven by the ability to create a regional product with a consistent set of class definitions. After closer examination the adopted scheme was based upon the GLC2000 classification, thus also allowing a direct comparison between the two products during the validation process. The reference data used to train the classifier has been generated following a stratified sampling approach based on the GLC2000 classification. This approach was preferred to using data from on ground surveys because of the heavy bias of the GIS database available for the project region towards managed forest areas. In this way we ensured a more robust training dataset, where all classes are well represented according to their actual distribution (assuming a high level of accuracy for the GLC2000 product.)
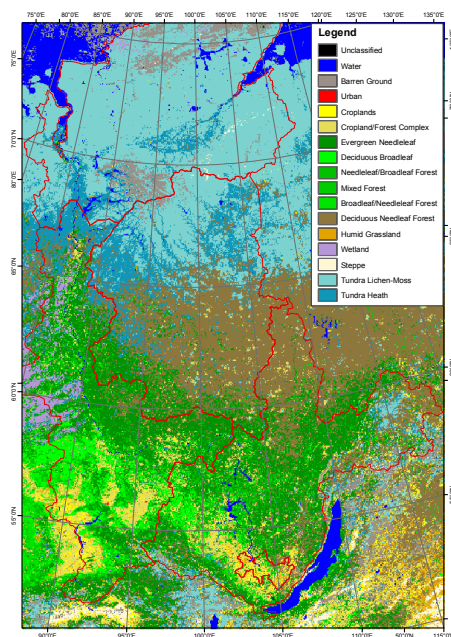
Figure 1. Land cover classification for 2003 based on 8-days MODIS temporal composites.

For the accuracy assessment of the land cover product a two-fold strategy has been implemented. Confusion matrix and kappa coefficient were determined on pixel level for each year (2001–2004) first and then the proportional distribution of classes in a 10x10km raster has been correlated (see Tables 1 and 2). On pixel level significant variation exists due to confusion between the class signatures, differences in resolution (1km vs. 500m resolution) and geolocational mismatches. These effects are being reduced when comparing only the proportion of each class in 10x10 km grid cells. Thus, values in Table 2 represent a more reliable measure of agreement. Nonetheless, uncertainties are high in both the GLC2000 and the SIBERIA-II products. Quantification of error is being prevented by lack of appropriate reference data.

	SIBERIA-II 2001	SIBERIA-II 2002	SIBERIA-II 2003	SIBERIA-II 2004
GLC2000	0,44	0,46	0,43	0,44
SIBERIA-II 2001		0,70	0,65	0,62
SIBERIA-II 2002			0,68	0,65
SIBERIA-II 2003				0,62

Table 1. Kappa coefficients of pixel level comparison.

	SIBERIA-II 2001	SIBERIA-II 2002	SIBERIA-II 2003	SIBERIA-II 2004
GLC2000	0,61	0,63	0,60	0,61
SIBERIA-II 2001		0,91	0,87	0,84
SIBERIA-II 2002			0,88	0,85
SIBERIA-II 2003				0,84

Table 2. Correlation coefficients (R^2) of 10x10km grid comparison.

Generally, it can be stated that the small variations between the independently derived SIBERIA-II products (Tables 1 and 2) have proven the robustness of the classification methodology. The land cover maps are suitable for regional to global scale users likewise the existing land cover products (GLC2000, UMD, IGBP). The higher spatial resolution of the SIBERIA-II products may even provide more detailed information, whereas the topicality of the products is to be seen as an additional advantage. In depth quality assessment of the derived products remains an issue and the availability of reliable validation data has been identified as a major problem.

2.2 LAND COVER AND GHG ACCOUNTING SCHEMES

Previous work has demonstrated shortcomings of traditional classified land covers for an application in a DVM (Beer, 2003). It was shown that a Vegetation Continuous Fields (VCF) product containing the percentage coverage of all Plant Functional Types (PFTs) in the model would be most applicable. For this reason in SIBERIA-II the MODIS VCF product, which contains the percentage coverage of tree canopies and grass is used. Nevertheless, since this product neither distinguishes between the different tree species nor indicates agricultural areas, a surrogate was developed by also using the information about the dominant species provided by the SBERIA-II land cover product. In detail, the information in the MODIS VCF product (500 m pixel size) was aggregated to a 0.5° pixel size as needed by the LPJ-DVM, and in doing so the SIBERIA-II land cover information (500 m pixel size) assisted by allocating dominant tree species to the whole tree coverage in each MODIS pixel. As a result, one map for each PFT was generated storing the percentage coverage of this PFT on a 0.5° grid-cell basis.

These maps were then used as an additional input in the LPJ-DVM. The vegetation is simulated dynamically as before (Sitch *et al.*, 2003) but the max potential area of each PFT is constrained by the indication from the land cover input. In doing so, Net Primary Productivity (NPP) was reduced in Central Siberia (Figure 2a). Results of the land cover constrained model run are well comparable to findings by forest inventory studies of 254 and 305 gC/m²/a in the middle and southern Taiga, respectively (Shvidenko *et al.*, 2001). The improvement in NPP coincides with an improvement in biomass estimates. By incorporating the land cover information these are even halved in many forest regions of Siberia (Figure 2b) and now better comparable to forest inventory findings by IIASA (Shvidenko *et al.*, 2000).

These results demonstrate both the capability of satellite data to support simulation results of a DVM, and the reliability of the LPJ-DVM over vegetated areas. The fraction of a 0.5°x0.5° region that is low or even not vegetated due to topography, water bodies, agriculture or other unfavourable environmental conditions like permafrost, which are not represented by the climate input data, can now be considered during the simulation of dynamic processes by using the additional land cover information.

For the GIS based delineation of Greenhouse Gas Compartments (GGCs), i.e. polygons having the same characteristics concerning pools of carbon and fluxes of CO_2 and CH_4, several EO and ground data sets are needed. Since vegetation and land surface characteristics play a crucial role in the carbon cycle, land cover is a major input parameter for this concept. Giving information about the distribution of vegetation communities (evergreen or broadleaf species, agricultural land, grassland), wetlands, urban regions, water etc., regions of CO_2 and CH_4 emissions to and absorption from the atmosphere can be delineated. This information is input for the two coarser of the three different spatial scales of the GGC concept, namely the regional scale, covering the entire SIBERIA-II study region, and the subregional scale, covering a SIBERIA-II sub-region, namely the Krasnoyarsk Kray. The finest spatial scale is test site based and uses forest inventory data.

3 ARD

In the Kyoto Protocol (KP) carbon emission inventory land cover changes are referred only to areas directly affected by human action through ARD. In SIBERIA-II the objectives of the ARD product are the evaluation and monitoring of Afforestation, Reforestation and Deforestation processes in Siberia for selected test territories with extensive forest enterprise information. The final product is a change map from 1989 to 2000 with change classes referring to temporal definitions of Afforestation, Reforestation and Deforestation (ARD) neglecting the term "human induced" for Reforestation and Afforestation. Additionally other classes are defined in order to exclude specific areas from the overall statistics (clouds, cloud shadows etc.)
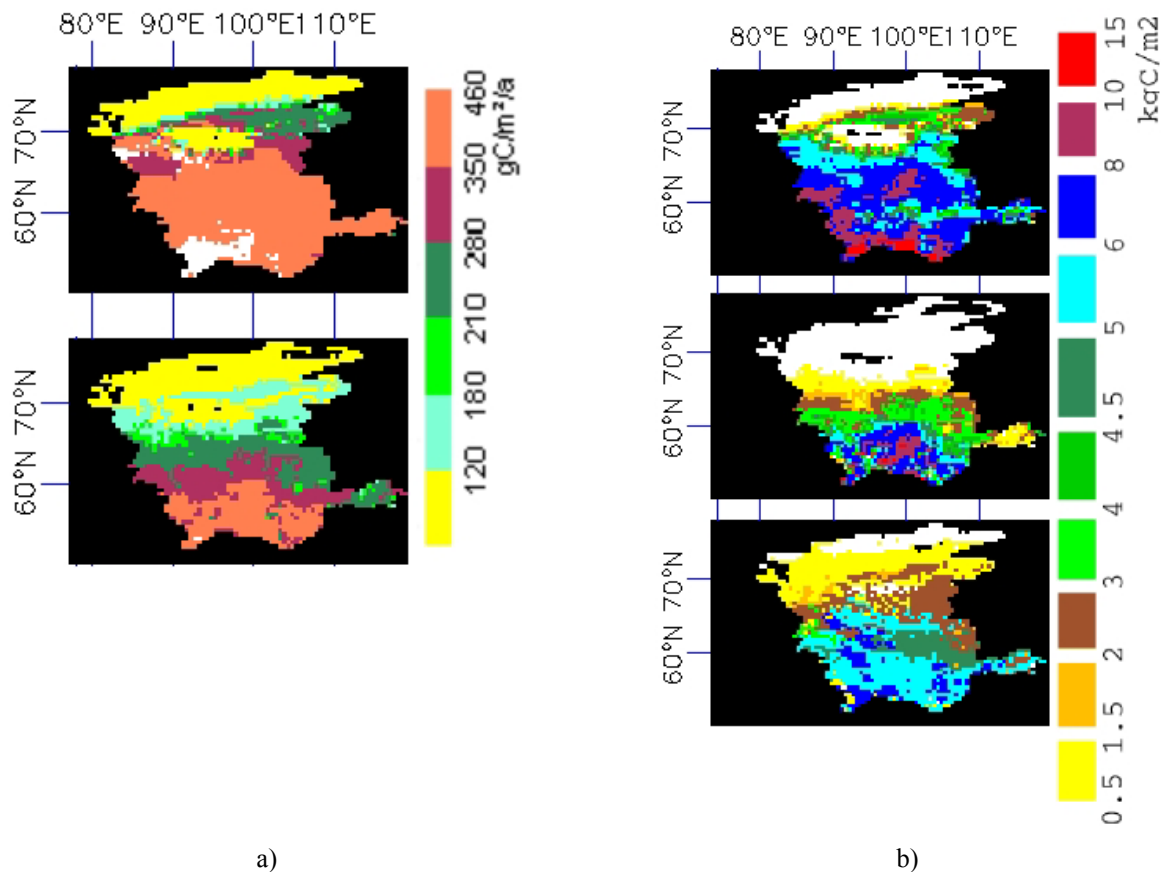
Figure 2. Illustration for the SIBERIA-II study region of a) NPP in gC/m²/a in 2002 obtained from LPJ model runs without land cover (top) and with land cover incorporation (bottom), and b) vegetation carbon density in kgC/m² averaged over 1988-1992 obtained from LPJ model runs without land cover (top), with land cover incorporation (middle) and IIASA forest inventory results (Shvidenko *et al*., 2000) (bottom).

As multi temporal analysis is performed comparing the 1989 baseline with the SIBERIA-II temporal status high resolution multi-temporal Landsat TM 5 and ETM 7 has been used for four test territories. The data is co-registered and atmosphere corrected. Since accumulation of a two-stage classification error complicates the analysis of very small changes, direct two-date change detection is preferred to post-classification.

ARD classification is pursued using a change detection algorithm based on an object-oriented approach. This change detection method makes use of image segmentation information into object primitives and attribution of object characteristics (spectral information, object shape, texture and relations to sub-objects in different scales). Multi-temporal data is segmented into three object layers with different scales. Clouds and cloud shadows are classified using class-related features and ratios of mean spectral object values. The resulting classes are grouped together with the class water and are used as a mask for the supervised classification of ARD and other classes. The "change"-category is differentiated with subclasses that describe "Reforestation" and "Deforestation" using a direct two-date supervised classification approach. Deforestation is subdivided into subclasses "potential_ClearCut" and "potential_FireScar" using shape-features based on polygons of the original segments. Additionally, the relationship to linear objects is analyzed to use context information for the class description. The underlying cause of the deforestation remains nevertheless to a certain degree unclear. A detailed description of the class hierarchy used can be found in (Hese, 2004). Figure 3 illustrates results of ARD classification for the Bolshe-Murtinsky test sites where first area statistics report 5.97 % Reforestation, 9.38 % Deforestation and no Afforestation.

The accuracy assessment is done with independent test sites where ground information is available and updated to 2002 (IIASA GIS for test territories). Compared with traditional classification accuracy analysis one difference is the use of trainings- and test objects (instead of pixels). Depending on the used object scale for the segmentation level the number of objects for evaluation is critical and usually cannot be extended very much. This context and the limited number of polygons from the IIASA test territories lead

to only a small number of reliable trainings and test objects for a classification. The reliability of the accuracy assessment is therefore severely limited. First results from error matrix analysis still indicate problems differentiating clear cuts (user accuracy: 0.92, producer accuracy: 0.39) from fire scar areas (user accuracy: 0.52, producer accuracy: 0.70), although a complex context based approach was used (overall accuracy of the analysed quarter Landsat scene: 0.807 with a KIA of 0.780). It is clear that the features used (object shape) do not flexible classify all characteristics of a specific class, i.e. not all clear cut objects show a high rectangular fit of object shapes. Classifying without the differentiation into fire scars and clear cuts would achieve much better classification accuracy but the potential of object-oriented classification (including shape classification) would not be fully utilized.
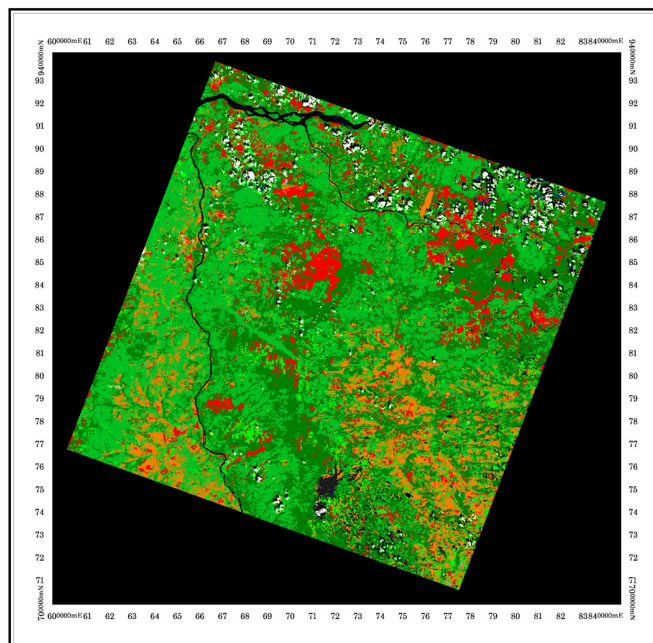
Figure 3. Forest cover change map Bolshe Murtinsky with additional non-change classes (Landsat 142/20). Deforestation is in red, reforestation in light green.

ACKNOWLEDGMENTS

REFERENCES

McIver, D.K. and Friedl, M.A. 2001. Estimating pixel-scale land cover classification confidence using non-parametric machine learning methods. *IEEE Trans. Geosci. Rem. Sens.*, 39:1959-1968.

Beer, C., Skinner, L., Lucht, W. and Schmullius, C. 2003. Assimilation of satellite-derived land cover into a process-based terrestrial biosphere model, *In Proceedings of IGARSS'03*, Toulouse, France, pp. 3178-3180.

Sitch, S., Smith, B., Prentice, C., Arneth, A., Bondeau, A. et al. 2003. Evaluation of ecosystem dynamics, plant geography and terrestrial carbon cycling in the LPJ dynamic global vegetation model. *Global Change Biology*, 9:161-185.

Shvidenko, A., Nilsson, S., Stolbovoi, V., Gluck, M., Schepaschenko, D. and Rozhkov, V. 2000. Aggregated estimation of the basic parameters of biological production and the carbon budget of Russian terrestrial ecosystems: 1. Stocks of plant organic mass. *Russian Journal of Ecology*, 31:371-378.

Shvidenko, A., Nilsson, S., Stolbovoi, V., Rozhkov, V., Gluck, M. 2001. Aggregated estimation of the basic parameters of biological production and the carbon budget of Russian terrestrial ecosystems: 2. Net Primary Production. *Russian Journal of Ecology*, 32:71-77.

Hese, S. and Schmullius, C. 2004. Approaches to Kyoto Afforestation, Reforestation and Deforestation mapping in Siberia using object oriented change detection methods. *In Proceedings of 1st Göttingen GIS & Remote Sensing Days*, Göttingen, Germany, Vol. 113, revised edition, pp. 349-354.

DEVELOPMENT OF SUPPORTING TOOLS FOR PLANNING & MONITORING OF SUSTAINABLE CARBON OFFSET PROJECTS. – COIN

Nadine Schmidt[a], Hanjo Kahabka[a], Felicitas von Poncét[a] and M. Köhl[b]

[a] Infoterra GmbH, D-88039 Friedrichshafen email: nadine.schmidt@infoterra-global.com;
Hanjo.Kahabka@infoterra-global.com; Felicitas.Poncet@infoterra-global.com
[b] Institut für Weltforstwirtschaft, Leuschnerstr. 91, 21031 Hamburg, weltforst@holz.uni-hamburg.de

ABSTRACT

The development of a monitoring concept for carbon offset projects in the forestry sector based on SAR data (COIN - Carbon Inventory) has been carried out in frame of the ProSmart II Extension project funded by DLR and bmb+f (Förderkennzeichen: 50 EE 0212). Focus of the ProSmart project was the development and demonstration of the feasibility of products and services based on airborne E-SAR data simulating future TerraSAR data as close as possible. The upcoming TerraSAR-X satellite, providing high-resolution X-band data, is planned for launch in April 2006.

Within the scope of Kyoto Protocol related projects a monitoring concept for Carbon Offset Projects in the forestry sector has been developed. The concept provides cost efficient, objective and comprehensive methods to enable reliable third party validation and verification of carbon offset projects. Furthermore, the mapping and monitoring products can support project developer in the improvement of their forest management concept in order to combine economic, silvicultural and carbon offset aspects.

The developed concept is based on EO data in combination with up-to-date field data (combined inventory). SAR data shows advantages due to the daytime and weather independency. Therefore, the sensor is able to provide a higher data acquisition frequency. Furthermore, SAR data -especially L-band- is highly correlated with biomass and also shows benefits in discrimination of different tree species in younger forest stands. During the development investigations on the suitability of SAR with focus on L- and X-band data for classification and biomass assessment purposes were performed.

This document provides an overview of the potential of SAR data for monitoring purposes in the forestry sector. A classification of tree species and biomass assessment were performed. In further steps the information derived from SAR data is used for the combined inventory concept, which results in the estimate of sequestrated carbon.

The evaluation by a reference customer proved a high accuracy of carbon storage estimation and a high cost-efficiency compared to traditional methods. Furthermore, the concept supports an independent and transparent carbon offset project certification process.

Keywords: Biomass assessment, SAR-data,

1 INTRODUCTION

The main objective of a carbon offset project is the determination of sequestrated carbon dioxide equivalents. Because of the impossibility to directly assess the stored carbon dioxide in a forest, auxiliary variables need to be assessed. The COIN development demonstrated that the combination of field measurements and information gained from L-band SAR, is an efficient and reliable way to deliver a biomass estimation as a basis for current carbon stock retrieval of forests. The advantage of the combined inventory approach is 1) the cost efficiency compared to purely field based methods and 2) the information on the accuracy of the estimates of current biomass respective carbon equivalents of a forest and thus a high reliability of the results. Furthermore, the combined approach allows to overcome one of the well known problems of L-band radar remote sensing in biomass retrieval namely the saturation problem, describing the decreasing sensitivity of L –band information to high biomass levels. This can be compensated by the allocation of more field samples in dedicated biomass levels.

2 SAR DATA ANALYSIS AND PROCESSING

For the development of a monitoring concept for carbon offset projects in order to support the project manager and the certifiers a suitable test site was chosen. The test site "Altenberg" is located in the eastern Ore Mountains in Germany and is characterized by large areas of reforested stands with different development stages and several tree species. Furthermore, the hard growing conditions in the eastern Ore mountains result in inhomogeneous stand structures. The detection of such inhomogeneous structures is an important information for project developers in order to optimize forest management measures. For the test site fully polarimetric L-band data and X–band data in HH and VV polarization were available acquired in Sept. 1998 and April 1999 by the E-SAR sensor.

The analysis and processing is based on geo-coded radiometrically corrected SAR data. Both, the following classifications and timber volume estimation are based on objects of uniform backscatter produced by different segmentation methods. The choice of segmentation algorithm and respective parameterization depends on the scale of evaluation appropriate to the information retrieval step. For forest classification a hierarchical approach is used, first discriminating areas covered by forest from other land use and second separating different species relevant for carbon retrieval. Using the information on biomass storage achieved during the field campaign the correlation between radar backscatter and biomass was analyzed and a robust inversion function developed. The results achieved with SAR-data are input to the combined inventory.

Table 1 shows the confusion matrix for producer accuracy for the species groups classification. The verification data set used is derived from the forest inventory database. The overall kappa coefficient reached is 88%, which is an excellent result.

Table 1. Confusion matrix (producer) for species groups classification

	Spruce	Pine	Larch	Deciduous
Spruce	84.58	10.67	15.59	25.77
Pine	9.54	85.20	8.53	10.51
Larch	2.78	2.51	65.72	5.18
Deciduous	3.10	1.62	10.16	58.55

The best classification accuracy is achieved for the class Pine, followed by Spruce and Larch. The accuracy for deciduous stands is not satisfying. However, the selection of classification samples for the class Deciduous was very difficult, due to the very small proportion of deciduous stands in the test areas and the occurrence of different tree species (oak, beech, birch, etc.). In addition, most of the deciduous stands contain a high proportion of coniferous trees (Schmidt *et al.*, 2004).

Additional analysis of the derived results of the COIN project proved, that the used SAR data is very suitable to detect inhomogeneous structure within forest stands. Especially for younger stands the analysis showed very good results in the discrimination between forested and non-forested areas and also the differentiation of different species groups. In comparison to the available CIR data, SAR has a higher potential for classifications and analyses of these younger age classes.

3 COMBINED INVENTORY AND COST BENEFIT

3.1 COMBINED INVENTORY

The main objective of a carbon offset project is the determination of sequestrated carbon dioxide equivalents. Because of the impossibility to assess the stored carbon dioxide in a forest, auxiliary variables need to be assessed. Volume of trees, especially tree trunks, is the most important carbon storage in forest. As non-destructive assessment of volume in a field is in practice impossible the tree height, diameter at breast height and number of trees per plot are measured. A volume function enables to derive the total stand volume. This is converted by a tree species-specific function into tonnes per ha of carbon dioxide equivalents. Thus the assessment of stand volume and tree species is most important. If the species have similarly wood density the stocking volume is the only needed parameter and estimation error of volume and carbon dioxide is equal because the transformation into CO2 equivalent tonnes is done by a constant factor.

The interest of a potential carbon project manager is to sell many verified credits on sequestrated tonnes of carbon dioxide equivalents. In the verification phase the minimum reliable estimates of stored tonnes carbon are transferred into verified credits and can be sold. Therefore the assessment needs to be done up to a specific accuracy and the lower bound of a confidence interval is assigned as minimum reliable estimate of carbon storage. The range of estimated carbon depends on the variation within the site, the number of samples plots and survey design. With help of additional plots the lower bound of confidence interval can be increased. But for each design there is point were the costs for additional plots are higher than this attempt will increase the benefit. This point is test site specific and depends on the market value of tonnes carbon dioxide equivalents and the inventory cost.

Combined inventories allow (compared to one phase inventories, purely field based assessments) to reduce the sampling error and therefore to increase the benefit by maximising the lower bound of the confidence interval.

Within the project COIN different sampling designs (stratification schemes, regressions and density of sample plots) for one time assessment of the total stored volume were analyzed. The gain in sampling error reduction for different combinations of stratification methods and sample grid densities was analyzed (see table 2 for test site "Altenberg" specific results). The 400b grid is shifted to include more sample plots of younger stands than in grid 400a. Thus the variation and the error of grid 400b are lower. The used combination methods perform much better. Also for the 600 meters grid with 31 plots the error is smaller than the 10% error defined by the reference client. One-phase terrestrial survey meets only marginally the demand with the 200 meters grid with 250 samples plots.

Table 2: Comparison of different combination methods and grid densities for the estimation error.

Grid density [m]	Stratification scheme			
	One-phase terrestrial	Stratified SPECIES	Stratified LHH 100	Regression
200	9,13%	0,52%	0,45%	0,52%
400a	18,92%	2,33%	1,99%	2,61%
400	16,03%	2,12%	1,37%	2,22%
600	24,66%	3,62%	3,92%	4,91%

The analysis of different design alternatives, grid densities and combination methods showed the following results for the Altenberg test site:

- combined inventories maximize the benefit compared to single terrestrial inventories (reduction of samples in combination with reduction of estimation errors)

- 400 m grid seems to be sufficient and lead to the biggest benefit

- for mainly young stand a stratification into volume groups performed best (400b)

- sites with more than 30% mature forest proportion 400a and 600 a stratification on species leads to higher benefit

3.2 COST BENEFIT FOR CARBON OFFSET PROJECTS

The methodologies developed during the COIN project showed promising results to support carbon offset projects. A cost-benefit analysis was performed in order to show the advantages of the methodology for the participating parties of a carbon sequestration project.

It is assumed that carbon offset projects conducted in the frame of Kyoto Protocol will have a runtime of 30 years. Looking at a typical scenario for a carbon sequestration project the project developer has to consider the following expenses during lifetime of the project:

Fixed expenses:

- Certification costs (PDD)

- Administration fee per year

- Inventory costs all 5 years

Variable expenses:

- Afforestation costs
- Maintenance after 5 and 10 years run-time

The first benefits of the project will occur after the first verification of the sequestrated carbon after 5 years run-time.

A cost-benefit analysis of a carbon offset project will show a typical development:

The afforestation is the most important investigation of the whole project run. As already mentioned after the first five years the first profits of the project can be added to the cost-benefit analysis and after each five years additional profits. The biggest benefit is expected in the last year of the project.

The main results of the cost-benefit analysis are:

- Variable cost, like the afforestation or maintain activities, are the major costs.
- Cash receipts in the early stage of the project have a positive impact, due to the reduction of the loan.
- Costs in the early stage of the project have a negative impact. The interest on the loan leads to an accumulation of debts.
- Planting losses or damages (pests or drought) that result in a decreasing sequestrating potential in early times of the project run have a bigger overall impact than interferences in the end of the project.
- The costs for inventory are circumstantial to the overall costs.
- The controlling of planting as a further tool of the inventory can efficiently help to reduce replanting cost, which are very crucial

The independency towards weather and daytime in combination with physical interaction between biomass, as main source for sequestrated carbon, and radar backscatter makes radar a powerful tool for carbon monitoring. In terms of overall benefit the first years of the project are the most important ones. The monitoring of afforestation success and the early warning towards calamities can be done very well with radar. Especially the accurate and effective inventory method in the first decade(s) of the project leads to higher benefits in the end. The investigated variation in the COIN Project, in terms of age classes, growing differences or species mixtures, was much bigger than it can be expected in a real carbon offset project. Therefore fewer terrestrial plots will be needed to achieve the same accuracy and the cost will be reduced and the benefit will increase further more. The impact of the saturation of the radar signal, as it is described in literature, to the inventory efficiency was not studied within the COIN project. But the developed sampling method responds dynamically by increasing the number of terrestrial samples to achieve the needed accuracy.

High potentials of radar time series were not studied with in this project due to lack of data availability. In future this information will enable further detailed cheep monitoring products and an optimised stratification.

4 SUMMARY

The project showed the great potential of SAR data for forest applications, namely the discrimination of tree species and biomass retrieval. In case of the species discrimination SAR data provides a high potential especially for young growth, where a differentiation between tree species in optical data is often inaccurate. Generally, the combination of multi-polarized X- and L-band data showed a good feasibility in discriminating different tree species groups. For biomass retrieval results of former investigations (ProSmart II projects RACOON and INVENT) on biomass retrieval with SAR data were confirmed. Furthermore, it was demonstrated that the combined inventory approach leads to a quantification of carbon storage with high accuracy and high cost efficiency compared to traditional methods.

The COIN (Carbon Inventory) project has established tools for cost efficient project area inventory and monitoring for carbon sequestration projects in order to maximize customer benefits such as:

- Support of independent and transparent project certification.

- Quantification of carbon storage with high accuracy.

- High cost efficiency compared to traditional method.

- Re-quantification of carbon sequestration potential during project lifetime.

- Early detection and localization of forest disturbances and damages to enable quick reaction and mitigation.

The developed service supports certification companies seeking for cost efficient, objective and comprehensive methods to enable reliable third party validation and verification of carbon offset projects in the Forestry Sector. Furthermore insurance companies guaranteeing the sustainable management of a forest support emission trading and thus benefit as well from regular and independent monitoring of the carbon offset project area. Even to a greater extend these mapping and monitoring efforts are suitable for project developers to improve their forest management concepts in order to combine economic, silvicultural and carbon offset aspects.

REFERENCES

N. Schmidt, F. von Poncét, J. Janoth (2004): Retrieval of biomass for carbon budget estimation based on airborne E-SAR data. In: *"Processings of 4th International Symposium on Retrieval of Bio- and Geophysical Parameters from SAR data for Land Applications"*, 16-19 Nov. 2004, Innsbruck

THE ROLE OF REMOTELY-SENSED DATA TO ASSESS SPANISH FORESTS AS CARBON SINKS IN THE KYOTO PROTOCOL CONTEXT

S. Merino-de-Miguel, F. González-Alonso, S. García-Gigorro, A. Roldán-Zamarrón, J.M. Cuevas

Remote Sensing Laboratory-INIA. Ctra. A Coruña, km 7.5 Madrid 28040 Spain. Email: alonso@inia.es

ABSTRACT

The Kyoto Protocol intends to limit or reduce CO_2 and other greenhouse gas emissions to 1990 (base year) levels and allows carbon emissions to be balanced by carbon sinks represented by vegetation (e.g. forests). The present paper is focused on three key aspects related to the capabilities of remote sensing data and techniques to help in monitoring forest ecosystems as carbon sinks or sources. The first one attempts to find statistical relationships between satellite-derived NDVI (Normalized Difference Vegetation Index) data and field measurements from the Spanish National Forest Inventory (NFI), on a province basis. If reliable, such relationship could be used to predict forest biomass at different dates. The second is focused on elaborating forest cartography in order to produce forest masks and for assessing the evolution of forested areas (increases or decreases). The third one tries to produce medium resolution biomass maps using ground data from the NFI and remotely-sensed images of various resolutions. These three tasks were carried out using several types of satellite data (NOAA-AVHRR, SPOT-VEGETATION, Envisat-MERIS and SPOT5-HRG) and ancillary information (NFI sample plots, land use maps and forest cartography). The study area is the whole Spanish territory. Results reached so far reveal that satellite information may play a key role in the spatial and temporal expansion of ground data, helping in the assessment of the carbon balance of Spanish forests on a regular basis.

Keywords: biomass estimation, NDVI, stem volume estimation, forest cartography, forest biomass map.

1 INTRODUCTION

The Kyoto Protocol intends to limit or reduce CO_2 and other greenhouse gas emissions an average value of 5% of 1990 levels and allows carbon emissions to be balanced by carbon sinks represented by vegetation. The assimilation of atmospheric CO_2 by the Earth's vegetation ecosystems, especially by forests which represent a long-term pool, is a very important component of the global balance of carbon. The vegetation pool gains carbon from productivity investment in its components (wood, bark, branches, leaves, etc) and loses carbon because of aging, mortality, fire, etc (Myneni *et al.,* 2001). In most cases, forest ecosystems tend to behave as carbon sinks during almost all their lives.

The Kyoto Protocol entered into force on 16 February 2005. Since it is an international and legally binding agreement, the Protocol will need of different control and monitoring mechanisms for treaty verification. These mechanisms should be implemented on both national and global basis in a very near future. For those aspects referred to carbon accounting in case of land use change (deforestation, reforestation or afforestation) or changes in forest productivity (changes in the amount of biomass), reliable systems will be a key point in reducing uncertainties in traditional practices. In this context, the remote sensing community seems to be very well positioned: (i) land cover change identification using remote sensing is widely applied (Richards, 2003) and (ii) forest biomass estimations using satellite and ground data are reliable (Tompoo *et al.*, 2002; Dong *et al.*, 2003).

Long-term NOAA (National Oceanic and Atmospheric Administration)-AVHRR (Advanced Very High Resolution Radiometer)-based studies carried out during the last years have shown a clear tendency through an increase in the carbon pools of boreal and temperate forests, both at global and regional scales (Myneni *et al*., 1997, Myneni *et al*., 2001, Dong *et al*., 2003, González-Alonso *et al*., 2003, González-Alonso *et al.,* 2004a). In the case of Spain, ground data from the Second (1986-1996) and Third (1996-2006) NFI also confirm an increase in the amount of both forest biomass and forested lands. However, a 10 years gap between successive inventories might be a too long period, specially if the Spanish Government wants to properly report of greenhouse gases related to forests. In this sense, satellite data might help in the expansion of ground data, either spatially or temporally. The objective of the present work is to develop

reliable remote sensing techniques that should help in the assessment of Spanish forests as carbon sinks or sources in the Kyoto Protocol context.

2 STUDY AREA

This paper presents results of a project of which study area is the whole Spanish territory. However, not all the processing was carried out within the whole area. As said before, the main objective of the present work was divided into three tasks. The first one, that consisted on finding statistically significant relationships between NDVI and ground data, was applied to the whole country. The second one, that aimed at producing updated forest cartography, was applied to up to five Spanish provinces of a total of fifty. The third one, that tried to produce forest biomass maps, was attempted in a small test area in west Spain.

3 MATERIAL AND METHODS

The following sections describe each one of the three tasks in which the present work is divided. In each case, materials and methods will be introduced. Reached results will be presented in section 4.

3.1 FOREST BIOMASS ESTIMATION THROUGH NDVI COMPOSITES

This part of the work involved the use of (i) field data from the Second and Third NFI (NFI2 and NFI3), (ii) the European land use database Corine Land Cover (CLC2000) and (iii) remotely-sensed data from Vegetation on-board SPOT (Système Pour l'Observation de la Terre) and from NOAA-AVHRR. Image processing was carried out with ENVI 4.1 and ArcView 3.2, while statistical analyses were performed with Statgraphics Plus 4.1. Results were always obtained on a province basis.

Stem volume data from the Forest Inventories were used (both in m^3 and m^3/ha): NFI3 data from 19 provinces, and NFI2 data from 48 provinces. Canarias, Ceuta and Melilla were not considered, as satellite information for those areas was not available. CLC2000 was employed to obtain forest cartography for the 48 study provinces, as NFI3 cartography is not complete.

Satellite information consisted on NDVI (Normalized Difference Vegetation Index) data. This index has previously shown a strong relationship with photosynthetic activity and with forest parameters (González-Alonso et al., 2003, González-Alonso et al., 2004a, Myneni et al, 1997, Myneni et al,. 2001). SPOT-VEGETATION dataset was obtained from VITO (Flemish Institute for Technological Research), and NOAA-AVHRR dataset from DLR (German Aerospace Center). The main characteristics for both sets of data are shown in Table 1.

Table 1.- Main characteristics for SPOT-VEGETATION and NOAA-AVHRR NDVI datasets

	Period	Months considered	NDVI composites	Spatial resolution
SPOT-VGT	1998-2004	February-October	10-day maximum (27/year)	1000 m
NOAA-AVHRR	1996-2004	March-September	monthly maximum (7/year)	1000 m

The two datasets were processed separately, and mean annual NDVIs were calculated (from 27 10-day maximum NDVI composites per year for SPOT and 7 monthly maximum NDVI composites per year for NOAA). From these annual values, mean NDVIs for the study period were obtained (98-04 for SPOT and 96-04 for NOAA). A forest-land mask was made from the CLC2000, and it was applied on the two mean NDVI files previously obtained. Finally, mean NDVI values from forested land for the study period were obtained for each province.

Table 2.- Description of the applied regression analyses

	Regresión type	Independent variable(s)	Explained variable
SLR	Simple Linear	Mean NDVI for the period	NFI3 stem volume data
MLR	Multiple Linear	Mean NDVI for the period /NFI2 stem volume data	

Available information for the statistical process was: mean NDVI values plus IFN2 stem volume data for the 48 study provinces, and IFN3 stem volume data for 19 of them. Statistical analyses were performed on data from those 19 provinces, in order to obtain a prediction equation for the whole set of 48 provinces. Stem volume and mean NDVIs were related through simple and multiple linear regressions (SLR and MLR, as explained in Table 2). These analyses were repeated for both sensors and for stem volume both in m^3 and m^3/ha.

3.2. FOREST CARTOGRAPHY

The material used for the present task falls into three main categories: (i) satellite images, (ii) field data and (iii) cartography. Five different Spanish provinces were processed. Satellite data were extracted from several FR (Full Resolution-300m) MERIS (Medium Resolution Imaging Spectrometer) images provided by ESA. Field data came from the Third NFI sample plots that are located on the ground according to a regular net. Used cartography was compounded by land use-land cover map (raster format, CLC2000) and forest cartography (vector format, that was supplied together with the NFI ground plots information and is better known as Spanish Forest Map, SFM). Maximum Likelihood supervised classification was carried out using different MERIS images. Regions Of Interest (ROIs) for training classifiers and for accuracy analysis, were delimitated on MERIS 'pure pixels', based on information from the NFI and CLC2000. The NFI was used for drawing ROIs in three forest categories (Deciduous broadleaved, Coniferous and Mixed), while the rest of classes were delimitated by means of CLC2000.

3.3. FOREST BIOMASS MAP DEVELOPMENT

Forest biomass map development involved the use of: (i) satellite images, (ii) field data, (iii) cartography and (iv) a digital elevation model (DEM). The area in which the different analysis were carried out is located in west Spain, near the border between Spain and Portugal. Satellite data were extracted from two different datasets: SPOT5-HRG (High Resolution Geometric instrument) and Envisat-MERIS FR. Field data came from the NFI3. Used cartography was the SFM.

Regularly-produced forest biomass maps would give an unique picture of the evolution of forest resources. In order to be affordable, such a product would ideally have a medium spatial resolution and an annual or bi-annual temporal resolution. Provided that the relationship between NFI and MERIS data was not reliable enough (González-Alonso *et al*., 2004b), a high resolution SPOT5-HRG image (10m) was then used as an intermediate step between field data and MERIS pixels. The processing consisted on two phases: (i) firstly, a 10m forest biomass map was developed using sample plots, SPOT5-HRG data and a DEM, (ii) secondly, a 300m forest biomass map was developed using the previous one and a MERIS FR scene.

The 10m forest biomass map was developed using: (i) SPOT5-HRG image, (ii) stem volume (m^3/ha) sample plots values, (iii) information derived from a DEM, (iv) a SPOT5-HRG unsupervised classification (for stratification purposes) and (v) a set of Biomass Expansion Factor. The latter allows the conversion of stem volume values into forest biomass on a species basis. The method for forest biomass map production consisted on two steps: (i) statistical analyses in order to find a significant relationship between ground measurements and satellite information and (ii) application of the former equation to remotely sensed data. The first step was solved through the development of multiple linear regression using stem volume as dependant variable and a set of satellite bands (single bands and ratios between bands) and terrain characteristics as independent variables. The sample was stratified into 3 groups as resulted from a SPOT5-HRG unsupervised classification, thus three multiple regressions were produced. The resulting 10m biomass map was then rescaled (scaled down) to a 300m pixel size image. The 300m forest biomass map was developed using: (i) the SPOT5-based 300m forest biomass map and (ii) a MERIS FR image. The method consisted on finding a statistically significant relationship between both sets of data. The resulting equation was then applied to a sub-scene of the original MERIS-FR image.

4 RESULTS

4.1. FOREST BIOMASS ESTIMATION THROUGH NDVI COMPOSITES

The first result which is worth pointing out is that mean NDVI values for the studied period from both sensors are highly correlated ($r^2 = 86.10\%$), even though the two datasets have different characteristics and temporal coverage (see Table 1).Mean NDVI values showed a stronger correlation with stem volume referred to surface (m^3/ha) than with m^3, as former studies had shown (González-Alonso *et al*., 2004a). From here on, only results obtained for m^3/ha will be considered. R-squared (r^2 expressed as %) and Root Mean Square Errors (RMSE expressed in m^3/ha) for the SLR and the MLR are shown in Table 3, together with the "mean relative error" expressed in percentage (MRE=[($\sum$(y'/y)/n)*100]-100, where: "y" means real value and "y'" predicted value).

Table 3.- Results for regressions obtained from mean NDVI values and stem volume data (m³/ha)

	SLR			MLR		
	r^2	RMSE	MRE(%)	r^2	RMSE	MRE(%)
SPOT-VEGETATION	82.38	14.781	10.793	95.73	6.856	2.688
NOAA-AVHRR	82.16	14.874	12.055	95.44	7.091	2.987

As can be observed, results are quite similar for both NDVI datasets, although slightly better for SPOT-VEGETATION. R-squared values for the regression between NFI3 and NDVI data (SLR) are quite high at a 1% confidence level, which indicates the strong relationship between forest parameters and NDVI mean values. Nevertheless, although the MRE is acceptable, the RMSE is considered too high, as it is close to NFI3 stem volume values for some provinces. When NFI2 stem volume dataset is included as a independent variable (MLR), the statistical parameters improve considerably, so MLR was considered more reliable than SLR. Prediction equations from MLR were applied to the whole set of 48 provinces, and predicted m³/ha values were obtained. Predicted m³ were calculated using the forested areas from CLC2000 as expansion factors, and increases over NFI2 on a provincial basis were obtained. Figures for some provinces are clearly overestimated, which suggests the convenience of performing a stratification of the sample based on vegetation and soil type, which will be considered for future work. According to results from SPOT-VEGETATION data, stem volume decreased only in two provinces (Álava and Valladolid) while from NOAA results Álava is the only province that shows a stem volume decrease. The rest of provinces show an increase in their figures. The stem volume increase at a national scale was calculated using NFI3 values for the19 available provinces, and estimated data for the rest of them. National increase over NFI2 was 45.03% from SPOT –VEGETATION data, and 45.77% from NOAA-AVHRR. Stem volume increase over NFI2 for the 19 provinces with available NFI3 data is 48.3%, so figures obtained through the proposed method of estimation are quite close to those extracted from ground information (NFI).

4.2 FOREST CARTOGRAPHY

Overall accuracy and Kappa coefficient for the five studied provincies are shown in Table 4. Accuracy for deciduous broadleaved and coniferous classes is also presented in Table 4. Results correspond to classifications where 100% ROIs were employed for both training and verification.

Table 4. Overall accuracy, Kappa coefficient and deciduous broadleaved and coniferous forests accuracies.

	La Rioja	Murcia	Navarra	Madrid	Lérida
Overall accuracy (%)	86.80	77.80	79.27	73.08	80.04
Kappa coefficient	0.8429	0.6971	0.7288	0.6944	0.7496
Deciduous broadleaved accuracy (%)	88.59	-	82.72	73.46	84.71
Coniferous accuracy (%)	78.34	72.30	72.68	76.11	86.24

4.3 FOREST BIOMASS MAP DEVELOPMENT

Table 5 presents the main parameters of the three multiple regression that were used to produce the SPOT-based 10m forest biomass map. As independent variables, a set of satellite bands (either single bands or ratios between bands) were used. Table 6 summarizes the main parameters of the multiple regression that was used to produce the MERIS-based 300m forest biomass map. Thirteen reflectance bands were used as independent variables in this case.

Table 5. SPOT-based 10m forest biomass map: multiple regression parameters ([a]: mean absolute error; [b]: root mean squared error).

multiple regression	independent variables	sample size	r^2-ajusted (%)	MAE[a] (m³/ha)	RMSE[b] (m³/ha)
1	6	39	95.65	6.62	8.44
2	6	22	94.68	3.56	4.71
3	2	28	96.95	14.72	25.53

Table 6. MERIS-based 300m forest biomass map: multiple regression parameters

multiple regression	independent variables	sample size	r^2-ajusted (%)	MAE (m^3/ha)	RMSE (m^3/ha)
1	13	14120	61.13	13.83	19.69

5 CONCLUSIONS

Reached results revealed the importance of remote sensing techniques and data in order to assess and monitor forest resources, specially if those Parties involved in the Kyoto Protocol want to properly and timely report about the variations in their forested carbon sinks or sources. Results reached so far are promising.

Forest biomass estimation through the use of NDVI composites revealed a highly dependant relationship between forest inventory results and satellite data. The use of coarse images, that are available through the Internet, allows to take into account larger data sets what results highly valuable for such studies. Reached results were quite similar for both sensors (AVHRR and VEGETATION), thus the method may be assumed to be robust.

MERIS-based cartography has produced promising results in the context of the current research. These preliminary results show the potential of MERIS images as a valuable source of information for updating forest cartography, either at regional or global scale, in a efficient and regular manner.

The development of forest biomass maps on a regular basis would give us valuable information about the evolution of forest ecosystems. Reached results allow to conclude that medium-resolution forest biomass map generation using field and satellite data is reliable provided that a high-resolution images are used as an intermediate step.

ACKNOWLEDGMENTS

REFERENCES

Myneni, R.B., Dong, J., Tucker, C.J., Kaufmann, R.K., Kauppi, P.E., Liski, J., Zhou, L., Alexeyev, V. and Hughes, M.K., 2001. A large carbon sink in the woody biomass of Northern Forest. *Proceedings National Academy of Science*, 98(26):14784-14789.

Richards, G., 2003, The Expanding Role of Remote Sensing in Greenhouse Gas Accounting. *In 30th International Symposium on Remote Sensing of Environment*, Honolulu, Hawai.

Tompoo, E., Nilson, M., Rosengren, M., Aalto, P. and Kennedy, P. 2002. Simultaneous use of Landsat-TM and IRS-1C WiFS data in estimating large area tree stem volume and above ground biomass. *Remote Sensing of Environment*, 82: 156-171.

Dong, J., Kaufmann, R.K., Myneni, R.B., Tucker, C.J., Kauppi, P.E., Liski, J., Buermann, W., Alexeyev V. and Hughes M.K., 2003, Remote Sensing estimates of boreal and temperate forest woody biomass: carbon pools, sources and sinks. *Remote Sensing of Environment*, 84, 393-410.

Myneni, R.B., Keeling, C.D., Tucker, C.J., Asrar, R.G. and Nemani, R.R., 1997. Increased plant growth in the northern high latitudes from 1981-1991. *Nature*, 386:698-702.

González-Alonso, F., Calle, A., Merino De Miguel, S. and Cuevas, J.M., 2003. Using Remote Sensing Techniques to assess Terrestrial Carbon Sinks in Spain. *30th In.t Symposium Remote Sensing of Environment*, Honolulu, Hawai.

González-Alonso, F., Cuevas, J.M., Calle, A., Casanova, J.L. and Romo, A., 2004a. Spanish vegetation monitoring during the period 1987-2001 using NOAA-AVHRR images. *Int. J. Remote Sens.* 25(1):3-6.

González-Alonso, F., Merino-de-Miguel, S., García-Gigorro, S., Roldán-Zamarrón, A. and Cuevas, J.M, 2004b. Monitoring forests as carbon sinks using remote sensing. *In the Proceedings of the ENVISAT Symposium, CD (SP-572)*. ENVISAT Symposium Salzburg, Austria.

CHARACTERIZATION OF ALPINE TREELINE ECOTONES: AN OPERATIONAL APPROACH ?

R.A. Hill[a], K. Granica[b], G.M. Smith[a] and M. Schardt[bc]

[a] Centre for Ecology and Hydrology, Huntingdon, Cambs, PE28 2LS, UK., email: rhill@ceh.ac.uk
[b] Joanneum Research, Forschungsgesellschaft mbH, Wastiangasse 6, A-8010 Graz, Austria
[c] TU Graz, Institute of Remote Sensing and Photogrammetry, Steyrergasse 30, A-8010 Graz, Austria.

ABSTRACT

An ecotone is a zone of vegetation transition between two communities, which can result from natural or anthropogenic environmental gradation or a positive feedback between vegetation community and environment. The transition with altitude from dense subalpine forest to alpine meadow or even tundra represents an ecotonal gradient relating to increasingly harsh environmental conditions. We demonstrate the use of class probability mapping to produce a soft classification of an alpine treeline ecotone in Austria using a SPOT 5 HRG image. The partitioning of class membership probabilities from a Maximum Likelihood algorithm between classes partially reflects the land-cover composition of mixed pixels in the ecotone. By identifying thresholds in the membership probability scores we map the alpine treeline ecotone as a zone of transition. This approach supplies more detailed information relating to alpine forests in this treeline ecotone than is displayed in a standard hard classification (Core Service Landcover map).

Keywords: soft classification, probability, SPOT, ecotone, alpine treeline.

1 INTRODUCTION

The term ecotone was introduced by Clements (1905) as a zone of vegetation transition between two distinct communities. Ecotones can have higher biodiversity than either neighbouring community and can help maintain species flows between them. In addition, ecotones can influence the flux of materials and energy in the landscape and can be early indicators of ecological response to environmental change (di Castri *et al.,* 1988).

Ecotones can be classified as environmental, anthropogenic or switch, resulting from natural or anthropogenic environmental transition over space or a positive feedback between vegetation community and environment (Walker *et al.*, 2004). The transition with altitude from dense subalpine forest to open alpine meadow represents an ecotone gradient relating to increasingly harsh environmental conditions, particularly climate. Clearly, where an ecotone is determined by an environmental gradient, its nature and spatial configuration are highly susceptible to environmental change. Anthropogenically induced climate change will impact alpine treeline ecotones (Hansen-Bristow *et al.*, 1988), although local scale environmental factors such as topographic complexity, geology, disturbance patterns, resource availability and biotic interactions will also be relevant (Stevens and Fox, 1991).

In remote sensing applications, ecotones have tended to be something of a 'grey area'. Johnston and Bonde (1989) examined ecotones in north-central Minnesota using a Landsat Thematic Mapper (TM) image. They employed two different approaches which focussed on boundaries in vegetation cover. First, they performed unsupervised classification of image spectral characteristics to map land cover types with ecotones identified as the spatial boundaries between each vegetation class. The six land cover types mapped were: water, herbaceous/cut-over, low deciduous shrubs, low conifers/muskeg, conifer trees, and deciduous trees. Second, they identified 'biomass ecotones' as areas of maximum contrast in Normalised Difference Vegetation Index (NDVI) over a 3x3 pixel window. This dual approach gave information of where the clearest vegetation boundaries occurred and which land cover types tended to border each other. However, little information was revealed as to the nature of transition between vegetation types, i.e. no distinction was made between a vegetation community boundary and an ecotone transition.

A more thorough examination of ecotones was provided by Allen and Walsh (1996). They investigated the alpine treeline ecotone in Glacier National Park, Montana, using two Landsat TM images. They used a

hierarchical approach to create a supervised classification of six forest types (closed-, medium, open-canopy spruce-fir, forested scree, dense krummholz, krummholz-scree) and five non-forest vegetation types (krummholz-meadow, lush or wet meadow, sparse or dry meadow, grass/shrub, dense tundra). The vegetation classes were mapped with an overall accuracy of over 90%, and together were taken as representing the alpine treeline ecotone. Cluster analysis of spatial and compositional pattern metrics derived from their thematic map was used to infer six treeline forms which differed among terrain types.

The recognition and treatment of vegetation communities in the classification of remotely sensed imagery depends entirely on the spatial scale of the vegetation communities and their zones of transition in relation to the spatial resolution of the imagery. An ecotone may appear as an edge, a boundary of mixed pixels or a zone of continuous variation in a remotely sensed image. Typically in image classification, an ecotone is either ignored if it falls within a width of one or two pixels, or part of it may be mapped as a separate vegetation community if it covers an area of several pixel widths. In the two examples of ecotone mapping outlined above, Johnston and Bonde (1989) ignored the ecotone during their classification process, identifying it by default as the spatial boundary between vegetation classes, whilst Allen and Walsh (1996) mapped the ecotone as separate vegetation communities but with no recognition of a gradual transition between those communities. These are both examples of so called 'hard' classifications in which each pixel in an image is allocated to the class with which it has the highest probability of membership, regardless of how strong or weak that probability is. In an area of vegetation transition, image pixels will often have a mixed composition. Allocating a mixed pixel to one vegetation class, which may not even be one of the component classes, thus does not provide a realistic or accurate representation of land-cover transition (Foody, 1996).

In fact, there is no analogy between 'hard' classification methods applied to vegetation analysis in remotely sensed data and the ordination methods commonly used in vegetation analysis, which examine gradients of change between vegetation communities (Wood and Foody, 1989). Hard classification is wasteful of information generated on the strength of class membership, which can partially reflect the land-cover composition of mixed pixels in boundary or ecotone areas (Foody, 1996). The probability information can be used to 'soften' the output of a hard classifier by outputting the probabilities of membership each pixel has to each class (Foody, 1992). Alternatively, fully 'soft' classification techniques exist such as linear-mixture modelling (Quarmby et al., 1992) or fuzzy c-means clustering (Cannon et al., 1986) which seek to unmix the composition of pixels at land cover boundaries. The relationship between the output of these techniques and the proportional composition of land cover per pixel will depend on the spectral separability of the chosen 'end-member' land cover types and the ability of these to depict the structural and floristic complexity of the land cover types present (Fisher and Pathirana, 1990; Foody and Cox, 1994).

In an area of heathland vegetation in Surrey, southern England, Foody et al. (1992) showed that the probability measures derived from Maximum Likelihood (ML) classification of Airborne Thematic Mapper data related to the vegetation canopy. For areas classified as heath it was possible to indicate the likelihood of heath, degrees of similarity to coniferous woodland, and different degrees of likelihood of wet heath and bog. This information provided increased accuracy in producing spatial estimates of each vegetation class and was displayed visually as a probability map by setting the grey scale in proportion to the strength of class membership for each vegetation type (Wood and Foody, 1989). This example provided a map of vegetation mosaicity rather than of ecotone transition along an environmental or anthropogenic gradient, but is a good early example of the technique of class probability mapping to produce a soft classification. Ranson et al. (2004) used a Landsat Enhanced Thematic Mapper (ETM+) image, amongst others, for assessing the tundra-taiga ecotone in Russian Siberia. They performed both a hard classification of six land cover classes (water bodies, taiga, tundra, bogs, riparian vegetation, and sand bars) and a linear-mixture model based on dense taiga forest and treeless tundra end-members as a demonstration of possibility.

In this paper we map the alpine treeline ecotone at an Austrian field site. As part of a European Framework 6 Integrated Project called GEOLAND, we compare the results of soft classification of EO data with the Core Service Landcover (CSL) product generated by standard hard classification.

2 FIELD SITE AND DATA PRODUCTS

The field site is located in the Hohe Tauern Mountains National Park, in the south of the Austrian provinces of Salzburg and Carinthia. The area lies in the crystalline Central Alps, which are mainly

metamorphic rocks (mica schists, gneiss and amphibolites). The field site includes three ecosystem regions from high subalpine forest to a montane zone, all within the sub-continental inneralpine zone. In the high mountains, the dominant tree species are Norway spruce (*Picea abies*), European larch (*Larix decidua*), mountain pine (*Pinus cembra*), dwarf mountain pine (*P. mugo*) and green alder (*Alnus crispa*). Broadleaf species occuring at lower altitudes are grey alder (*A. incana*), mountain alder (*A. viridis*), mountain ash (*Sorbus aucuparia*), sycamore maple (*Acer pseudoplatanus*), common ash (*Fraxinus excelsior*), and wych elm (*Ulmus glabra*). The alpine range above the timberline is characterised by a belt of dwarf-shrubs (*Vaccinium gaultherioides*, *Rhododendron ferrugineum*, *Loiseleuria procumbens*), whilst higher areas are covered by more or less closed alpine grassy heathlands on detritus soils.

The EO data used in the analysis of ecotones was a SPOT 5 HRG 1 scene acquired on 20 July 2003. The scene covers approximately 65 x 60 km, centred on latitude N47^0 02' 23" and longitude E13^0 35' 50". The four HI bands are: Band 1, 0.49 - 0.61μm (green); Band 2, 0.61 - 0.68μm (red); Band 3, 0.79 - 0.89μm (near infra-red); and Band 4, 1.58 - 1.75μm (short-wave infra-red). The spectral responses in Bands 1-3 (10 m spatial resolution) were used to sharpen Band 4 (originally 20 m spatial resolution). The 2.5 m spatial resolution PAN band (0.49 - 0.69μm, green-red) was also available. These data were georeferenced and topographically normalised. Displacement errors caused by topographic relief had to be removed to optimise the absolute geometric location accuracy of the geocoded image (Raggam *et al*., 1991). In the course of geocoding, these errors were removed through the integration of a 90 m spatial resolution Digital Terrain Model (DTM). The calculated root mean square error was 0.54 pixels (with max. of 1.26) for the multi-spectral bands and 1.01 pixels (with max. of 2.04) for the PAN band. Based on past experience the parametric Minnaert correction was used for topographic normalisation (Schardt *et al*., 2000).

The CSL map for the study area identified 10 classes (see Figure 1a) and was produced from a hierarchical and hybrid approach using ASTER scenes and a DTM (for more details see www.gmes-geoland.info/CS/CSL/index.php).

3 SOFT CLASSIFICATION OF THE ALPINE TREELINE ECOTONE

A total of 52 training areas were identified to capture the spectral variance of the SPOT 5 HRG scene components. These included components that were not relevant to mapping the ecotone (cloud, cloud shadow, water bodies, snow, built surface, bare soil, crops, pasture and felled forest) and components that were of relevance (bare rock, sparse herbaceous vegetation, natural grass, scrub, and forest of different age and species composition). These training data were used for ML classification. However, because the classification probability was to be retained per pixel for each training class, the number of spectral variants per land cover class and of land cover classes themselves was kept to a minimum. Hence, the training data were amalgamated into eight classes: cloud, cloud shadow, snow, water bodies, non-vegetated surface, sparse herbaceous vegetation, pasture & natural grass, scrub & forest. The classification probability for each of these eight classes was calculated as a percentage of the total Euclidean Distance values output from the ML algorithm.

The treeline ecotone could be represented by the probability image for the vegetation class 'scrub & forest' (Figure 1b). To identify whether the percent probability of 'scrub & forest' related to the proportional cover of trees per pixel, a tree map was produced using the 2.5 m spatial resolution PAN band. Tree canopy was identified as having a DN value of between 40 and 57 in the PAN band and with an NDVI, calculated using Bands 2 and 3, of < 0.25. This provided the proportional tree cover in sixteenths per 10 m pixel of the 'scrub & forest' probability image. The correlation co-efficient between the proportional tree cover and the probability score for 'scrub & forest' from soft classification was 0.79.

A histogram of the probability scores for 'scrub & forest' for all pixels classified in the CSL map as forest is shown in Figure 1c. Note that in the CSL map forest has a canopy closure of > 30%. The histogram covers a range of probability scores of 0% to 100%, and is bi-modal with peaks at 4% and 90%. The second peak is by far the larger, starting at a probability score of around 80% and containing one-third of the total histogram. The average probability score of all pixels classified in the CSL map as forest is 55%. The CSL map has been smoothed to remove isolated clumps of pixels, and so this would account for the occurrence of pixels apparently classified as forest in the CSL map but which have a low probability score for 'scrub & forest' in the soft classification. Nevertheless, it is clear that the CSL map of forest contains much of the treeline ecotone and so is generalising some important ecological information.
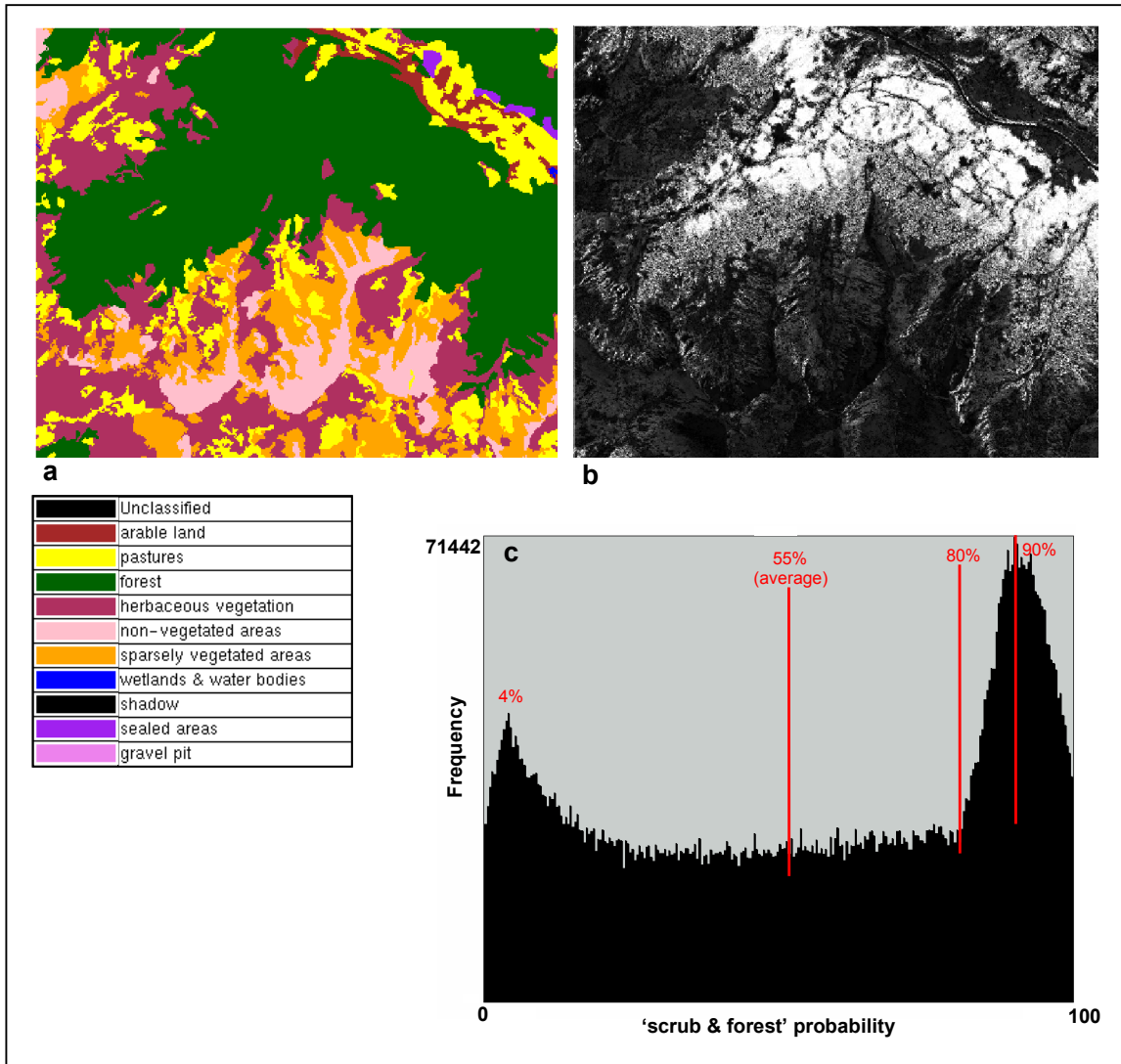
Figure 1. a) CSL map for a 6.5 x 4.5 km sample area of the field site, b) probability image for 'scrub & forest' from soft classification of SPOT 5 HRG image: dark = low probability, white = high probability, c) histogram of all probability pixels within the CSL class 'forest'.

Although the probability image for 'scrub & forest' has been shown to be meaningful in terms of forest composition, this is not by itself adequate to fully represent the treeline ecotone, since the transition is in fact between the vegetation classes 'pasture & natural grass' and 'scrub & forest'. For example, an area of clear felling or natural disturbance (e.g. windfall) within a woodland patch will have low probability classification as 'scrub & forest' but is not part of the treeline ecotone. A more intelligent treatment of the ecotone needs to consider the classification probability of both 'scrub & forest' and 'pasture & natural grass'. In Figure 2, the two end-members of *natural grass* and *forest* are defined by a probability of > 85% for 'pasture & natural grass' and for 'scrub & forest' respectively. For the three transitional classes, all pixels have a combined probability for 'pasture & natural grass' and 'scrub & forest' of > 50%, with the probability of 'scrub & forest' increasing from 15-35 % for *pasture with scrub*, to 36-65 % for *open scrub woodland*, and to 65-85% for *scrubby forest*. Note that *pasture* and *lowland forest & scrub* were separated from this ecotone map using the DTM, taking a threshold of 1400 m elevation and 10° slope.

4 CONCLUSIONS

Retaining the probability scores from a standard ML classification can enable the much more detailed characterization of an alpine treeline ecotone than a traditional 'hard' classification (such as in the CSL map). By simplifying the classes prior to classification and examining the transition between land cover types that grade between each other, the generation of ecotone maps could become an operational service of the GEOLAND project for habitat mapping across Europe.
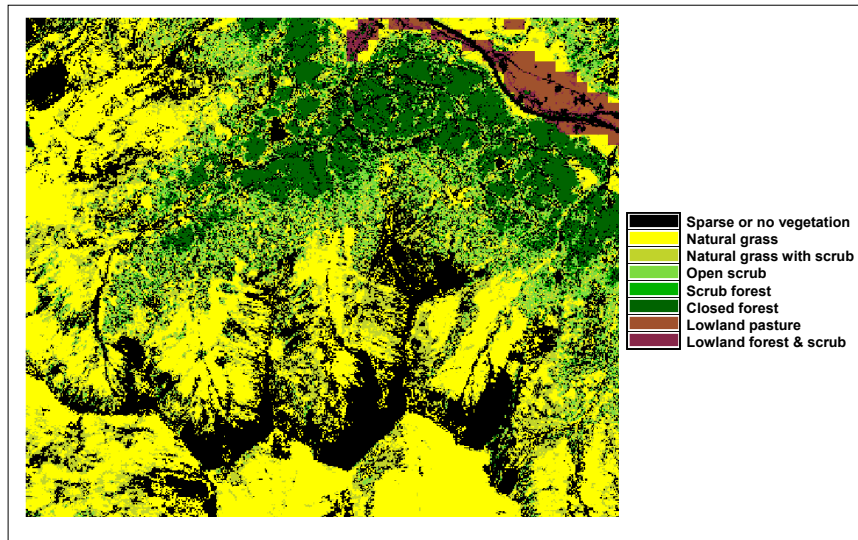
Figure 2. Ecotone characterization map for a 6.5 x 4.5 km sample area of the test site based on soft classification of a SPOT 5 HRG image.

REFERENCES

Allen, D.S. and Walsh, S.J. 1996. Spatial and compositional patterns of Alpine treelines, Glacier National Park, Montana. *Photogramm. Eng. Rem. S*. 62:1261-1268.

Cannon, R.L., Dave, J.V., Bezdek, J.C. and Trivedi, M.M. 1986. Segmentation of a Thematic Mapper image using the fuzzy c-means cluster algorithm. *IEEE Trans. Geosci. Rem. Sens*. 24:400-408.

Clements, F.E. 1905. *Research Methods in Ecology*. University Publishing Company. Lincoln, USA.

Di Castri, F., Hansen, A. and Holland, M.MN. 1988. A new look at ecotones: emerging international projects on landscape boundaries. *Biology Int.*, Special Issue 17.

Fisher, P.F. and Pathirana, S. 1990. The evaluation of fuzzy membership of land cover classes in the suburban zone. *Remote Sens. Environ*. 34:121-132.

Foody, G.M. 1992. A fuzzy set approach to the representation of vegetation continua from remotely sensed data: an example from lowland heath. *Photogramm. Eng. Rem. S*. 58:221-225.

Foody, G.M. 1996. Fuzzy modeling of vegetation from remotely sensed imagery. *Ecol. Model*. 85:3-12.

Foody, G.M. and Cox, D.P. 1994. Sub-pixel land cover composition estimation using a linear mixture model and fuzzy membership functions. *Int. J. Remote Sens*. 15:619-631.

Foody, G.M., Campbell, N.A., Trodd, N.M. and Wood, T.F. 1992. Derivation and applications of probabilistic measures of class membership from the Maximum-Likelihood classification. *Photogramm. Eng. Rem. S*. 58:1335-1341.

Hansen-Bristow, K.J., Ives, J.D. and Wilson, J.P. 1988. Climatic variability and tree response within the forest-alpine tundra ecotone. *Ann. Assoc. Am. Geog*. 78:505-519.

Johnston, C.A. and Bonde, J. 1989. Quantitative analysis of ecotones using a geographic information system. *Photogramm. Eng. Rem. S*. 55:1643-1647.

Quarmby, N.A., Townsend, J.R.G., Settle, J.J., *et al*. 1992. Linear mixture modeling applied to AVHRR data for crop area estimation. *Int. J. Remote Sens*. 13:415-425.

Raggam, H., Almer A., Strobl D. and Buchroithner M.F. 1991. RSG - State-of-the-Art Geometric Treatment of Remote Sensing Data. In *Proc. of 11th EARSeL Symposium: Europe: From Sea Level to Alpine Peaks, from Iceland to the Urals*, Graz, Austria, pp. 111-120.

Ranson, K.J., Sun, G., Kharuk, V.I. and Kovacs, K. 2004. Assessing tundra-taiga boundary with multi-sensor satellite data. *Remote Sens. Environ*. 93:283-295.

Schardt, M., Granica, K., Schmitt, U. and Gallaun, H. 2000. Monitoring of protection forests in alpine regions. In *Proc. of the 4.02.05 Group Session 'Remote Sensing and World Forest Monitoring', IUFRO XXI World Congress*, Kuala Lumpur, Malaysia.

Stevens, G.C. and Fox, J.F. 1991. The causes of treeline. *Annu. Rev. Ecol. Syst*. 22:177-191.

Walker, S., Bastow Wilson, J., *et al*. 2004. Properties of ecotones: evidence from five ecotones objectively determined from a coastal vegetation gradient. *J. Veg. Sci*. 14:579-590.

Wood, T.F. and Foody, G.M. 1989. Analysis and representation of vegetation continua from Landsat Thematic Mapper data for lowland heaths. *Int. J. Remote Sens*. 10:181-191.

TRANSITIONAL AND ABRUPT EDGES OF FOREST TO NON-FOREST BOUNDARIES ON MEDIUM RESOLUTION LANDSAT TM WINTER IMAGES

Kersti Püssa[a], Jaan Liira[a], Urmas Peterson[b,c]

[a]Institute of Botany and Ecology, Tartu University, Tartu, Estonia Institute of Botany and Ecology, University of Tartu, Lai 40, Tartu 51005, Estonia Kersti.Pyssa@ut.ee;
[b]Tartu Observatory, Tõravere 61602, Tartumaa, Estonia
[c]Faculty of Forestry, Estonian Agricultural University, Kreutzwaldi 5, Tartu 51014, Estonia

ABSTRACT

Forest management has produced fragmented landscapes in which edges are a dominant feature. In remote sensing, the accuracy of the detection and location of forest boundaries depends on the sharpness of the boundary, the spatial resolution of the available data as well as the subsequent methods used to detect them. Sampling is often constrained to large areas of classes with boundary areas are excluded from comparisons mainly to avoid misregistration problems and to enhance high confidence with the reference data set. As a result the accuracy statements can be biased and be not representative to the whole image area. In current study forest edges were delineated on Landsat Thematic Mapper (TM) images made in late winter under plain snow cover conditions. Our recent studies show that the threshold value, calculated as average of the 2nd and the 98th percentiles, is the best for the detection of forest edge location. We also found that the TM bands 2-4 are all equally good for the detection of the forest edge location on winter image, and we could not find any significant shadow effects when edges stable for several tens of years were observed. We found that late winter image with snow-covered ground is phenologically the best-timed images for detecting forest areas regionally because there are no differences between forest site types. When we focused on relatively recently cut and sharp forest to clearcut edges, the results of the analyses show that the contrast of Landsat TM measured radiance in the visible and near infrared spectral region between forest and clearcut area depends on adjacent forest parameters and on clear-cut area age.

Keywords: Forest change, forest edges, forest mapping, Landsat TM winter image, image classification

1 INTRODUCTION

The delineation of landscape patch boundaries between neighbouring vegetation communities is important for several aspects of land use management planning and in the compilation of resource inventories. The location and accuracy of the delimited vegetation boundaries, however, depend on the sharpness of boundary, the spatial and temporal resolution of the available data, as well as the subsequent statistical methods used to detect them (Fortin and Edwards 2001).

In a recent study, Landsat Thematic Mapper images from late winter - a non-traditional season for forest mapping, were used (Peterson 2003). The results of the study showed that forest mapping with winter images can give rather accurate results, with overall accuracy exceeding 90% when compared to forest boundaries derived from a coregistered map with forest boundaries delineated from orthophotos. Both commission and omission errors tended to fall within a two-pixel-wide zone around the forest patches.

Winter in boreal and hemi-boreal latitudes is the season with the greatest target to background contrast on predominantly two-class images composed of forest and non-forest classes. In winter, forest patches are surround on all sides by open areas with bright snow cover.
Change detection between two or more time periods is one of the most important uses of satellite remote sensing data in forestry applications and in monitoring land cover change in general. Pair wise image comparison methods have been a more widely used technique in change detection studies (Lawrence & Ripple 1999).

In northern temperate zone boreal and boreo-nemoral forests are characterized by marked seasonal variations. The seasonal changes in forest reflectance may be much greater than those caused by subtle,

year-to-year long-term changes (Nilson et al. 2003). It has been shown that if comparison of isolated dates has been applied in change studies the results vary from the detection of very large changes to no detected change, depending on the dates of the images being compared (Lambin 1996). Some authors (Cihlar 2000) have suggested that a "phenological correction" could be feasible in digital change detection of seasonally changing communities. Correcting for this type of error continues to be of interest in remote sensing research because it has been shown to be a significant cause of omission error in change detection (Mas 1999, Rogan et al. 2002).

A significant problem with per-pixel characterization of land cover is that a substantial proportion of the spectral signal apparently from the land area represented by a pixel actually comes from the neighbouring pixels (Townshend 1981). This is a consequence of many factors including the optics of the instrument, the detector and electronics, atmospheric effects, and image resampling (Schowengerdt 1997, Townshend et al. 2000). To find out differences that are not the real changes of forest area we delineated forest boundaries from two Landsat TM images that were taken on close dates.

The aim of our study was to: 1) Determine in which Landsat TM band, and at which threshold level, forest edges are most clearly detected. We assumed that the reflectance contrast between neighbouring pixels (pixel zones) should be the greatest at a forest edge. 2) Assess differences in forest edge contrast according to their azimuthal direction. 4) We tested whether there are any statistically significant differences in the reflectance of forest clear-cut communities on winter image. We also attempted to answer the following question: Do the stand parameters at the forest edge (e.g. stand height and tree canopy composition) and edge azimuth direction have an effect on the contrast of radiance at a forest edge? 5) To assess the stability of the edge location.

2 MATERIAL AND METHODS

2.1. SATELLITE DATA

A Landsat TM scene, Path 187 Row 19 according to the Landsat Worldwide Reference System, dated March 10, 1996 was used for determination of the optimal threshold level and Landsat TM band, and also for testing the reflectance properties in of forest clear-cut communities (Figure 1). Solar elevation at the image acquisition time was 23º26', solar azimuth was 148º35´, which is roughly from the south-east. The snow cover had remained at a thickness of about 30 cm for two weeks preceding Landsat overpass, with daily mean temperatures remaining below zero. Total precipitation as snow in the first ten days of March was 3 mm. Tree crowns, which can be heavily loaded with snow around Christmas time, are mostly bare in late winter, in March. The second, Landsat 7 Enhanced Thematic Mapper (ETM+) image acquired on 06 March 2003, Path 187 Row 19 in Landsat Worldwide Reference System, was used for studying the effect of adjacent forest parameters on the contrast of radiance at a forest edge (Figure 2). Solar elevation at the image acquisition time was 24º; solar azimuth was 159º (reference to the North). The snow cover had remained at a thickness of about 15 cm for two weeks before the time of data capture and was measured at 13 cm at the Estonian Meteorological and Hydrological Institute weather station at Tõravere, located within the study area. Atmospheric haze level was low in both years.

All used images were georeferenced using 1 m resolution 1:10 000 panchromatic digital orthophoto quadrangles. The images were geometrically registered to the Estonian National Coordinate System (Lambert-Est) using the nearest neighbor resampling algorithm and a linear transformation. For registration of both multispectral and panchromatic images, the total root mean square error was kept below 0.4 pixels. Atmospheric correction was not applied because statistical analyses relied on relative radiance differences of neighboring pixels within one scene and within a restricted area. Relative units of the scanner data, the so-called digital numbers (DN), in the 8-bit radiometric scale were used in these analyses.

2.2. STATISTICAL TREATMENT

Radiance contrast at forest-to-open area edges was defined as the difference between the mean DN value of the (last) boundary pixel zone of the open area and the mean DN value of the (first) boundary pixel zone of forest adjacent open area. For selection of the optimal threshold level for each Landsat TM band was defined as the strongest contrast of reflectance on a forest edge as the deepest regression slope value of reflectance intensity change from the last pixel zone inside the forest to the first (neighbouring) pixel zone of the open area. In the open area adjacent to forest, the forest clear-cut areas, the analysis of the reflectance dependency on clear-cut age and forest type group was performed. For exact description of statistical methods see Peterson et al. (2004) and Püssa et al. (2005). All significance tests were performed using the General Linear Model (GLM) module in Statistica Version 6.0.

3 RESULTS AND DISCUSSION

We tested a method for forest mapping by the thresholding of a Landsat Thematic Mapper image made in late winter in plain snow cover conditions in boreal and hemi-boreal bio-geographical zones. The optimal edge threshold level can be defined by looking for a maximum reflectance contrast of neighbouring pixels in a boundary area. While verifying the optimal forest delineation threshold, we found that the brightness contrast at the forest boundary is the greatest at around the mean threshold level, calculated as average of the 2nd and the 98th percentiles, and that the contrast of reflectance between neighbouring pixels decreases when diverging from that optimal threshold (Figure 3). Sub-sample analysis was performed to compare brightness contrast between spectral bands and intermediate cardinal points at an intermediate threshold level. Our results suggest that the most effective determination of the forest boundary on a wintertime satellite image could be carried out using average satellite image brightness intensity in Landsat TM bands 2, 3 or 4 (see also Peterson et al. 2004). The results support one global threshold level over the whole sub-scene area, since we did not detect significant differences in the contrast of differently exposed patch edges. No clear preference could be given to any of the Landsat TM visible bands in forest boundary delineation. Band 1 is significantly less effective and could be excluded from further studies. However, it should be noted that band 1 tends to be saturated at later dates in March.

Resampling of the forestland from two images taken in 9 days interval revealed that the mis-classification error at forest edges using presented methodology is about 3.6% of total forest area. At the same time, total area of forest doest not vary – 36.7 % on one and 36.2% on another. The reasons for error variation should be analysed.

Rapid changes of reflectance on clear-cut areas and reflectance contrast at edges are caused by the reforestation vegetation succession. Right after clear-cut logging, the clear-cut area is a sunlit ground that will rapidly be covered with herbaceous layer, usually within the first growing period. While monitoring year-to-year successional changes it is necessary to minimize phenological changes, which can be very apparent and can obscure subtle year-to-year changes. In the thick snow cover conditions in the winter image, the tree cover determines the radiance in visible bands, since young trees start to reach the crowns above snow. However, the coverage of tree stems and litter of herb plants above the snow surface is low and therefore, clear-cut areas do not show any significant variations between habitat type conditions during the first ten years of reforestation in winter conditions (see also Püssa et al. 2005).

Winter images have proved to be a suitable tool for forest–clear-cut boundary detection and zone radiance contrast description in visible and near-infrared spectral bands. The forest stand height adjacent to the clearcut, as well as conifer stem volume, were the most important factors determining the gradient of forest to clearcut radiance contrast in the studied mixed northern temperate and boreal forests in Estonia.

Our studies suggest the potential importance of considering edge effects in landscape-scale estimates of measuring clearcut-sized openings with abrupt edges in forests on Landsat-type medium spatial resolution satellite images.

4 FIGURES AND TABLES
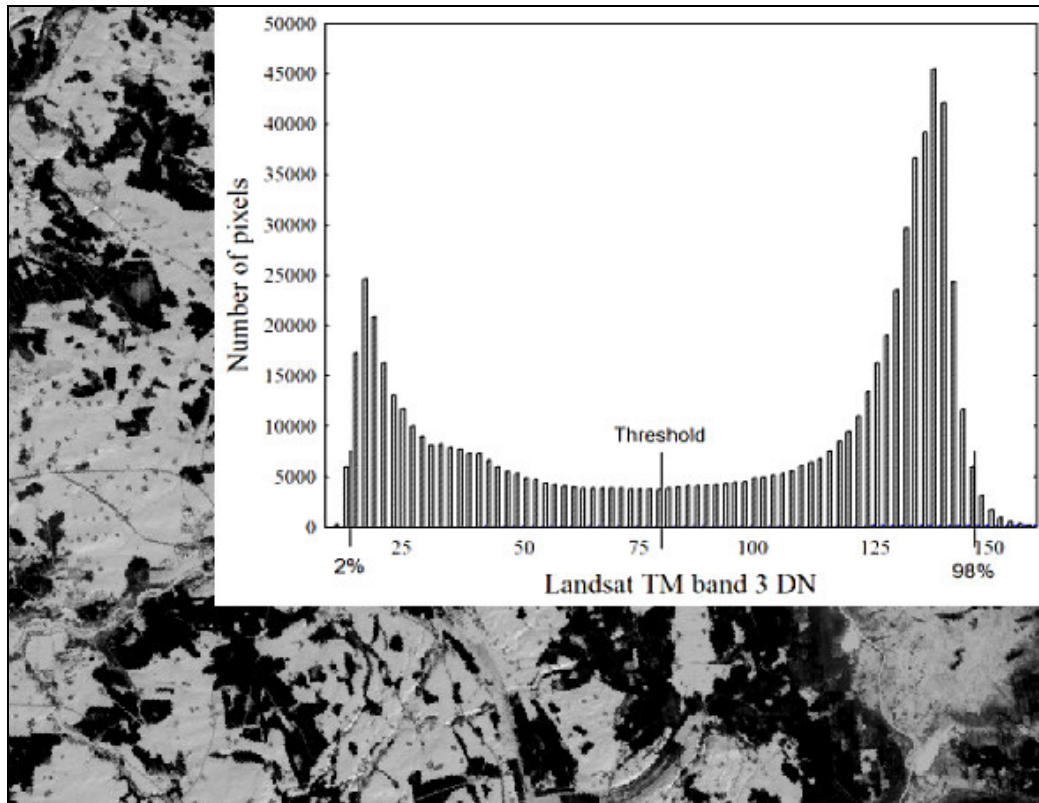
Figure 1. A fragment of a Landsat TM image representing an area of 25 x 15 km on the ground and a frequency distribution of the image pixel brightness values. Dry snow cover causes a significant radiometric contrast between open areas and forests. Two levels dominate in the frequency distribution. The highest radiance values correspond to snow-covered bare areas or areas covered with very low vegetation. The lowest randiance values correspond to conifer-dominated and mixed forests. Forest to non-forest boundary is thresholded between the 2nd and the 98th percentile values.
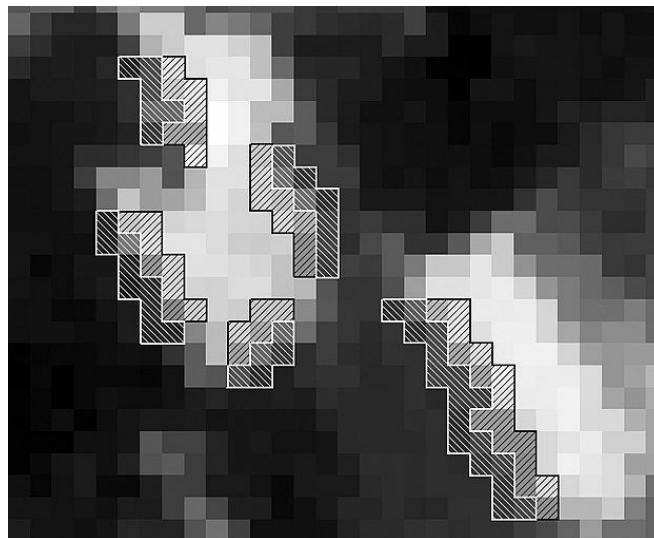
Figure 2. The sub-sample of Landsat ETM+ images in band 3 (TM3; pixel size 30m). Two clear-cut areas are seen as brighter areas. Edges with boundary zones, whose radiance is analysed, are marked with boxes. A white box frames the first pixel zone inside a forest and a black box denotes the first pixel zone inside a clearcut area. In analyses the average radiance value of pixels within a closed box were used.
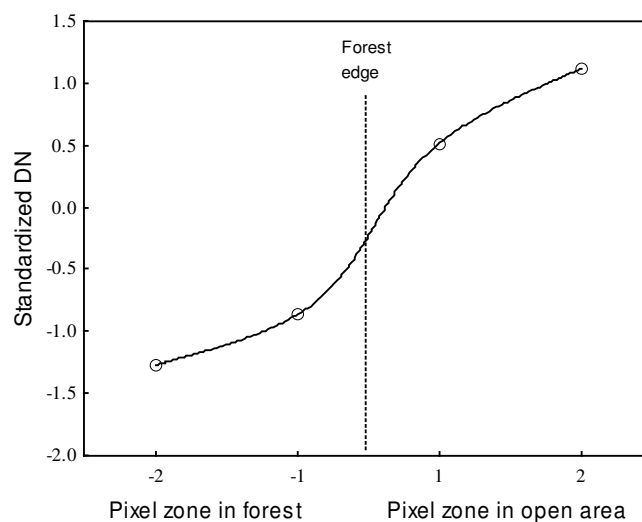
Figure 3. The reflectance pattern (mean standardized DN values) at the forest edge pooled over four Landsat TM bands at intermediate threshold level. Mean values of the first and second pixel zones in forest areas and in open areas are presented (Peterson et al. 2004).

5 ACKNOWLEDGMENTS

6 REFERENCES

Cihlar, J. 2000. Landcover mapping of large areas from satellites: status and research priorities. International Journal of Remote Sensing, 21: 1093-1114.

Fortin, M.-J. and Edwards, G. 2001. Delineation and analysis of vegetation boundaries. In Spatial Uncertainty in Ecology. Implications for Remote Sensing and GIS Applications, edited by C. T. Hunsaker, M. A. Friedl, M. F. Goodchild and T. J. Case, Springer, New York, pp. 158-174.

Lambin, E. 1996. Change detection at multiple temporal scales: seasonal and annual variations in landscape variables. Photogrammetric Engineering and Remote Sensing, 62: 931-938.

Lawrence, R. L. and Ripple, W. J. 1999. Calculating change curves for multitemporal satellite imagery: Mount St. Helens 1980-1995. Remote Sensing of Environment 67: 309-319.

Mas, J. E. 1999. Measuring land-cover changes: a comparison of change detection techniques. International Journal of Remote Sensing, 20: 139-152.

Nilson, T., Kuusk, A., Lang, M. and Lükk, T. 2003. Forest Reflectance Modeling: Theoretical Aspects and Applications. Ambio, 8: 535-541.

Peterson, U. 2003. Forest mapping for Eastern Baltic region with Landsat Thematic Mapper winter images. Research for Rural Development. Conference Proceedings held in Jelgava, Latvia on 21-24 May 2003, Jelgava, Latvian University of Agriculture.

Peterson, U., Püssa, K. and Liira, J. 2004. Issues related to delineation of forest boundaries on Landsat Thematic Mapper winter images. International Journal of Remote Sensing, 24: 5617-5628.

Püssa, K., Liira, J. and Peterson, U. 2005. The effects of successional age and forest site type on radiance of forest clear-cut communities. Scandinavian Journal of Forest Research, (in press).

Rogan, J., Franklin, J. and Roberts, D. A. 2002. A comparison of methods for monitoring multitemporal vegetation change using Thematic Mapper imagery. Remote Sensing of Environment 80: 143-156.

Schowengerdt, R. A., 1997, Remote sensing: models and methods for image processing, Academic Press, San Diego.

Townshend, J. R .G. 1981. Spatial resolution of satellite images. Progress in Physical Geography, 5: 33-55.

Townshend, J. R. G., Huang, C., Kalluri, S. N. V., DeFries, R. G. and Liang, S. 2000. Beware of per-pixel characterization of land cover. International Journal of Remote Sensing, 21: 839-843.

ACCURACY ASSESSMENT OF FOREST STAND DELINEATION USING VERY HIGH SPATIAL RESOLUTION SATELLITE IMAGES

J. Radoux and P. Defourny

Department of Environmental Science, Université catholique de Louvain,
Croix du Sud 2 bte 16, 1348 Louvain-La-Neuve, Belgium
Email: radoux@mila.ucl.ac.be, defourny@enge.ucl.ac.be

ABSTRACT

Per-field classification with very high resolution multispectral imagery improves the discrimination within forest stands through the combined use of spectral, textural and contextual information in object based classification. Stands delineation therefore plays a major role for the quality of the results. This paper implements a method to assess the planimetric quality of remotely sensed boundaries produced by segmentation of IKONOS and SPOT 5 images. It also evaluates the effect of the Douglas-Poiker and a new mid-line generalisation algorithm on the delineated stands. Accuracy assessment was performed with a 1/10000 topographic map as reference and measured both the bias and the mean range of error around the borders. This method of validation offers a description of errors adapted to per field classification and expansible to other areas.

Automated versus manual segmentation by was found to be unbiased and had a range smaller than the pixel size. Compared to the reference dataset, the bias for the delineated stands was more than one meter and is mainly due to an uncorrected parallax. The effect of the viewing elevation angle on the delineation could be reported to the theoretical values and is largely above the other errors. Performance of SPOT 5 and IKONOS for the discrimination between non forest and coniferous or deciduous stand was very similar. The new generalisation algorithm improved both the rendering and the planimetric quality of the delineations.

Keywords: Accuracy assessment; Generalization; Very high resolution; Forest mapping ; Segmentation

1 INTRODUCTION

Up to date description of forest stands is of paramount importance for the sustainable management of forests. With the integration within geographic information system, large scale forest maps indeed become powerful tools for forest managers. Remote sensing has potential to provide such maps with greater coverage than is achievable using field sampling and foresters were amongst the first photointerpreters (Howard, 1984).

With the development of very high resolution satellites (SPOT 5, IKONOS-2, QuickBird, OrbView-3), automated and semi automated method have been developed in order to extract useful stand information from remotely sensed data. The increase of within class spectral variability becomes a hindrance to per pixel classification but sometimes has been taken advantage of textural analysis (Kayitakire, 2002). As pixel size becomes smaller than tree crowns, tree objects can be delineated as a primary step to improve classification (Leckie et al, 2003; Erikson, 2003). Furthermore, the use of image-object in the classification conveniently incorporates extra knowledge, like shape and context, that contributes to a more accurate classification. (Flanders, 2003; Benz, 2004).

While per-field classification has proven its advantages in VHR remote sensing, the segmentation step is a key to its efficiency (Peterson, 2004; de Wit and Clevers, 2004). Due to the heterogeneity of pixel value in VHR forest images, region-based segmentation performs better than edge-based (Pekkarinen, 2002). Several methods of morphological mathematics (region growing, region splitting, pattern recognition and semi-variogram), have been developed to delineate more accurately forest stands from remote sensing data (Dorsen et al, 2003; Wang et al, 2004 ; Flanders, 2003 ; Leckie et al, 2003).

The aim of this study is to quantitatively assess the quality of stands delineation of IKONOS-2 and SPOT 5 images for topographic and forest management purpose. It contains a post processing algorithm for boundaries generalisation to improve the rendering of the data. An edge specific method of accuracy assessment addresses the quality control of the resulting delineation.

2 REFERENCE DATA

The reference dataset for orthorectification and geometric quality assessment came from the 1/10 000 topographic vector database (topo10GIS) of the National Geographic Institute (NGI). It guarantees less than 1 m of error in 95 % of the cases and describes 7 forest classes, namely coniferous, mixed with coniferous dominance, mixed with broadleaves dominance, mixed, broadleaves in coppice and broadleaves regular or irregular forest. The digital elevation model was produced from contour lines with altitudinal steps of 5 meters.

In order to test the segmentation independently from the geometry of the image, a subset of the single IKONOS image was manually delineated and worked as a second reference dataset. This subset was embracing a deciduous/coniferous interface of 16 km.

3 SITE DESCRIPTION

A study area of 2900 hectares was chosen for its diversified forest stands representative of the major species in Belgium, its relatively gentle slopes and the availability of ancillary data. This area is dominated by various forest stands. Peat swamps and rural areas are also present.

The study area is located in Southern Belgium, about 15 km on the south of Francorchamps. The main tree species are spruce (*Picea abies*), beech (*Fagus sylvatica*) and oak (*Quercus sp*). Other coniferous, like *Pseudotsuga menziesi* and *Larix decidua*, and broadleaves, like *Alnus glutinosa* and *Betula pendula*, are also present. About 60 percent of the forested area falls into public land and the remaining is privately owned.

4 IMAGE DATA AND PREPROCESSING

The image dataset includes one SPOT 5 and 3 IKONOS-2 (one single image and the 2 lids of a stereo pair) satellite images overlapping on the study area and acquired between 2003 and 2004.

The SPOT 5 image was panfused at 5 m of resolution with 4 spectral bands (green, red, near-infrared, middle-infrared). The single IKONOS image was used as a 1 meter panchromatic and a 4 meter multispectral image. The 2 lids of the stereo pair were provided as panfused 1 meter resolution images with 4 spectral bands each (blue, green, red and near infrared).

The viewing elevation angle of all the scenes was around 60 degrees, excepted for the second lid of the stereo pair (73 degree). The images were orthorectified by using ground control points and digital elevation model from our reference dataset. The area covered by clouds (including shades) represents about 4 % of the study area and was extracted from the data after manual delineation.

5 METHOD

5.1 GENERALISATION

The rough results of segmentation are not ready to be included as a GIS layer or to be used for a cartographic purpose. The negative visual effect of the stair like aspect due to the pixels will be removed using generalization algorithms.

In order to assess the effect of this generalisation on the geometric quality of the delineation, two algorithms were tested against the non simplified edges. The first one is the point removal algorithm developed by Douglas and Peucker (1973) and the second is a line averaging algorithm developed in the framework of this study.

As the objective of these algorithms was to produce smoother borders without degrading the scale, the maximum allowable offset for point removal algorithm of Douglas and Poiker was fixed to 1.5 pixel size, thus a bit more than the diagonal of the pixels.

The second generalization was conducted using the mid-line generalization algorithm. Its goal was to produce generalized edges without affecting their spatial accuracy but decreasing their range of variation around the reference. It starts by building two outer lines passing either through the left or through the right extrema of the line within a given search radius. Once the "left" and "right" outer lines are created, the mid-line is created by joining vertices located at equal distance from their edges. We used here a tolerance of 3 pixels.

5.2 GEOMETRIC QUALITY ASSESSMENT

Each image was segmented using the commercial software e-Cognition (Baatz and Schappe, 2000). From the parameters used by the segmentation algorithm, the scale and the compactness where iteratively adjusted in order to create compact segments including no more than one forest type.

The key source of error in per-field classification is the location of the edges. Information on the edges can help to better identify these errors and evaluate the reliability of a method for different purposes. It is thus well suited to the assessment of a delineation methodology even if it is heavy to implement. Furthermore, a rough estimate of the edge length in a new study area can give a good prediction of the final accuracy of a new cartographic product using a given methodology.

The planimetric quality of the edges was evaluated based on the concept of accuracy and precision. The first estimator was the bias and the second, the mean range. These estimators were derived after intersecting the image objects with the reference dataset. The area of the non-matching polygons was counted as negative when it induced an underestimate of the stand area and as positive in the other case. The bias is then calculated by adding the signed areas for each interface type, and the mean range is defined as the sum of the unsigned area, minus the absolute value of the bias. These two estimators were normalized by the total interface length in order to be expressed in map unit.

6 RESULTS AND DISCUSSION

6.1 GENERALISATION

Considering the visual aspect of the two generalisation algorithms used in this project is difficult because it is subjective. However, generalization is definitely a major improvement compared to the rough data.

The Douglas-Poiker algorithm performs best when lines can be reduced to a single segment but its very angular shape does not well fit to curved boundaries. Additionally, this algorithm may cause independent lines to cross each other which results in the creation of artifacts. It appears thus that the mid-line algorithm presents a more adequate representation of the forest boundaries at the intended large scale for all the segmentations. Figure 1 shows the results of the algorithm on a coniferous / deciduous edge detected from the multispectral IKONOS image of June the 7th.
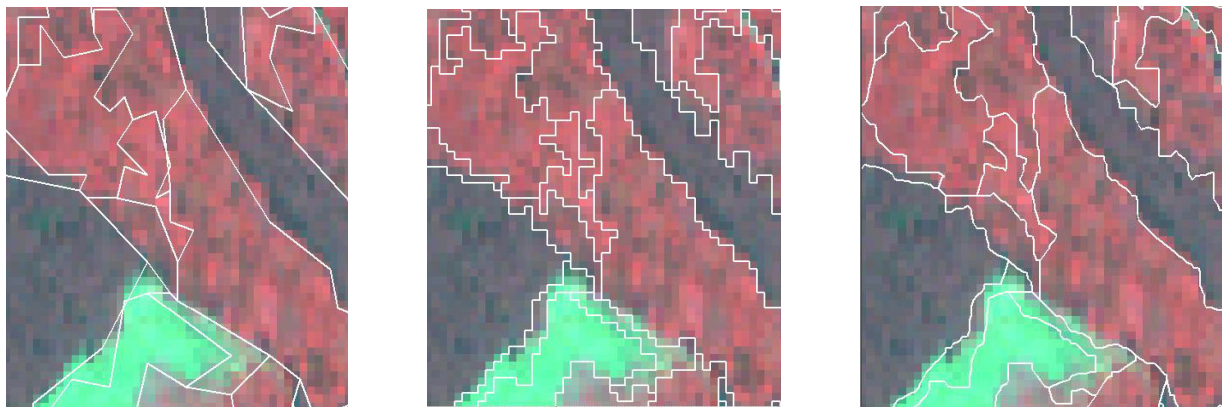
Figure 1. Results of the segmentation on the IKONOS multispectral image with the Douglas-Poiker algorithm (Left), without generalization (Center) and with the mid-line generalization (Right).

Beside its visual effect, the generalisation algorithm slightly affects the planimetric quality of the boundaries. As a general trend, running the mid-line algorithm decreases the mean range (up to 24 %) while the Douglas-Poiker point removal tends to increase this range of 5 percents in average. The effect of generalisation on the bias was much more dependent on the geometry of the objects, so that no tendency could be identified.

6.2 SEGMENTATION ASSESSMENT

Accuracy assessment of the IKONOS multispectral (4 m) image using the manually delineated stands showed that the method of segmentation was close to be unbiased. After mid-line generalisation, the bias was of 0.11 meters in favors of the coniferous stands and the range as low as 3.6 m. The variance

minimizing segmentation algorithm indeed preferably groups (darker) shaded pixels with the dark coniferous region than with the (lighter) deciduous stands.

6.3 GROUND TRUTH VALIDATION

The stand delineation obtained by the segmentation of the different images compared to the ground reference dataset showed bigger bias and range of values. Some of the errors came from the reference dataset itself (not up to date) but the most important source of error is the geometric deformation of the image. The bias on the forest / non forest edge is indeed around 1.75 m for most images. The origin of these errors is mainly the parallax remaining despite the orthorectification (because the height of the stand could not be accounted for). This displacement away from the satellite is given by the formula:

"Height difference" / TAN (viewing elevation angle).

Figure 2 shows the effect of the parallax on the two images from the IKONOS stereo pair. Theoretical displacement for a stand height of 20 m is 11.5 m for the 60 degree elevation image and of 6.88 for the elevation image. This difference was effectively observed on the images and induced an overall increase of the bias of 2 meters between the second lid of the stereo pair and the other images.

The value of the mean range is close to the pixel size for the multispectral IKONOS image and for the fused SPOT 5 image for forest / non forest edges (respectively 4.3 and 5.1 m), and is around 3 meters for the IKONOS fused and panchromatic 1 meter images.
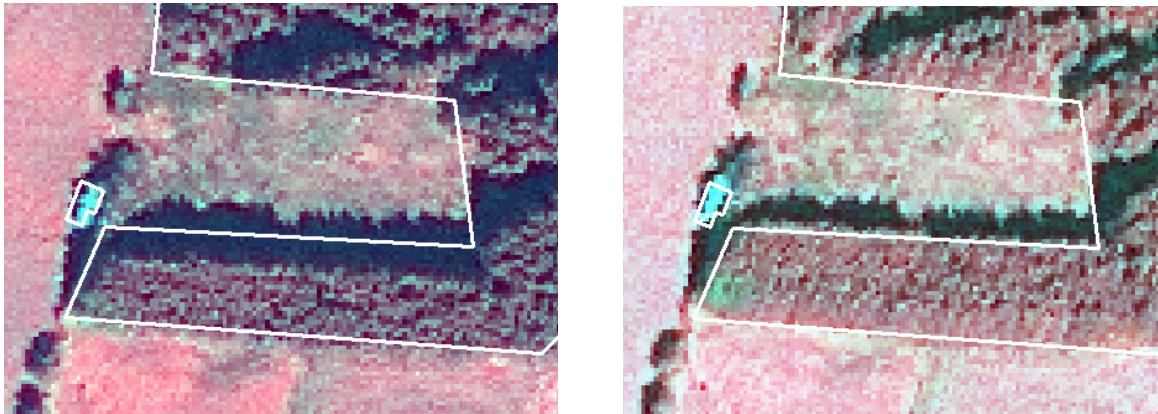
Figure 2. Error due to the parallax on the two elements from the stereo IKONOS pair. The viewing elevation angle was 71 degrees of the left image and 60 degrees on the right image.

7 CONCLUSION

The quality of forest stand delineation from automated segmentation is above the planimetric quality of a single image orthorectified without prior knowledge of the stands height. Due to their similar precision and accuracy in stand delineation, SPOT 5 and IKONOS are thus both adapted to the discrimination between non forest, deciduous forest and coniferous. However, as SPOT 5 is more cost effective than IKONOS, it represents a better alternative. Classification potentials from the middle infra red bands of SPOT 5 or the higher textural information of IKONOS have to be considered in this choice.

Boundary generalization using the mid-line algorithm is well suited to cartographic purposes. It achieves indeed a better visual rendering of the delineation without negative effect on the quality of the information in terms of bias and mean range.

The bias shows a tendency to overestimate the forest stands. It is mainly due to the remaining parallax after orthorectification and would need a prior knowledge of the stands height in order to be corrected from a single image. Forest mapping from small elevation viewing angle is thus an issue and would not produce reliable forest maps at a scale larger than 1/50000 without specific post processing.

REFERENCES

Howard, J.A. 1984 *Remote sensing of forest resources: Theory and application* Chapman 418 p

Kayitakire, F., Giot, P. and Defourny, P. 2002 Discrimination automatique des peuplements forestiers à partir d'orthophotos numériques couleurs *Canadian Journal of Remote Sensing* 28 (5) pp 629-640

Leckie, D.G., Gougeon, F.A., Tinis, S., Nelson, T., Burnett, C.N. and Paradine, D. 2005 Automated tree recognition in old growth conifer stands with high resolution digital imagery *Remote Sensing of Environment* 94 pp 311-326

Erikson, M. 2003 Segmentation of individual tree crowns in colour aerial photographs using region growing supported by fuzzy rules *Canadian Journal of Forest Research* 33(8) pp 1557-1563

Flanders, D., Hall-Beyer, M. and Perverzoff, J. 2003 Preliminary evaluation of eCognition object based software for cut block delineation and feature extraction. *Canadian Journal of Remote Sensing* 29(4) pp 441-452

Benz, U.C., Hofmann, P., Willhanck, G, Lingenfelder, I. And Heynen, M. 2003 Multiresolution, object oriented fuzzy analysis of remote sensing data for GIS ready information *ISPRS journal of Photogrammetry and Remote Sensing* 58(3-4) pp 239-258

Peterson, U., Pussa, K. and Liira, J. 2004 Issues related to delineation of forest boundaries on Landsat TM winter images *International Journal of Remote Sensing* 25 (24) pp 5655-5668

De Wit, A.J.W and Clevers, J.G.P.W. 2004 efficiency and accuracy of per-field classification for operational crop mapping *International Journal of Remote Sensing* 25(20) pp 4091-4112

Pekkarinen, A 2002 A method for the segmentation of very high spatial resolution images of forested landscapes *International Journal of Remote Sensing* 23(14) pp 2817-2836

Dorsen, L.K.A., Maier, B. and Seymonsbergen, A.C. 2003 Improved Landsat based forest mapping in steep mountainous terrain using object based classification *Forest Ecology and Management* 183(1-3) pp 31-46

Wang, L., Sousa, W.P. and Gong, P. 2004 Integration of object based and pixel based classification for mapping mangroves with IKONOS imagery *International Journal of Remote Sensing* 25(24) pp 5655-5668

Leckie, D.G, Gougeon, F.A., Walsworth, N. and Paradine, D. 2003 Stand delineation and composition estimation using semi-automated individual tree crown analysis. Remote Sensing of Environment 85(3) pp 355-369

Baatz, M., and Schäpe, A. (2000): Multiresolution Segmentation – an optimization approach for high quality multi-scale image segmentation. In: Strbl, J. et al. (Hrsg.): Angewandte Geographische Informationsverarbeitung XII (pp. 12–23). Beiträge zum AGIT-Symposium Salzburg 2000, Karlsruhe, Herbert Wichmann Verlag .

Douglas, D.H. and Peucker, T.K 1973 Algorithms fort he reduction of the number of points required to represent a digitized line or its caricature Canadian Cartographer 10 (2)

MAPPING STORM DAMAGES TO FORESTS USING OPTICAL AND RADAR REMOTE SENSING. THE CASE OF THE DECEMBER 1999 STORMS IN FRANCE

N. Stach[a] , M. Deshayes[b] T. Le Toan[c]

[a] IFN, 32 Rue Léon Bourgeois 69500 Bron, France , email: nstach@lyon.ifn.fr
[b] Cemagref UMR TETIS, 500 rue J-F. Breton, 34093 Montpellier Cedex 5, France
[c] CESBIO 18, avenue Edouard Belin BPI 2801, 31404 Toulouse Cedex 4, France

ABSTRACT

After the 1999 storms in France, IFN has considered using satellite imagery to map the damages caused to forests. After a first disappointing urgency test using winter images, IFN gave up this solution and ordered aerial coverages. Two years later, IFN, Cemagref and Cesbio decided to re-explore the use of optical and radar satellite imagery. They developed and validated methods on several test sites representative of French forest conditions in lowland and hill situations. The mapping of the damages with optical images was based on a change detection method and carried out in three steps, a pixel-based supervised classification of difference-images, a segmentation of pre-storm images in homogenous objects, and an integration of the pixel-based classification and the segmentation to produce the final damage map.The positive results obtained with SPOT summer data allow to envisage operational applications of these methods.

Keywords: Storm damage, optical, radar, change detection, segmentation

1 INTRODUCTION

In end-December 1999, France and other countries on Europe's western edge were hit by two consecutive storms with a power and violence that had never been experienced before. French forests sustained severe damages: about 100,000 ha of forest were affected and about 170 million cubic of wood was either felled or broken. In January 2000, the French ministry in charge of forests entrusted IFN (French National Forest Inventory) with mapping the affected zones and estimating the extent of damage. In view of the huge area to be covered, IFN considered the use of satellite imagery. In the absence of any previous comparable experience, IFN set up an expert group to conduct a preliminary feasibility study. This preliminary study found that it would be difficult to do the job using satellite data acquired in winter and for areas with topography. IFN thus decided to map the damage using photo-interpretation of aerial photographs, with the exception of the maritime pine of the Aquitaine massif (1 million ha) for which it mapped the damage using Landsat TM images (Stach, 2000). Since the mapping by photo-interpretation was proving very time-consuming (results produced in first and second 2001 semesters ???), IFN, Cemagref and CESBIO decided to re-explore the possibilities of mapping the damage using satellite remote sensing with the objective of developing and validating methods that could be used for any future event of similar nature

2 TEST SITES AND DATA

2.1 STUDY AREAS

In order to obtain general results on the possibilities and limits of mapping storm damage from satellite imagery, the tests were performed on different test sites, as representative as possible of French forest conditions in lowland and hilly situations. 8 test sites distributed in 3 regions of interest have been defined. Table 1 describes the forest conditions present in the 8 test sites.

Table 1. Test sites description

Region of interest	Test Site	Main forest types	Relief	Damages;Intensity	Damages distribution
Région 1 South west massif central	Double	Maritime pine high forest Pine High forest and coppice Coppice	Flat hills	Massive	Both large area and sparsely distributed
	Limousin Plateaus	Coniferous high forest	Undulating Plateaus	Massive	Sparsely distributed
	Limousin chestnut grove	Coppices (chestnuts) Broad-leaved high forest and coppice Coniferous high forest	Hills	Massive	Sparsely distributed
	Braconne forest	Broad-leaved high forest Broad-leaved high forest and coppice	Low flat plateaus	Massive	Large area
Region 2 Parisian basin Border	Othe forest	Broad-leaved high forest Coniferous high forest Broad-leaved high forest and coppice	Low plateaus	Heavy	diffuse
	Wet Champagne	Broad-leaved high forest Coniferous high forest Broad-leaved high forest and coppice Poplar	Plain	Heavy Mainly in Coniferous	Large area
	Burgundy Plateaus	Broad-leaved high forest Coniferous high forest Broad-leaved high forest and coppice	Plateaus	Locally important	Locally concentrated
Region 3 Normandy	Ecouves forest	Broad-leaved high forest Coniferous high forest Broad-leaved high forest and coppice	Hills	Massive mainly on coniferous	Locally concentrated

2.2 DATA

The question of map delivery delay being crucial in an operational context of storm impact assessment, it was decided to test the method with different types of satellite data acquired at different seasons. As the methods are based on a change detection process, one reference image before the storm and one after-storm image is acquired on each test site and season (Table 2).

Table 2. Optical imagery acquired on test sites

Test Site	Winter / early spring images	Spring images	Summer images
Double		SPOT4 26/05/99 SPOT4 24/05/00	Landsat 5 TM 11/08/98 and 31/07/00
Limousin Plateaus			Landsat 5 TM 11/08/98 and 31/07/00
Limousine chestnut grove			Landsat 5 TM 11/08/98 and 31/07/00
Braconne forest	SPOT2 09/02/98 SPOT4 12/02/00		Landsat 5 TM 11/08/98 and 31/07/00
Othe forest	SPOT2 01/04/99 SPOT1 07/04/00		Landsat 5 TM 11/08/98 and 31/07/00 SPOT4 30/07/99 and SPOT2 19/07/00
Wet Champagne			Landsat 5 TM 11/08/98 and 31/07/00
Burgundy Plateaus			Landsat 5 TM 11/08/98 and 31/07/00
Ecouves forest			SPOT1 25/06/00 and 28/06/00 SPOT4 03/08/98 and 29/06/00

In the microwave domain, active sensors have their own source of emission and the signal is not affected by clouds. The question of acquisition season is less crucial but a long chronological series of images is needed for reducing speckle using multitemporal filtering. Two series of before-storm and after-storm ERS2 images were acquired on Othe and Double main test sites (Table 3).

Table 3. Radar imagery acquired on test sites

Test site	Othe test site	Double test site
Sensor	ERS2 Frame 2637 Track 423	ERS2 Frame 2691 Track 237
Before-storm images (1999)	June, July, November, December	June, August, October
After storm images (2000)	January, March, June, July	January, March, August

In addition to satellite imagery, other data were used in this project including digital terrain elevation models, topographic maps, IFN vegetation maps and IFN forest damage maps produced by photo-interpretation of large scale aerial photos. These last maps were used as reference data for image interpretation and accuracy assessment.

3 IMAGE PROCESSING

3.1 RADAR REMOTE SENSING

3.1.1 Image preprocessing

Image preprocessing was realized with *Gamma remote sensing* softwares. It includes spatial and temporal filtering and image geocoding. Spatial and temporal filtering are done to reduce the speckle in radar images. For a temporal series of M images, the filtered value of image i (Ji)is given by given

$$J_i = \frac{\sigma_i}{M} \sum_{j=1}^{M} \frac{I_j}{\sigma_j} \qquad 1 \leq i \leq M \tag{1}$$

with σi the backscatter coefficient of image i, Ij the Intensity value of image j and σj the backscatter coefficient of image j.

Temporal filtering is performed with an adaptive filter that reduces the speckle but preserves the radiometric edges in original images.

3.1.2 Radiometric analysis

The analysis of radiometric signatures of different landcover types extracted from the IFN vegetation maps on the two test sites has shown that forest could be characterized by:

2. a backscattering coefficient ranging from –3db to –11db whereas it could range from +7db to –14db in other types of landcovers,

3. a temporal stability of backscattering coefficient. This was assessed through 3 criteria, temporal variance of backscattering coefficient, maximum variation given by the ratio between highest and lowest temporal value and the mean temporal (*mv*) variation given by

$$mv = 10\log\left[\frac{2}{N(N-1)}\sum_{i=1}^{N-1}\sum_{j>i} R_{ij}\right], \qquad \text{with } R_{ij} = \max\left\{\frac{\hat{I}_i}{\hat{I}_j}, \frac{\hat{I}_j}{\hat{I}_i}\right\} \tag{2}$$

3.1.3 Damage mapping

On the two test sites, one before-storm forest mask and one after-storm forest mask have been produced classifying respectively before-storm images series and after-storm images series. The classifications were performed by applying thresholds for the 4 criteria presented above: mean backscattering coefficient, temporal variance, max temporal variation and mean temporal variation. The thresholds were determined interactively to fit to the reference stands extracted from IFN vegetation maps.

The damaged areas were deducted from these two forest maps as being the areas that were in the before-storm forest mask no more in the after-storm forest mask.

3.2 OPTICAL REMOTE SENSING

3.2.1 Image preprocessing

SPOT images used in this project were acquired at level 3, which is to say that they were already orthorectified with a residual error lower than 1 pixel (30 m). All Landsat images have been geocoded with a polynomial transformation model based on ground control points.

For each before-storm / after-storm image couple, a relative radiometric normalization has been realized in order to make them comparable independently of the atmospheric conditions. The normalization method is a linear model defined on no-change targets of the images. For each band, the normalized digital count (DCnorm) is a linear function of the original digital count (DC):

DC norm = a DC + b , with a and b being estimated from a linear regression between the digital counts of no-change objects in the two images.

Once the two images of each couple are normalized, an image difference has been computed as the pixel to pixel difference between the second image of the couple and the first image in every spectral band.

3.2.2 Radiometric analysis

In every test site, two samples of reference stands in each forest type have been extracted from IFN maps: one sample of damaged stands and another of not damaged stands. The radiometric signatures of these two samples in the corresponding difference-images were extracted and analyzed. The significance of the difference between damaged and not damaged stands radiometric evolution has been analyzed depending on the forest types, the acquisition season and the spectral bands.

Confirming previous experiences it was found that the discrimination of damaged stands using winter images was very low, except for some rare cases in pure coniferous high forest on flat terrain. On the other hand, significant differences were obtained with spring (from May) and even more with summer images.

Concerning spectral bands, it appears that the more performing bands were in the SWIR spectral domain (SPOT 4 XS4 or TM5 and TM7). The visible bands (XS1, XS2, TM1, TM2, TM3) were slightly less performing but presented some significant differences between damaged and not damaged stands. The worst results were obtained in the NIR domain (XS3, TM4), where very few significant differences could be observed between the two samples.

3.3.3 Damage mapping

The mapping of the damages was realized in three steps. The first is a pixel-based supervised classification of difference-images. In the same time, the original images were segmented in homogenous objects. At the end, the pixel-based classification was integrated in the segmentation and a damage intensity was affected in each object of the segmentation in order to produce the final damage map.

The pixel based classification was performed on every difference-image with a supervised process based on the maximum likelihood criteria. It produces for each test site, sensor and acquisition period a 3-class classification : not damaged pixels, partially damaged pixels and totally damaged pixels.

The segmentation was performed with *Definiens eCognition* software (Baatz & Schäpe, 2000). It proposes a multiscale segmentation. Its segmentation algorithm uses 5 parameters: the scale parameter corresponding to the maximum heterogeneity tolerated inside each resulting segment, the shape and color factors determining the respective weight of shape and radiometry in the segmentation process and the smoothness and compactness factors. The parameters have been interactively fixed for each image from trial and error procedure on sub-samples of the images and then applied to the whole images.

The last step of damage mapping consists in integrating the pixel classifications and the segmentations results. The number of pixels of each class detected in each homogenous segment has been counted. The damage of the segment was then computed, with the following formula:

Segment_Damage = Nb_totally_damaged_pixels + k . Nb_partially_damaged_pixels, with $0 \leq k \leq 1$,

k being a coefficient which was calibrated using a set of representative training segments with known rate of damage. The method ended by classifying the segment in one of the 5 classes of damage depending on the percentage of area affected by the damages : 0 to 10%, 10 to 50%, 50 to 90% and more than 90%.

4 RESULTS AND DISCUSSION

In the radar domain, the discrimination between forest and other landcover gives quite good results in the Othe test site. About 90% of the closed forest on IFN maps were classified as forest and the false detection rate was about 26%. On the Double test site the results were more disappointing. About 80% closed forest was correctly classified as forest but the false detection rate reached more than 60%. Moreover, in the two test sites, the damage maps obtained by comparison of before-storm and after-storm masks were very disappointing. A visual comparison of these maps with the reference IFN maps showed very important differences and no further time consuming quantitative accuracy assessment was carried out.

In the optical domain, a very intensive validation process has been carried out. Every satellite derived map has been crossed over in a GIS with the reference IFN damage maps. In order to take into account the obligatory part of subjectivity contained in IFN human made maps, the difference between satellite derived maps and reference was not necessary consider as errors but re-interpreted on the large scale aerial photos acquired for damage mapping. The differences were classified in omission errors, commission errors (false detection), confusion errors (damage map on both reference and satellite maps but with a different intensity class) or false errors (due to subjectivity). The control has been realized on more than 26 000 ha of forest among witch 10 000 ha of damaged stands. Obtained results varied as a function of the sensors and the season. Satisfactory results were obtained with SPOT summer data with omission rate ranging from 3% to 14%, commission rate ranging from 6% to 14% and confusion rate from 15% to 20%. With Landsat images the results were distinctly worse, specially in the test sites with sparsely distributed or diffuse damage patterns: the omission and confusion rates exceed 35% in the Double test site. As expected, results obtained with winter images were very poor, particularly in broad-leaved dominated sites: for example the omission rate in Othe test site was 93%.

5 CONCLUSION AND PERSPECTIVES

Most of the results obtained in this project confirm previous experiences using remote sensing to map storm damage to forest with satellite remote sensing (Schwarz et al. 2001). The interest is that these results have been obtained from intensive validation on a wide range of forest conditions representatives of French lowland and hills forests. The good results obtained with SPOT summer data let envisage the use of these remote sensing techniques in an operational context. In the case of winter storm, the necessity to wait for summer images excludes the use of optical imagery for urgency assessment of damaged areas, however the fact that the satellite derived maps present the same specifications and the same quality as photo-interpreted map allow to combine these two techniques with a higher efficiency. In 2003 for example, IFN realized the forest damage map on the "Vosges" 'département' combining satellite based methods on the hilly and flat regions of the 'département' and aerial photography in the mountainous areas.

ACKNOWLEDGMENTS

REFERENCES

Stach, N. 2000. L'IFN cartographie les dégâts de la tempête sur le massif aquitain de pin maritime. *Géomatique Expert*, 5: 15-17.

Baatz, M. and Schäpe, A. 2000. Multiresolutional segmentation – an optimization approach for high quality multi-scale image segmentation. *In: Strobl, J., Blaschke, T. and Griesebner (Eds.): Angewandte Geographische Informationsverarbeitung* XII: 12–23.

Schwarz M., Steinmeier C., and Waser L. 2001. Detection of storm losses in alpine forest areas by different methodic approaches using high-resolution satellite data. *21st EARSeL Symposium,* PARIS.

INTERPRETATION OF WIND DAMAGE IN CONIFER PLANTATION FORESTS FROM REMOTELY SENSED IMAGERY

D.N.M. Donoghue [a], K.B. McManus [b], R.W. Dunford [a] & P.J. Watt [a]

[a]Geography Department, Durham University, Durham, DH1 3LE, UK
email: danny.donoghue@durham.ac.uk
[b]CEH, Natural Environment Research Council, Monks Wood, Cambridgeshire, UK

ABSTRACT

Damage caused by wind poses a significant threat to the economic management of forests. In recent times, large storm events such as the 1999 Lothar storm and January 2005 gales have caused significant economic damage to areas of forest across Europe. However, wind damage also occurs at a smaller scale that may be harder to detect. Traditionally, vertical or oblique aerial photography has been the main method used to assess extent of new wind damage. Smaller areas of localised damage may not even be detected until the area is ready for harvest. The aim of this paper is to evaluate a variety of remote sensing systems as sources from which windblow can be interpreted manually by operators. The results show the influence of spatial resolution and spectral information on image interpretation. High spatial resolution appears very important for identifying internal wind damage while spectral information is more important within the 0.25-5m spatial resolution range. The results also illustrate the importance of training in image interpretation and of local knowledge.

Keywords: Wind damage, conifer plantations, image interpretation

1 INTRODUCTION

Wind damage of forest stands is represented by an area where trees have been blown over by a wind event. The result is an area displaying different structural, textural or spectral characteristics than the neighbouring area. This is most notable where trees have been blown right over and their bare trunks are visible in contrast to the green foliage. Some patches of wind damage can occur at the edge of the forest stand and are readily observed from the rides (Figure 1a).Trees within a forest stand can also be affected by wind damage but these are not so easy to locate at ground level (Figure 1b). Therefore, spaceborne or airborne remote sensing has great potential to provide a method for assessment of large areas more easily than ground based survey.

Figure 1a At edge of forest stand	Figure 1b Within forest stand
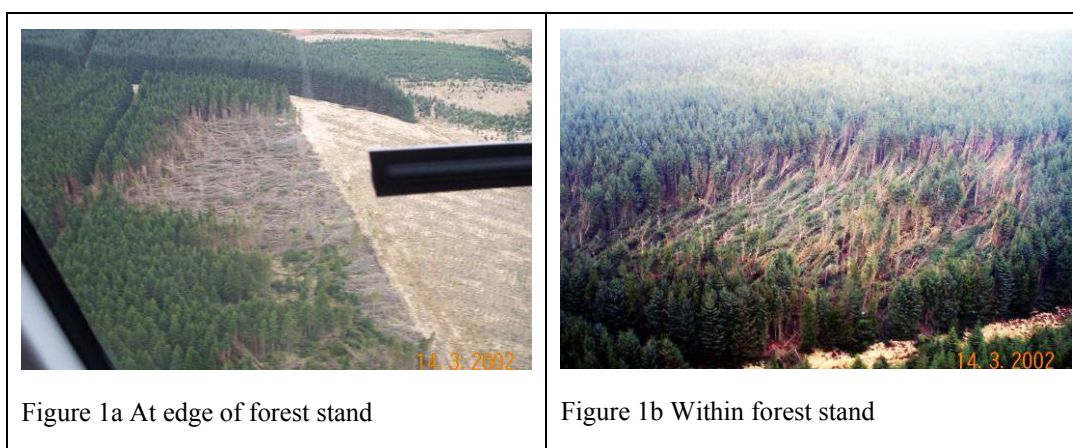
2 MATERIALS AND METHODS

2.1 IMAGE DATA

A series of digital images from a variety of remote sensing systems were acquired over the Kielder forest district, northern England between 2002 and 2003. The images provide a range of spectral and spatial resolutions for wind damage assessment that are currently available from commercial spaceborne or

airborne systems (Table 10). The images were geometrically registered to the UK WGS-84 geographical projection system with the satellite data radiometrically normalised to allow direct comparison of wind damage detection from the different image characteristics.

Table 10: Images used for wind damage assessment

Sensor	Acquisition Date yyyy-mm-dd	Spectral Resolution	Spatial Resolution
Landsat	2002-09-02	6-band VISB, VISG, VISR, NIR 2xSWIR	30m
SPOT	2002-10-26	4-band VISG, VISR, NIR, SWIR	20m
Landsat	2003-03-22	Panchromatic	15m
ASTER	2002-09-02	3-band VISG, VISR, NIR	15m
Ikonos	2002-03-13	4-band VISG, VISR,	4m
LiDAR	2003-03-28	Canopy Height	4m
Ikonos	2002-03-13	Panchromatic	1m
Aerial Photography	2001-2002	3-band Red, green, blue	0.25m

2.2 STUDY AREA

The spatial extent of the area to evaluate the images in detail was reduced to focus on a 14 km^2 area to the south of Kielder Reservoir, northern England. This area contains the optimum overlap in image data.

2.3 IMAGE PROCESSING

Each image was imported into ArcGIS for assessment of wind damage. An appropriate band combination was selected to optimise detection and the histogram stretched to enhance the visualisation. On this particular band combination (displaying the visible red band on the red display channel, the near-infrared on the green channel and the visible green on the blue channel) areas of potential wind damage are identified as areas of bright pink colouration compared with the neighbouring green foliage or alternatively showing a spectral, textural or tonal variation compared with the surrounding foliage (Figure 2).

Landsat Multispectral (3:4:2)	SPOT (2:3:1)	Landsat Panchromatic
ASTER (2:3:1)	Ikonos Multispectral (2:3:1)	LiDAR height
Ikonos Panchromatic	Aerial Photographs (3:2:1)	
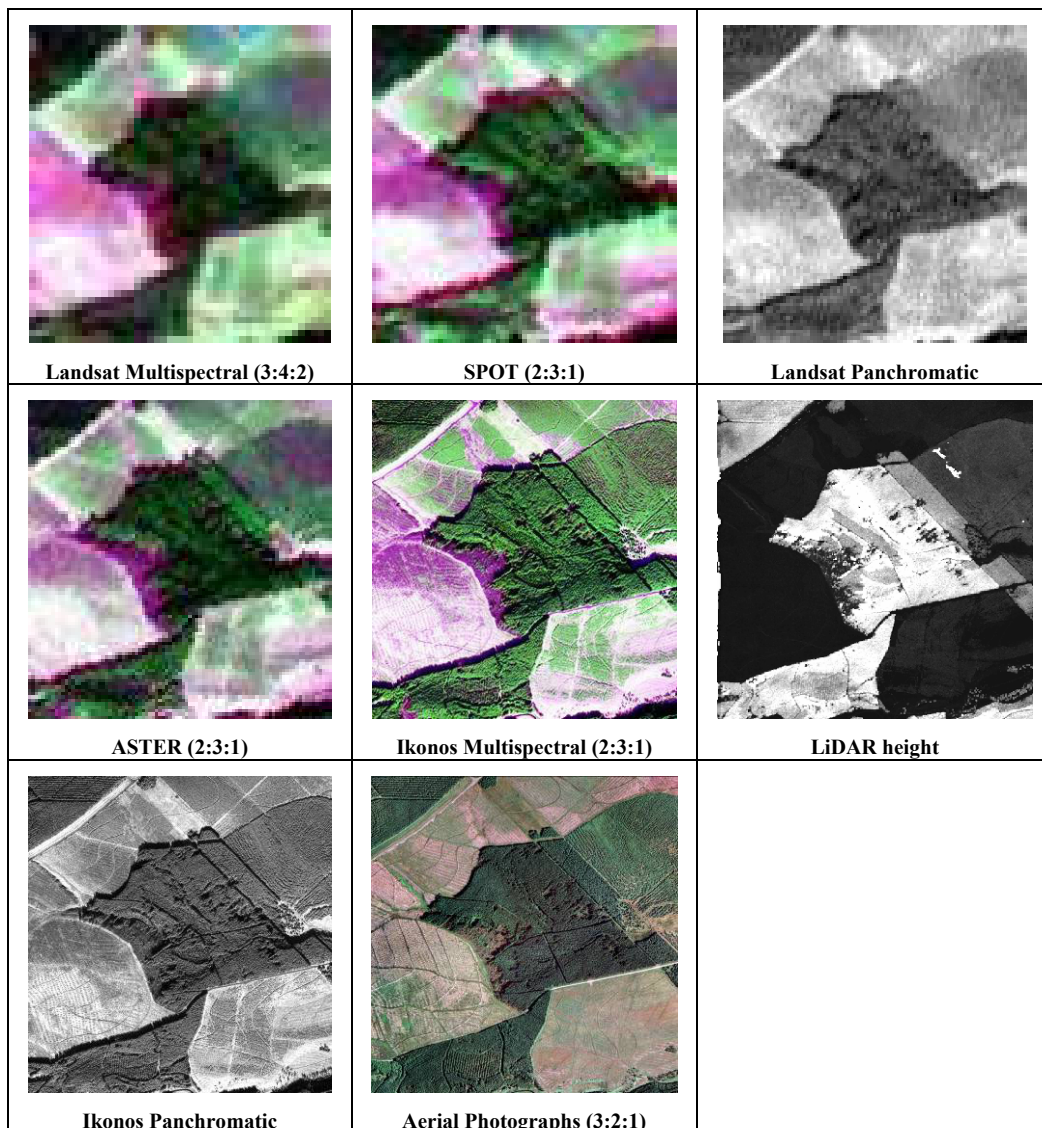
Figure 2: Comparison of spatial and spectral detail of a known area of wind damage

2.3 EXPERIMENTAL DESIGN

An experiment was designed to establish which type of commercial imagery would be most beneficial for wind damage detection. The evaluation involved the generation of a vector layer containing specific points of a range of wind damage categories, both within and at the edge of a forest stands and also at points where no wind damage occurred. The selected interpreters included, 5 professional foresters (all with varying levels of experience in forest management, aerial photography and image interpretation) the ForestSAFE team at Durham University (4 people) and a control group of non-foresters (8 people with little experience of forestry or image interpretation). Subjects were asked to mark each of 24 potential windblow sites within the focus area on a four-point scale from 0 (definitely no windblow) to 3 (definite windblow) for each of the 8 images.

3 RESULTS

In theory, wind damage (or windblow) should be identifiable from regions that have different, textural or spectral characteristics than unaffected area of forest. In practice however, the spectral and spatial resolutions of the sensors as well as the knowledge and skill of the individual interpreting the image, will all impact upon the accuracy of the interpretation.

Table 2 summarizes the interpretation of each sensor by the type of wind damage and by interpreter group.

Table 2. Summary of interpretation of each sensor by wind damage type and by interpreter group.

	Small Internal Windblow				
	All	UoD	FC	Expert	Students
Aerial Photography (25cm)	45	50	42	50	42
Ikonos Panchromatic (1m)	51	67	58	60	42
Lidar Height Grid (4m)	45	58	25	40	54
Ikonos multispectal (4m)	39	67	42	47	29
ASTER (15m)	25	8	33	20	33
Landsat Panchromatic (15m)	25	8	25	17	38
SPOT (20m)	25	17	17	17	38

	Large Internal Windblow				
	All	UoD	FC	Expert	Students
Aerial Photography (25cm)	69	81	56	73	69
Ikonos Panchromatic (1m)	74	100	75	88	59
Lidar Height Grid (4m)	74	100	63	75	75
Ikonos multispectal (4m)	69	100	81	85	47
ASTER (15m)	41	38	56	40	41
Landsat Panchromatic (15m)	18	0	19	8	28
SPOT (20m)	21	13	19	18	28

	Large External Windblow				
	All	UoD	FC	Expert	Students
Aerial Photography (25cm)	76	75	67	77	79
Ikonos Panchromatic (1m)	51	58	42	53	54
Lidar Height Grid (4m)	55	58	42	50	67
Ikonos multispectal (4m)	45	58	42	50	42
ASTER (15m)	33	33	33	33	33
Landsat Panchromatic (15m)	20	17	8	13	29
SPOT (20m)	57	58	67	60	54

	Non-Windblow				
	All	UoD	FC	Expert	Students
Aerial Photography (25cm)	88	87	96	92	85
Ikonos Panchromatic (1m)	86	88	96	92	79
Lidar Height Grid (4m)	87	87	92	90	83
Ikonos multispectal (4m)	82	87	94	92	71
ASTER (15m)	57	69	62	64	50
Landsat Panchromatic (15m)	82	92	90	90	74
SPOT (20m)	73	92	73	82	63

* Expert category is the FC and UoD groups combined

Of all the different windblow types, small internal windblow is the most difficult to detect. This is perhaps not surprising. However, the results suggest that these areas are just as likely to be identified using IKONOS panchromatic, multi-spectral or LiDAR data, especially if the user has some experience in interpreting these data. A similar pattern between the groups is also observed in the identification of large areas of either internal or external wind damage. As spatial resolution increases above 15 m the percentage of correctly classified windblow areas also increases. Although, in the case of Landsat panchromatic data the accuracy is lower when compared to similar/lower resolution multi-spectral imagery such as ASTER or SPOT. Spectral resolution also impacts on the interpretation, with the inclusion of the near infrared band leading to improved identification of some wind damage types. This is particularly relevant in the case of the LiDAR data as using just height data wind damage is still difficult to detect. Table 3 summarizes the overall accuracy of the wind damage interpretation by interpreter group and sensor.

Table 3. Summary of the accuracy of the wind damage interpretation by interpreter group and sensor.

	Overall Average (17)	Durham University (4)	Forest Industry (5)	All 'Experts' (9)	Students (8)
Aerial Photography (25cm)	77	80	78	81	74
Ikonos Panchromatic (1m)	74	83	80	81	67
Lidar Height Grid (4m)	74	82	71	75	74
Ikonos multispectal (4m)	69	83	78	79	56
ASTER (15m)	59	62	67	62	55
Landsat Panchromatic (15m	54	53	56	54	55
SPOT (20m)	54	61	55	58	51
Landsat (30m)	59	59	61	60	58

4. CONCLUSIONS

This study demonstrates that wind damage is not always interpreted accurately using aerial photography, even by the so called 'expert interpreters'. Interestingly, the IKONOS XS data was interpreted as well as aerial photography despite the difference in spatial detail. Satellite data with pixel sizes of 15 m or more were not interpreted accurately or consistently. LiDAR data on its own could not be interpreted easily. To make best use of LiDAR data it needs to be combined with spectral information.

ACKNOWLEDGEMENTS

EVALUATION OF USING SPACE- AND AIRBORNE RADAR FOR MAPPING OF WIND-THROWN FORESTS AFTER THE JANUARY 2005 HURRICANE IN SOUTHERN SWEDEN

L.M.H. Ulander[a,b], G. Smith[b], L. Eriksson[b], K. Folkesson[b], J.E.S. Fransson[c], A. Gustavsson[a], B. Hallberg[b], S. Joyce[c], M. Magnusson[c], H. Olsson[c], A. Persson[d], and F. Walter[e]

[a] Swedish Defence Research Agency (FOI), SE-581 11 Linköping, Sweden, email: ulander@foi.se
[b] Chalmers University of Technology, Göteborg, Sweden
[c] Swedish University of Agricultural Sciences (SLU), Umeå, Sweden
[d] National Board of Forestry, Jönköping, Sweden
[e] Dianthus, Boden, Sweden

ABSTRACT

Space- and airborne SAR have a potential for providing timely information of forest storm damage. In this paper, we compare Envisat, Radarsat and CARABAS with aerial photography and field data after the January 2005 hurricane in southern Sweden. The spaceborne Envisat and Radarsat C-band images are not able to detect the storm-damaged areas due to unfavorable frequency band and coarse resolution. The airborne CARABAS VHF-band SAR, on the other hand, detects most storm-damaged forest areas and even partly damaged which are often not detected in the aerial photography.

Keywords: Radar, SAR, CARABAS, Envisat, Radarsat, forest, wind-thrown, storm-damage.

1 INTRODUCTION

An intense low-pressure system with hurricane-force winds passed over southern Sweden on January 8-9, 2005. The maximum average wind speed was 33 m/s with wind gusts up to 42 m/s. Key bridges and airports were closed, all rail and ferry traffic was suspended, and the sea rose to record levels. Nine people were killed and 415.000 households lost electricity. Forests over a 300 x 350 km^2 area were damaged by the storm (see Figure 1). It is estimated that 75 million m^3 of timber, i.e. equal to the annual forest harvest in Sweden, has fallen down to a value of about 3 billion EURO.

Figure 1. The rectangle marks the 300 x 350 km^2 area where the forests were severely damaged by the storm. The green square by the arrow indicates the location of the test site.

The National Board of Forestry (NBF) has the responsibility for coordinating forest activities after a storm event. Directly after the storm, NBF therefore initiated an investigation to assess the extent of the damage. The immediate need was to obtain a synoptic view which was carried out using observations from low-altitude aircraft along sampling lines (Claesson and Paulsson, 2005). NBF was also interested in

exploring the possibility of using remote sensing. Both optical and radio-frequency systems were considered, including synthetic-aperture radar (SAR) with its all-weather and large area-coverage capability.

In this paper, we present results from evaluating both air- and spaceborne SAR images for mapping wind-thrown forests. We show example images over a common test site from two satellite systems, i.e. the European Space Agency's (ESA) Envisat and the Canadian Space Agency's (CSA) Radarsat, and one airborne system, i.e. the Swedish Defence Research Agency's (FOI) CARABAS-II low-frequency SAR (Hellsten *et al.,* 1996). The spaceborne data were obtained through The International Charter on Space and Major Disasters whereas the airborne data collection was funded by FOI and Ericsson Microwave Systems (EMW). Characteristics of the SAR data studied are summarized in Table 1.

Table 1. Characteristics of the analyzed SAR data.

System	Freq.	Polarization	Resolution
Envisat WSM	5.3 GHz	VV	150 m
Envisat IMP	5.3 GHz	VV	30 m
Envisat APP	5.3 GHz	HH/HV,VV/VH	30 m
Radarsat Fine	5.3 GHz	HH	9 m
CARABAS-II	55 MHz	HH	3 m

2 ANALYSIS

We have evaluated the SAR images over a 5 x 5 km^2 test site with significant forest storm damage. A map is shown in Figure 2. Lakes are shown in blue, and green areas are nominally forest land which may include newly clear-felled areas. Yellow areas are farm land and white areas are open land. The thick brown lines are major highways, smaller roads are marked in gray or black, and the black-white line is a railway. Elevation contours (5 m) are shown in brown. Brown areas are bogs. Figure 3 shows a high-altitude aerial photo over the same area after the storm. Five areas are indicated in white where 100% of the trees have been damaged by the storm.
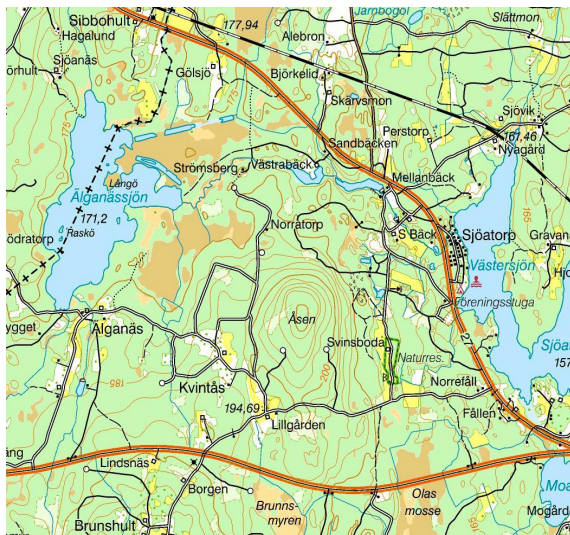
Figure 2. 1:50.000 map over the 5 x 5 km^2 test site (© LMV 2005).

Figure 3. Aerial photo from an altitude of 8 km with five areas marked in white where 100% of the trees have been wind thrown by the storm (© NBF 2005).

Most of the example images are from after the storm but there are also three examples from before for comparison. The first two images in Figures 4-5 show Envisat WSM wide swath images from before and after the storm. No significant structural change is evident besides the lakes, mainly because of the poor spatial resolution. The second two images in Figures 6-7 are Envisat IMP precision images which show a little more structure but still insufficient to detect forest storm damage. Figures 8-10 show Envisat APP images for different polarization after the storm (no images were available before the storm). Again, it is concluded that the Envisat images do not support detection of the forest storm damage.
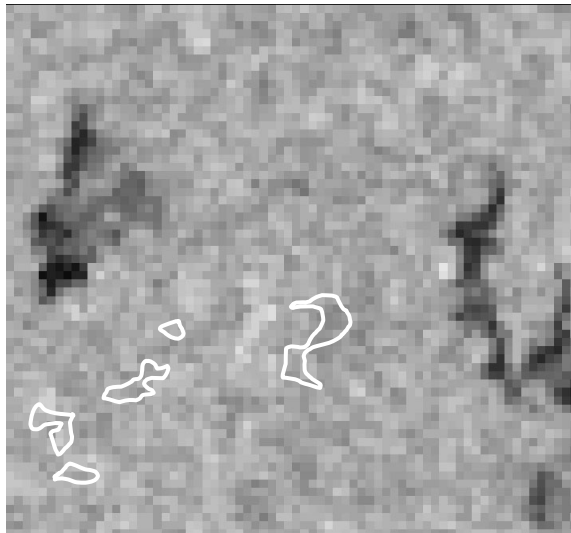
Figure 4. Envisat WSM 13-Dec-04, before storm (© ESA 2005).
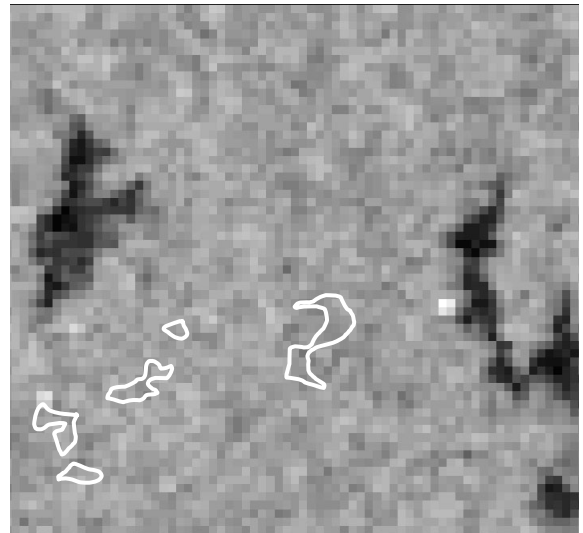
Figure 5. Envisat WSM 20-Jan-05, after storm (© ESA 2005).
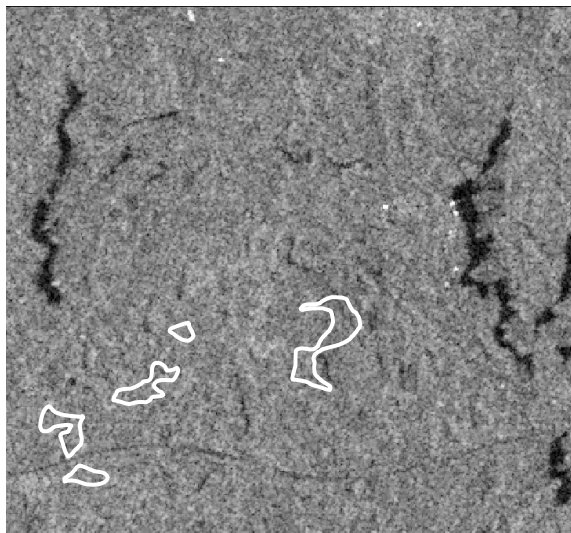
Figure 6. Envisat IMP IS2 05-Nov-04, before storm (© ESA 2005).
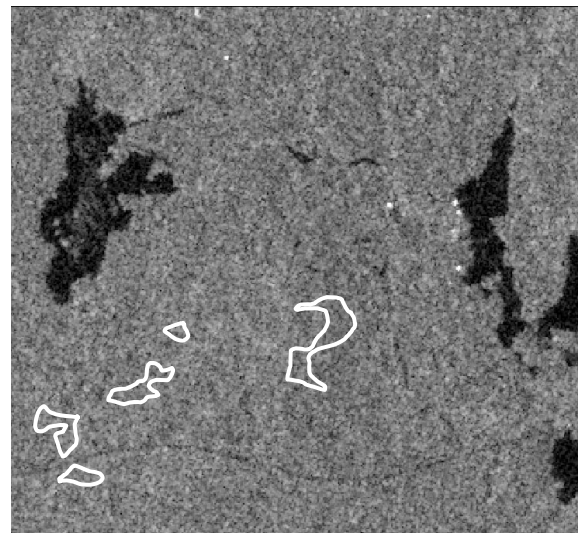
Figure 7. Envisat IMP IS2 14-Jan-05, after storm (© ESA 2005).
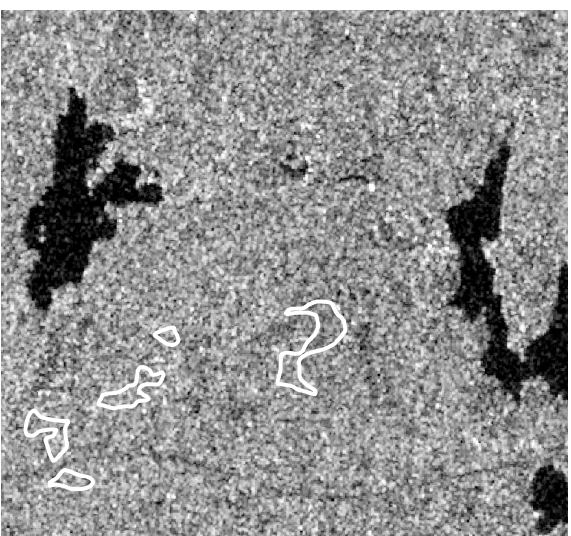
Figure 8. Envisat APP IS5 HH 23-Jan-05, ascending orbit, after storm (© ESA 2005).
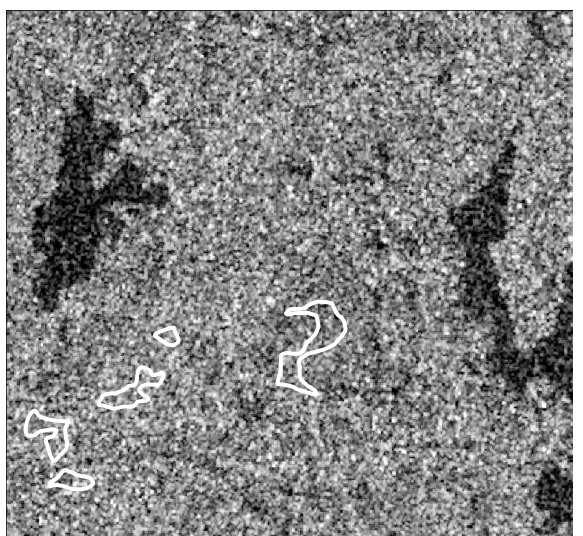
Figure 9. Envisat APP IS5 HV 23-Jan-05, ascending orbit, after storm (© ESA 2005).
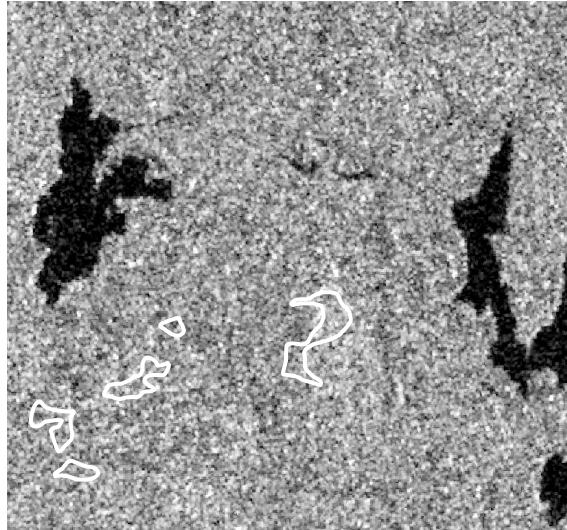
Figure 10. Envisat APP IS5 VV 23-Jan-05, descending orbit, after storm (© ESA 2005).

Radarsat images using fine beam modes with a spatial resolution of about 9 m are shown in Figures 11-12. These images show more structural information which seems to be related to forest characteristics, mainly by delineating boundaries by shadowing and foreshortening effects in the image before the storm. The image after the storm shows less structure which, to some extent, can be explained by storm damages. However, it is concluded that only a few storm-damaged areas (all with 100% wind-thrown trees) can be delineated in the Radarsat images.
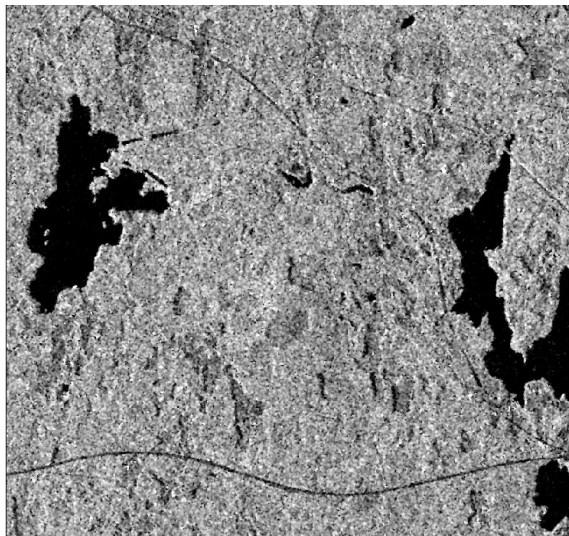
Figure 11. Radarsat Fine F2N 17-Jul-04, before storm (© CSA 2005).
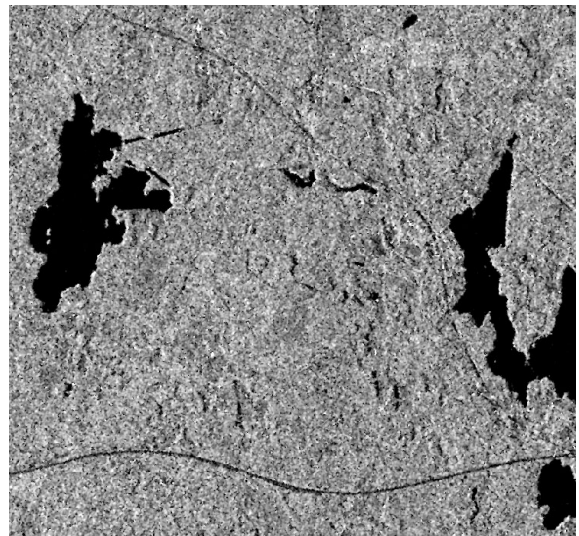
Figure 12. Radarsat Fine F3F 18-Jan-05, after storm (© CSA 2005).

The last image example in Figure 13 shows a CARABAS image with 3-m resolution. The use of low radar frequencies (20-90 MHz) results in very different information content. The response from horizontal trees is significantly higher than from vertical trees (Fransson *et al.*, 2002) provided the horizontal trees are not lying directly on ground and their axes are parallel to the flight track within about $\pm$ 30°. The storm-felled trees thus appear as bright and elongated objects. The image in Figure 13 has been produced by taking the maximum pixel brightness in three images corresponding to flight headings separated by 45°. This results in enhanced brightness in areas with storm-damaged trees.

A comparison of the CARABAS image with the aerial photo in Figure 3 shows that CARABAS detects significantly more and larger storm-damaged areas. Field observations verified that CARABAS also detects storm-felled trees in stands with standing forest and near borders with high trees. This is not possible in the high-altitude aerial photos due to shadowing from trees which are still standing. Close-up images are shown in Figures 14-15. The CARABAS image is a color composite where directive scattering objects are red whereas isotropic scattering objects are gray, i.e. storm-damaged areas are discriminated by a red color. The linear features which are seen in the CARABAS images are power lines or fences. They disappear in some areas, which indicate that they have been damaged and fallen to the ground.

Figure 13. CARABAS max. 3 headings 19-Jan-05, after storm (© FOI 2005).
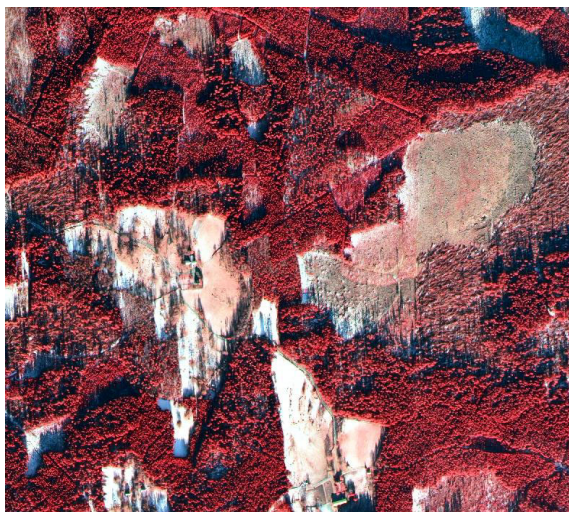
Figure 14. Aerial photo from within the yellow box indicated in Figure 13 (©NBF 2005).
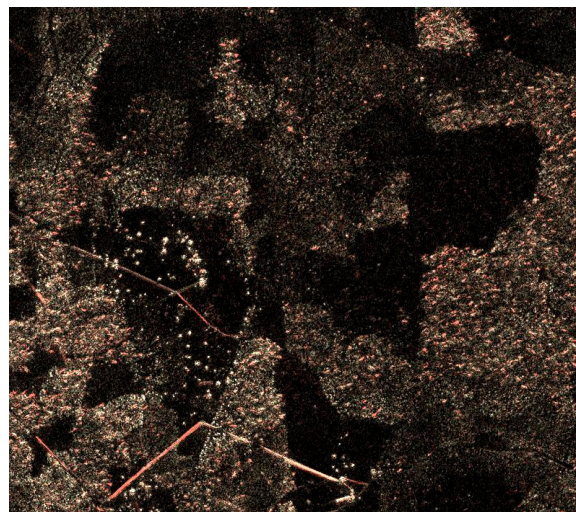
Figure 15. CARABAS color composite 19-Jan-05, after storm (© FOI 2005).

3 CONCLUSIONS

Analysis of the spaceborne Envisat and Radarsat C-band images shows that they are unable to detect forest storm damage due to unfavorable frequency and resolution. Future spaceborne SAR systems, e.g. ALOS and TerraSAR-L, will operate in L-band which is expected to improve detection. The CARABAS VHF-band SAR, on the other hand, is shown to detect most storm-damaged forests as well as power lines. CARABAS even detects partly damaged forests which are often not detected in aerial photography.

REFERENCES

Claesson, S. and Paulsson, J. 2005. *Flyginventering av stormfälld skog – januari 2005*. PM (in Swedish), National Board of Forestry.

Hellsten, H., Ulander, L.M.H., Gustavsson, A. and Larsson, B. 1996. Development of VHF CARABAS II SAR. *In Proc. Radar Sensor Technology*, Orlando, FL, 8-9 April 1996, SPIE vol. 2747, pp. 48-60.

Fransson, J.E.S., Walter, F., Blennow, K., Gustavsson, A. and Ulander, L.M.H. 2002. Detection of storm-damaged forested areas using airborne CARABAS-II VHF SAR image data. *IEEE Trans. Geosci. Remote Sensing*, vol. 40, no. 10, pp. 2170-2175.

REMOTE SENSING OF FOLIAR MASS AND CHLOROPHYLL AS INDICATORS OF FOREST HEALTH: PRELIMINARY RESULTS FROM A PROJECT IN NORWAY

S. Solberg[a], E. Næsset[b], L. Aurdal[c], H. Lange[a], O.M. Bollandsås[b] and R. Solberg[c]

[a] Norwegian Forest Research Institute, Ås, Norway, email: svein.solberg@skogforsk.no
[b] Norwegian University of Life Sciences, Ås, Norway
[c] Norwegian Computing Centre, Oslo, Norway

ABSTRACT

Variations in foliar mass and chlorophyll concentration are likely to reflect temporal variation in forest health well, by capturing both defoliation and discoloration symptoms. Canopy chlorophyll mass is the product of foliar mass and chlorophyll concentration. In the current project, we try to model these two variables using airborne LiDAR and hyper-spectral data, respectively. On ground we have data on foliar mass and chlorophyll concentrations from 16 sample plots dominated by Norway spruce (*Picea abies*). Based on the models, we use the airborne data to scale up estimates for both variables to a larger forest area. Up-scaled estimates are correlated to satellite data. The results are preliminary

Keywords: remote sensing, forest health, LAI, foliar mass, chlorophyll, laser scanning, spectral data.

1 INTRODUCTION

On the global scale, forests are threatened by population growth and human activities, including deforestation, air pollution; climate change; and spread of pests and diseases across continents. There is a need for quantitative information on forest health, and how it varies in space and time. Important here is the need for a quantitative and general health variable integrating across diagnoses, because the above mentioned threats to forest health may be manifested by a wide range of different damage types. Remote sensing might now provide useful tools for forest health monitoring at large scale. Remote sensing has already demonstrated its ability to provide forest health-relevant data, such as Leaf Area Index (LAI) and leaf loss (Brandtberg *et al.*, 2003; Lefsky *et al.*, 1999; Schaepman *et al.*, 2004), chlorophyll (Malenovský, 2002, Zarco-Tejada *et al.*, 2004), foliar nutrients (Martin and Aber, 1997), and identification of trees having root diseases (Leckie *et al.*, 2004). In the current project we try to develop methods for remote sensing of foliar mass per unit ground area (or LAI) and chlorophyll concentration, as suitable measures of variation in forest health. We intend to estimate the two variables using airborne LiDAR and hyper-spectral data, respectively. The two variables correspond to the traditional, ground based forest health variables defoliation and discoloration, as used by the European forest monitoring program UN-ECE/ICP-Forests since 1986 (Anon., 2002). The product of foliar mass and chlorophyll concentration is canopy chlorophyll mass per area, and is one general variable integrating effects across any type of forest damage. The aim of this paper is to present the outline and preliminary results from our project.

2 MATERIALS

The area for this study is located near Oslo, in south-eastern Norway (59º 50′N, 11º 02′E, 190–370 m a.s.l). The size of the area is 6 km^2, comprising mainly Norway spruce (*Picea abies* L. Karst.) and some Scots pine (*Pinus sylvestris* L.). A large part of the area consists of old forest stands only. This area is a forest reserve, where no clear-cuttings have been executed since 1940 and it is considered as a primeval forest, being partly multi-layered. The data were collected during summer 2003, except the airborne hyper-spectral data that were acquired in June 2004.

We subjectively selected 16 circular spruce sites (1000 m^2) as sample plots, being in four age-classes from young plantations to old stands. We used differential GPS/GLONASS for determining plot coordinates in field according to the procedures proposed by Næsset (2001; 2004). Positions of all trees were obtained by additional measurements of their polar coordinates within the plot. We recorded diameter at breast height (dbh), defoliation, discolouration, social status, and species of the

trees. On each plot, four of the non-suppressed trees were systematically selected as sample trees, in total 64 sample trees, with additional measurements and branch sampling for foliar mass and chlorophyll measurements. Branches were sampled from the lower, the middle and the upper parts of the crown. For 11 of the sample plots, we measured optical Leaf Area Index using a LiCor LAI-2000 plant canopy analyzer. For each plot, five LAI readings were obtained by measuring at the centre and 3 m away from the centre in each of the four cardinal directions. These LAI measurements were done as a measure of foliar mass, being an alternative approach to the foliar mass measurements of the sample trees. The forest area was classified into stands, with tree species and age class given for each stand. This was done as part of an operational forest inventory by a commercial company in Norway (Prevista).

Laser data were acquired on October 10, 2003, by a Hughes 500 helicopter carrying the ALTM 1233 laser scanning system produced by Optech, Canada. The leaf conditions were in an intermediate state, i.e. the deciduous trees were still foliferous at the time of the flight. The average flying altitude was approximately 600 m. First and last returns were recorded. The last return data were used to model the terrain surface. Hyper-spectral data were acquired on June 30, 2004, by a Cessna 172 airplane carrying the ASI (Airborne Spectral Imager) developed by Norsk Elektro Optikk AS, Norway (Anon., 2004). The average flying altitude was 900-1200 m above the ground. The data set was radiometrically calibrated to obtain radiance. We used the VNIR module of the ASI instrument, which is a pushbroom scanner covering 400-1000 nm in 160 bands. For both flights, GPS and inertial navigation system data were logged continuously to provide geometric correction and geo-referencing.

We have one SPOT quarter-scene aquired on August 17, 2003. The image is a level 3 SPOT image with a spatial resolution of 10x10 m; four spectral bands: green, red, NIR and SWIR. The image was geo-referenced and radiometrically corrected.

3 METHODS

In order to assign pixels from the airborne hyper-spectral data set uniquely to sample trees, the crown outlines were modelled using the LiDAR point cloud. This was done by filtering out the uppermost LiDAR points; making a digital canopy surface model (DSM) by smoothing these points into a grid; and applying a watershed algorithm to identify the tree crown outlines for each local maximum. These outlines (polygons) were then linked to the tree numbers from the ground data, based on the stem coordinates of the trees. Hyper-spectral pixels were then derived from an overlay of these polygons on the hyper-spectral images.

We estimated LAI from LiDAR data assuming that laser pulses penetrate the canopy layer in a similar way as solar radiation. The penetration of visible light through a canopy approximates the Beer-Lambert law:

$$\ln I_z/I_0 = -k\text{LAI},$$

where I_z and I_0 are light intensity below and above the canopy, respectively, and k is an extinction coefficient being species specific (Waring and Schlesinger, 1985). We assumed that the same applies for penetration of laser pulses through the canopy, and estimated a transformed version of this model:

$$\text{LAI} = a \ln N/n_g,$$

i.e. a linear, non-intercept regression model where N were the total number of LiDAR points and n_g the number of LiDAR points below the canopy (ground hits). We parameterized this equation using the eleven plots with ground based LAI-2000 measurements, together with LiDAR data for the circular 1000 m^2 sample plots. Recalculating the LiDAR data according to this model provided LiDAR based LAI estimates for the entire area, i.e. for every 10x10 m square matching the 10x10 m pixels in the SPOT data.

We selected chlorophyll concentrations measured in the upper part of the tree crowns for correlating with hyper-spectral data. In general, green plants have a very specific spectral signature, with low reflectance in visible light, and high reflectance in the near infrared range, i.e. the red-edge effect. We correlated chlorophyll concentrations to spectral variables that reflect this red-edge effect,

i.e. so far NDVI. We calculated NDVI by summing channels in accordance with the wavelengths used in SPOT 5, i.e. red = 610-680 nm, and NIR = 780-890 nm.

We search for empirical relationships between satellite data and foliar mass and chlorophyll concentrations, where the latter two variables are estimated at a large scale using airborne data together with models between airborne data and ground data.

4 RESULTS AND DISCUSSION

The modelling of the digital canopy surface model (DSM) based on LiDAR data was quite successful, although some of the plots had a rather heterogeneous structure (Fig. 1). The tree segmentation algorithm used identified the ground based trees fairly well. All predominant trees were identified, around 70% of the dominant trees and 45% of the co-dominant trees.
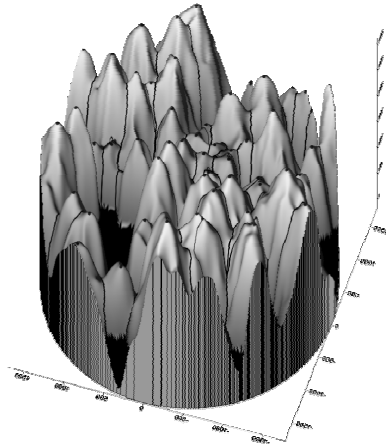
Figure 1. DSM model of a 1000 m^2 plot in an old Norway spruce stand, visualized in 3D. Local maxima, being tree top candidates, are marked.

As expected, the relationship between LiDAR data and ground based LAI values followed nicely the Beer-Lambert law, where the intercept was non-significant and was discarded, and with a high R-square (Fig. 2). This, together with SPOT satellite data and forest stand data produced a data set of 46,000 pixels having both LAI estimates and SPOT NDVI, and where the main tree species was Norway spruce (Fig. 3). There was a relationship between the two variables LAI and NDVI. High LAI values and high NDVI values were generally seen in dense or old forests, mostly in lower parts of the terrain, while low values were seen mostly in upper hillsides and hill tops, which are dominated by scattered pine and aspen trees, and on clear cuttings and young stands. A preliminary, non-linear model between LAI and NDVI, following the approach of Roberts *et al.* (2004), gave a weak but significant relationship (R^2=0.16), with a saturation point of ca. 0.8 for NDVI at LAI-values around 4 and higher, when excluding clear-cuttings.
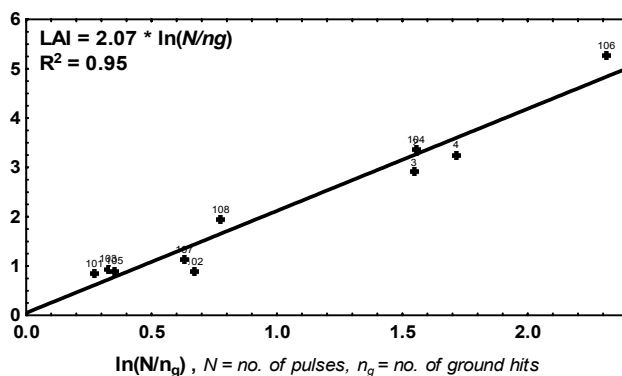
Figure 2. Linear regression of ground based LAI-2000 measurements against LiDAR 1. return data for eleven 1000 m2 circular plots of Norway spruce. Point labels = plot numberings.
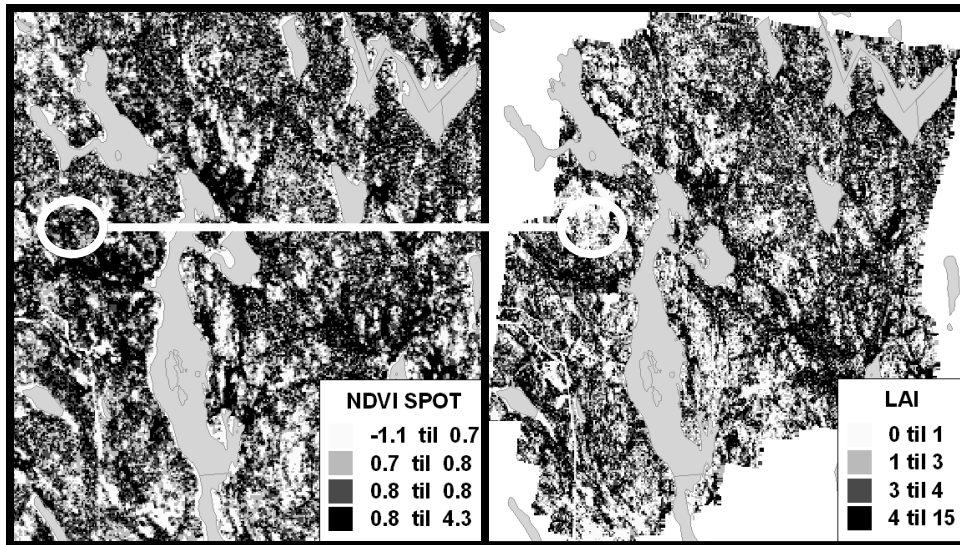
Figure 3. Comparison of SPOT NDVI (left) and LAI estimates based on airborne LiDAR (right) for the ~6km^2 forest area Østmarka. A general consistency is seen. However, also areas with low consistency are evident, one of which is marked with a white circle.

However, the match between NDVI and LAI was far from perfect. Some stands with young spruce trees had high NDVI values, but low LAI values. This is evident in the area marked with a circle in Fig. 3, being a spruce stand with tree heights around 1-2 m. A closer look on one of our sample plots in this area is shown in Fig. 4. The trees are evident in the normal black and white image, and they are also indicated by their crown segment polygons. However, in the NDVI-image the trees are no longer as clearly distinguishable from non-tree objects, likely due to chlorophyll-rich vegetation, seen as dark areas in-between the trees. This illustrates a possible limitation of the easily available spectral data from satellites.
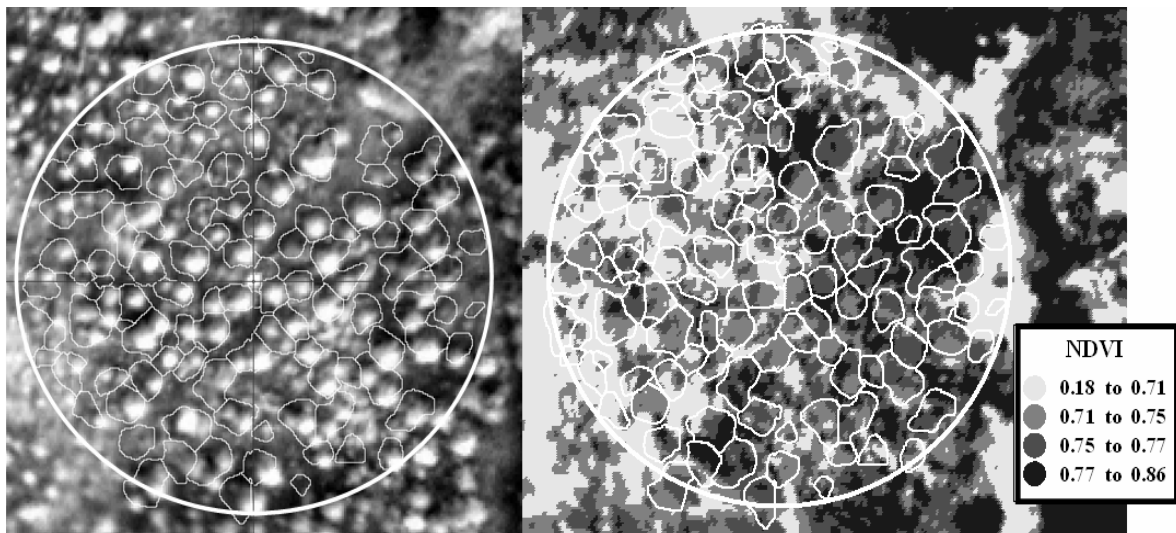
Figure 4. Polygons for the tree crown segments overlaid on black and white images of the airborne hyper-spectral data, normal black and white, i.e. visible light (left); and NDVI (right).

The second part of the work was the modelling of foliar chlorophyll concentrations using hyper-spectral data. Here we are in the beginning of the work only. We have started to overlay tree outline polygons on the hyper-spectral images, in order to derive hyper-spectral data for each of the 64 sample trees with chlorophyll concentration data. So far, we have data for 16 of the 64 sample trees. The spectral data followed the characteristic signature for vegetation, and this signature was quite stable within the entire tree crown, although the intensity varied from pixel to pixel (Fig. 5). Foliage

chlorophyll concentrations in the upper canopy were positively, but only weakly (R^2=0.12) related to NDVI in the hyper-spectral data.
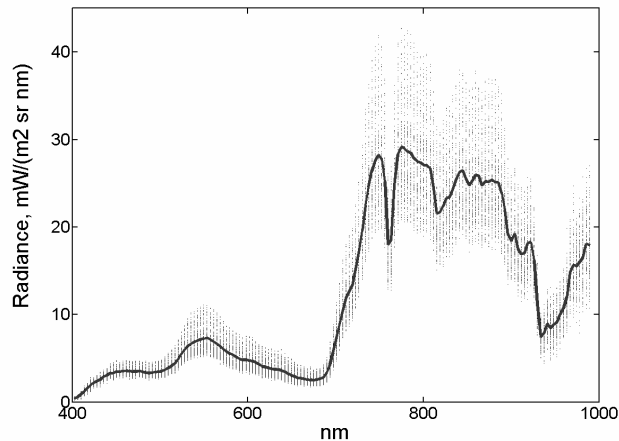
Figure 5. Spectral signature for one young spruce tree, comprising 116 pixels. Radiance for all pixels is shown as black dots, while the mean radiance across pixels is shown as a line.

ACKNOWLEDGMENTS

REFERENCES

Brandtberg, T., Warner, T., Landenberger, R. and McGraw, J., 2003. Detection and Analysis of Individual Leaf-off Tree Crowns in Small Footprint, High Sampling Density Lidar Data from the Eastern Deciduous Forest in North America, *Remote Sensing of Environment*, vol. 85, no. 3, pages 290-303.

Lefsky, M., Cohen, W., Acker, S., Parker, G., Spies, T. and Harding, D. 1999. Lidar Remote Sensing of the Canopy Structure and Biophysical Properties of Douglas-Fir Western Hemlock Forests, *Remote Sensing of Environment*, vol. 70, no. 3, pages 339-361.

Schaepman, M.E., Koetz, B., Schaepman-Strub, G., Zimmermann, N.E. and Itten, K.I. 2005. Quantitative retrieval of biogeophysical characteristics using imaging spectroscopy: a mountain forest case study. *Community Ecology*, in press.

Malenovský 2002. Investigation of functional parts and status of Norway spruce crowns using spectral remote sensing information. Thesis Report GIRS 25. Lab of Geo-Inf Science and Rem Sens, Wageningen Univ, pp

Zarco-Tejada, P.J., Miller, J.R., Morales, A., Berjón, A. and Agüera, J. 2004. Hyper-spectral indices and model simulation for chlorophyll estimation in open-canopy tree crops. *Remote Sensing of Environ* 90, 463-476.

Martin, M.E. and Aber, J. D. 1997. High spectral resolution remote sensing of forest canopy lignin, nitrogen, and ecosystem processes. *Ecological Applications* 7: 431-443.

Leckie, D.G., Jay, C., Gougeon, F.A., Sturrock, R.N. and Paradine, D. 2004. Detection and assessment of trees with Phellinus weirii (laminated root rot) using high resolution multi-spectral imagery. *International Journal of Remote Sensing* 25, 793-818.

Anon. 2002. UN/ECE & EC. / Lorenz, M., Mues, V., Becher, G., Müller-Edzards, Ch., Luyssaert, S., Raitio, H., Fürst, A., and Langouche, D. Forest Condition in Europe - 2003 Technical Report, Geneva, Brussels

Næsset, E. 2001. Effects of differential single- and dual-frequency GPS and GLONASS observations on point accuracy under forest canopies, *Photogramm. Eng. Remote Sensing* 67, 1021-1026.

Næsset, E. 2004. Practical large-scale forest stand inventory using small-footprint airborne scanning laser. *Scand. J. For. Res.*, 19, 164-179.

Anon. 2004. ASI – Airborne spectral imager. NEO (Norsk Elektro Optikk AS) http://www.neo.no/asi

Waring and Schlesinger 1985. *Forest ecosystems. Concepts and management.* Academic press. Orlando. 340 pp.

Roberts, D.A., Ustin, S.L., Ogunjemiyo, S., Greenberg, J., Dobrowski, S.Z., Chen, J. and Hinckley, T.M. 2004. Spectral and Structural Measures of Northwest Forest Vegetation at Leaf to Landscape Scales. *Ecosystems* 7, 545-562.

DETECTION OF FAILED REGENERATION WITH MULTITEMPORAL SATELLITE REMOTE SENSING

Steve Joyce and Håkan Olsson

Department of Forest Resource Management and Geomatics,
Swedish University of Agricultural Sciences. Umeå, Sweden.
email: Steve.Joyce@resgeom.slu.se

ABSTRACT

This study is an attempt to identify areas of failed forest regeneration from a time sequence of satellite imagery. All new clearfellings between 1990 and 1992 were detected and mapped from a pair of summer Landsat TM scenes within a 50 x 50km area in northern Sweden. A selection of these stands was visited in the field in 2004 to assess the current regeneration status. Spectral mean values in these stands were extracted from summer Landsat imagery from 2000 and 2004. The analysis showed that it was not possible to discriminate the failed regeneration areas in the image from 2000 (8 or 9 years after the previous stand was harvested), but there was significant separability in the image from 2004. The main factors that determined spectral separability were a combination of tree height and stocking density. It seems that during this early stage of regeneration, the re-colonization of the background vegetation and differences in site types dominate the satellite spectral signal before the trees make a significant contribution. Regeneration status was not apparent in the satellite imagery until the trees reached approximately 2.5m in height.

Keywords: change detection, regeneration assessment.

1 INTRODUCTION

Forest owners in Sweden are required by law to regenerate forest stands within 3 years of final felling and it is the responsibility of the regional forest authorities to verify that regeneration is adequate after 7 years. With large areas to monitor and limited resources for spot checks, the forest authorities could benefit from remote sensing tools to better focus their field verification efforts. There is also a wider public interest in mapping the extent of failed or poor regeneration, especially on marginal forest land near the Swedish mountains. Since the forest authorities are already acquiring satellite imagery annually when available, it is interesting to see if the regeneration status of individual stands can be inferred from remote sensing. At the very least, it would be useful to use satellite imagery to identify or rank priority areas for verification in the field.

1.1 BACKGROUND AND OBJECTIVES

The defining characteristic of a failed regeneration is that an insufficient number of suitable new trees have been established on a site some time after a stand is harvested. When looking at a single remote sensing image, failed regenerations are easily confused with more recent clearfellings and other mostly treeless areas (Foody et al, 1996). It is therefore important to consider the time (or age) dimension when judging regeneration success. Reflectance changes in regenerating stands show a rapid decrease in seasonal peak brightness and greenness during the first 15-20 years for normal growth (Peterson and Nilson, 1993), after an initial increase in the first years due to recolonization of the ground vegetation (Peterson, 1992). This can be attributed to changing proportions of sunlit ground vegetation, tree crowns and tree shadows (Nilson and Peterson, 1994), with considerable variability due to site types, tree species and growth rates. It should therefore be possible to identify failed regenerations from remote sensing by following the spectral properties of a stand during the years after stand establishment: normally regenerating stands will show a significant decrease in reflectance over time due to tree growth, whereas failed regeneration would remain fairly constant.

In this study we test this idea by first doing a change detection with a pair of historical Landsat images to identify a large number of individual stands that were all harvested at the same time (between 1990 and 1992). A number of these cohorts are visited in the field to identify the species composition and their current regeneration status. We then look at the stand spectral mean values in

more recent imagery (from 2000 and 2004) to see if the stands with failed or poor regeneration are distinct from those that are regenerating normally. The idea is that such a procedure could be routinely applied when a time sequence of historical imagery over an area is available and new images are acquired. The anticipation is that poor regeneration will be spectrally distinct or extreme, even if the specific site type, stocking density, and species planted is unknown. If the exact date of harvest is known from other sources such as cutting records, then this could be used instead of change detection with historical imagery. The main scientific question is how soon after stand establishment can failed regeneration be distinguished from "normal" development by satellite remote sensing. Further, what are the factors, in terms of site types and species composition, that influence the ability to detect these failed regeneration areas.

1.2 STUDY AREA

The study area covers a single mapsheet (22G Vilhelmina) from the Swedish Land Survey's 1:100,000 "Blåkartan" series and extends 50km x 50km including the town of Vilhelmina in the county of Västerbotten Sweden (Latitude 64°40', Longitude 16°20'). This area is in the foothills of the Swedish mountains with a minimum elevation of 334m at the large reservoir called Malgomaj, up to a maximum elevation of 724m on Blaikfjället. Forests in the area are intensively managed for wood production with final felling in patches of 2 to 20ha. Newly harvested areas are typically replanted within 1 to 3 years and site preparation in the form of soil scarification is used on some sites. The majority of stands are replanted with Norway spruce (*Picea abies*) or Scots pine (*Pinus sylvestris*), but it has also been popular in the past to plant lodgepole pine (*Pinus contorta*) which grows quickly and is less susceptible to moose browsing. Establishing regeneration after harvesting can be problematic on some sites in this region due to several factors. Sites at higher elevations can be at risk for frost damage which either kills young plants outright or destroys the current year's growth. Intensive moose browsing on pine in winter in the low-lying areas especially in river valleys and near lakes can also prevent or delay new stand establishment. It is estimated that up to 10% of regeneration areas fail to reach the established standards for regeneration success after 7 years.

1.3 SATELLITE IMAGERY

Table 1 shows the satellite imagery used in this study. All scenes are relatively cloud-free with clear atmospheric conditions and were processed to level 2c. The first two were used for change detection, and the others were used to assess regeneration status.

Table 1. List of satellite scenes and dates of acquisition.

Sensor	Path/Row	Date
Landsat-5 TM	196/15	1990-07-15
Landsat-5 TM	195/15	1992-06-11
Landsat-7 ETM+	195/15	2000-07-27
Landsat-5 TM	196/15	2004-06-03

Images were radiometrically normalized to compensate for differences in sensor calibration, solar illumination and atmospheric clarity by applying a linear transformation to each spectral band to match the distribution of pixel values under a forest mask using the image from 2000 as a reference. This approach doesn't give an absolute radiometric scale, but has the advantage of compensating for all sources of radiometric distortion simultaneously and has been shown to be preferable to other simplified approaches to image calibration for forests of this type (Olsson, 1994).

2 CHANGE DETECTION AND MAPPING

Procedures for change detection for forest land are fairly well developed (Coppin and Bauer, 1996) and after some experimentation we found it was sufficient to take differences in TM band 5 for identifying new clearfellings. The differences were thresholded based on statistics from the residual distribution to identify a number of change pixels. A majority filter was applied to smooth the groups

of change pixels and remove isolated small areas. After a raster-to-vector conversion, and applying a minimum size rule (2 ha) we were left with a number of stands that were known to be cut between 1990 and 1992 (fig. 3).

Figure 3. Change detection results. a) Landsat TM image from 1990, b) 224 stands identified as clearfelled between 1990 and 1992.
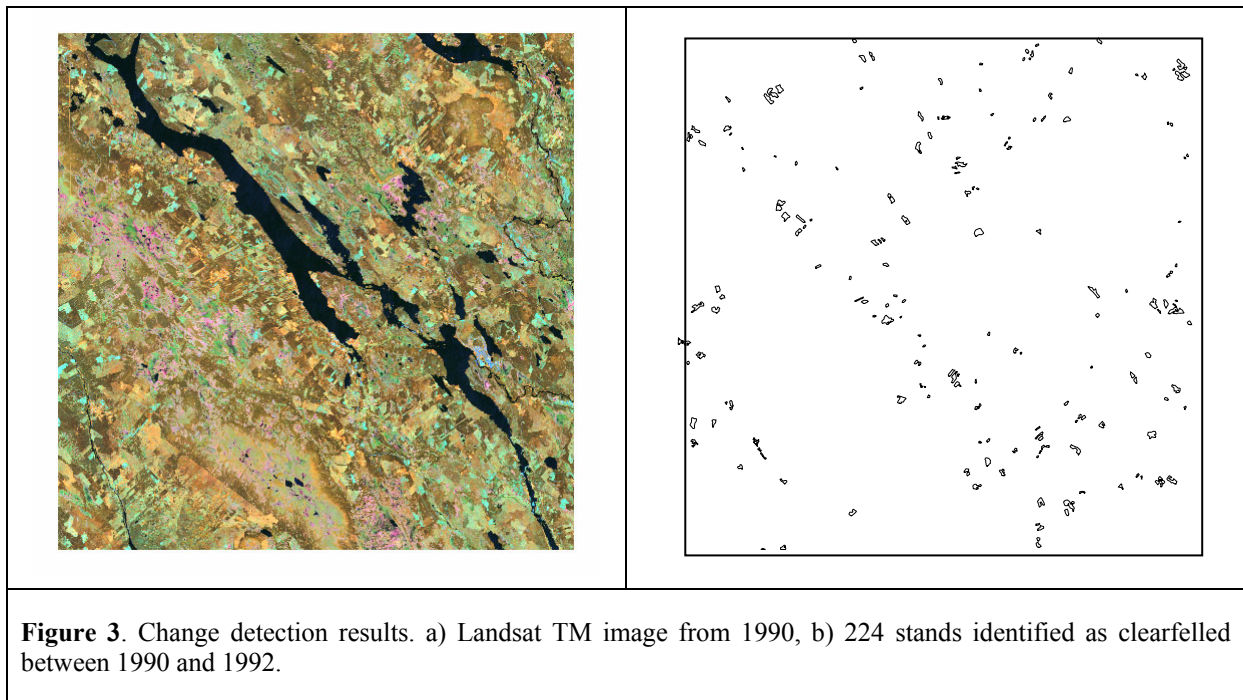
3 FIELD INVENTORY

The change detection with the images from 1990 and 1992 resulted in 224 stands within this 50x50km area identified as being harvested within this period. A selection of the stands was visited in the field in 2004 to assess their current regeneration status. Measurements of height, stem density, crown closure and species composition were taken and other information about the field layer and site type was recorded. In total 52 stands were visited and of those 6 were judged as "failed" regeneration, and a summary of the stand characteristics are shown in figure 4.

Figure 4. Selected characteristics of stands measured in the field
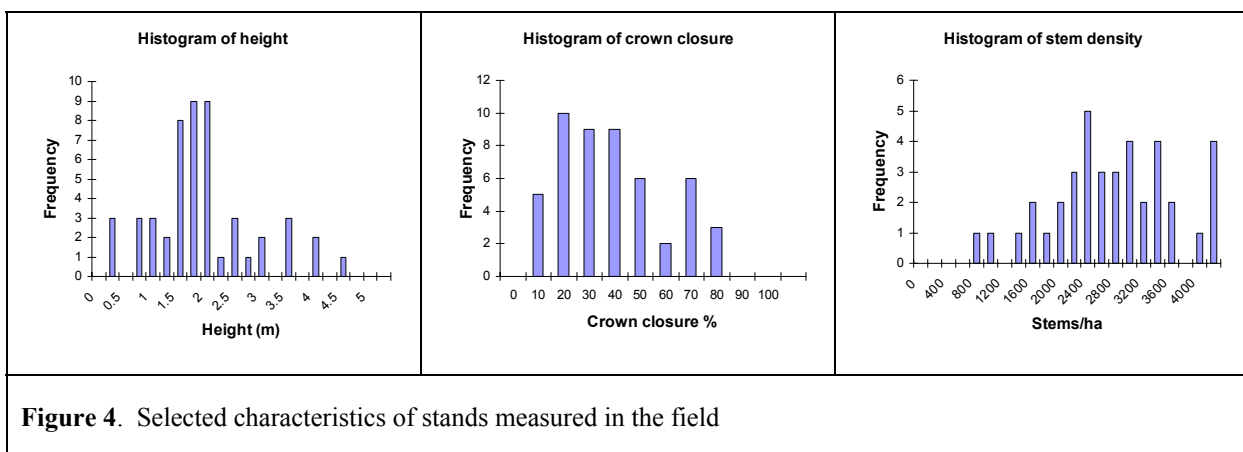
There were 4 main types of sites discovered in the field visit. Scots pine regeneration, mostly on well-drained sites, spruce regeneration on wetter sites with some fraction of birch, lodgepole pine plantations (fig. 5a) and open areas with no significant regeneration (fig. 5b). There were large differences in height of these stands, up to a maximum for 4.5m for some of the lodgepole pine plantations.

Figure 5. Extremes of regeneration success after 12 years. a) lodgepole pine plantation, b) failed spruce regeneration.

4 REGENERATION ASSESSMENT

Polygon mean values were extracted from the image data sources and a summary of the results are shown in figure 6. We focus mainly on TM band 4 and 5 which have been shown to capture most of the information associated with regeneration (Fiorella and Ripple, 1993). There are several points of interest from these graphs. First, clearfelling causes a strong increase in reflectance in band 5, and it doesn't start to decrease again until approximately 8 years after stand establishment. As expected, the strongest decrease is for lodgepole pine (contorta) sites which have both greatest height and crown closure compared to other sites. In band 4, the largest increase comes not from clearfelling, but in the following years, most likely due to recolonization of the ground vegetation. The peak seems to occur much later than that observed by Peterson (1992) for these site types.
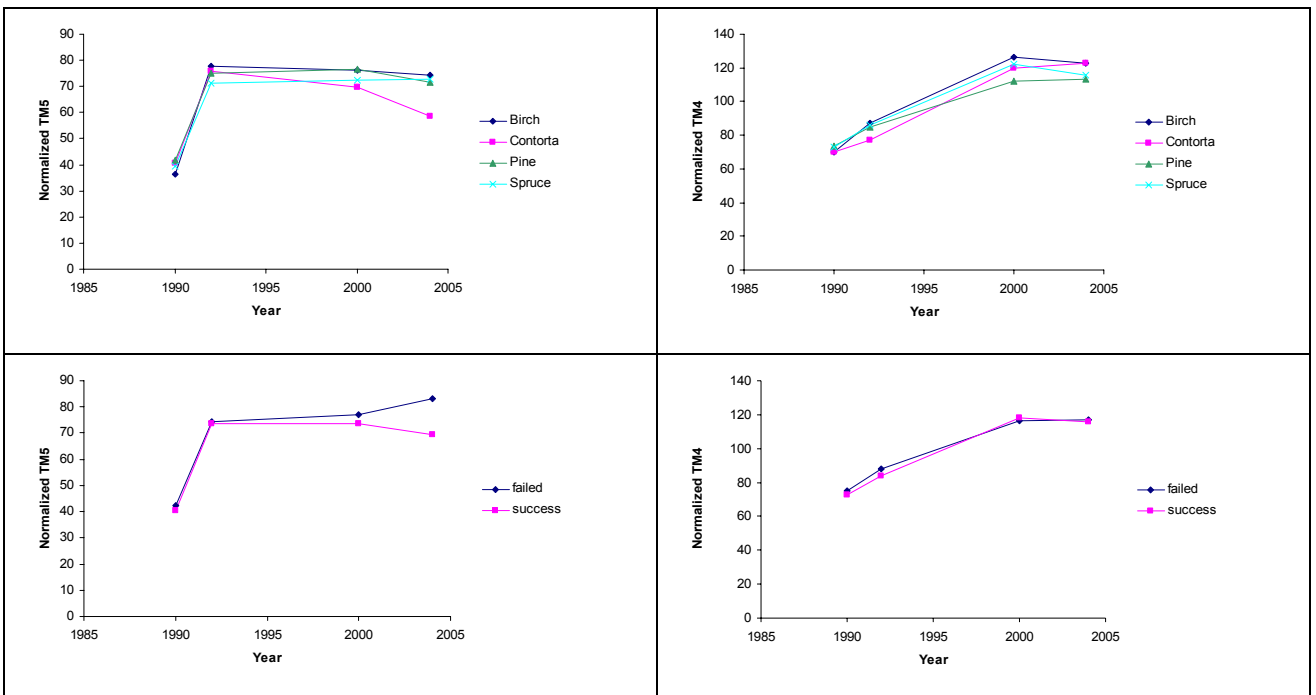
Figure 6. Spectral profiles of different site types for TM band 5 and TM band 4 in the 4 different images.

Figure 7 shows the differences in mean values calculated for the regenerating forest polygons in TM band 4 and TM band 5 compared to the image from 1992. In the image from 2000, those polygons

113

identified in the field as failed regeneration are not separable from other stands. In 2004, they tend to be much brighter in TM5 as expected. From this data it seems that the regeneration status was only apparent in the satellite imagery after 12 or 13 years for these relatively slow-growing stands.
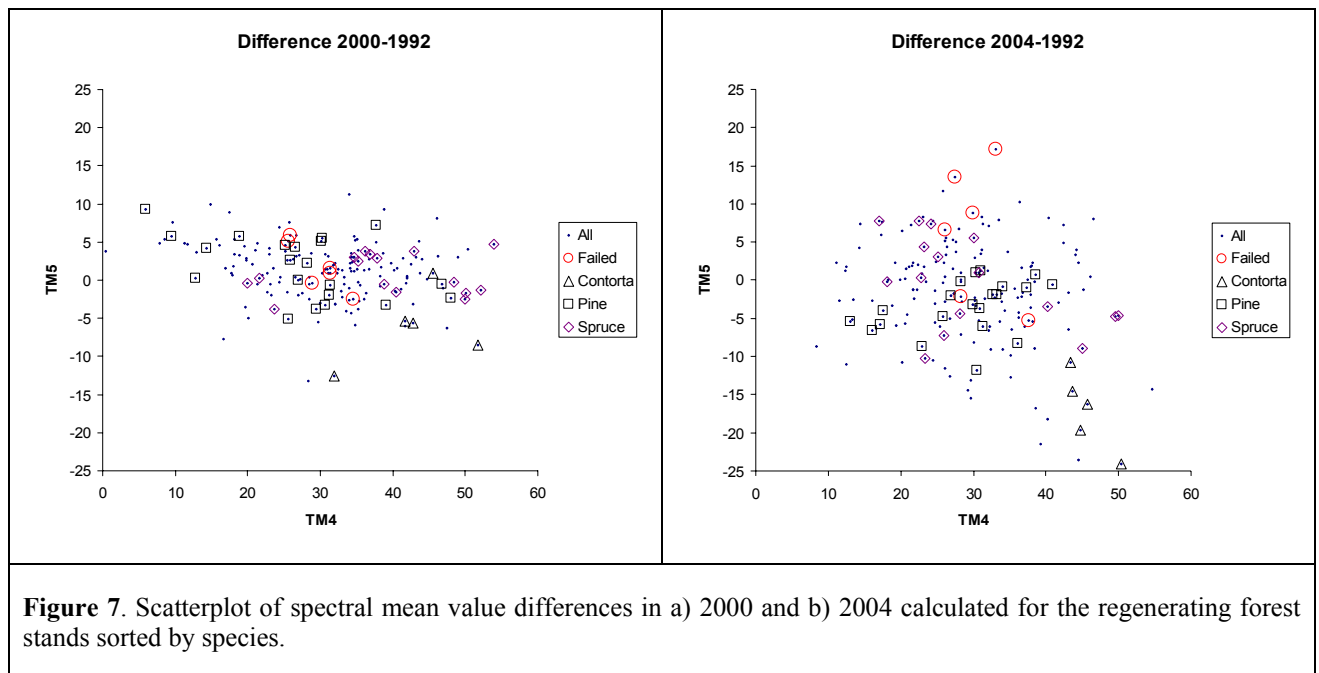
Figure 7. Scatterplot of spectral mean value differences in a) 2000 and b) 2004 calculated for the regenerating forest stands sorted by species.

5 DISCUSSION AND CONCLUSIONS

During the early years of regeneration, the spectral properties are mostly influenced by the recolonization of the ground vegetation, and differences in site types. The tree layer doesn't seem to make a significant contribution until they reach approximately 2.5m in height which can take more than 8 years. It was not possible to discriminate the failed regenerations from normal growth by remote sensing alone in the image from 2000 (8 years after felling), but there was a clear difference in the image from 2004. The time delay for detecting failed regeneration is a bit too long to make this a practical approach for operational requirements of the forest authorities, but it may prove to be a useful technique for mapping the extent of long-term failed regeneration. We can also expect better discrimination in areas with higher site productivity.

ACKNOWLEDGMENTS

REFERENCES

Fiorella, M. and Ripple, W. J., 1993. Determining successional stage of temperate coniferous forests with Landsat satellite data. *Photogrammetric Engineering and Remote Sensing*. 59(2):239-246.

Foody, G.M., Palubinskas, G., Lucas, R.M., Curran, P.J., and Honzak, M. 1996. Identifying terrestrial carbon sinks: classification of successional stages in regenerating tropical forest from Landsat TM data. *Remote Sens. Environ.* 55:205-216.

Nilson, T., and Peterson, U., 1994. Age dependence of forest reflectance: analysis of the main driving factors, *Remote Sens. Environ.*, 48:319-331.

Coppin, P. R., and Bauer, M.E. 1996. Digital change detection in forest ecosystems with remote sensing imagery, *Remote Sensing Reviews*, vol. 13, pp. 207-234, 1996.

Olsson, H. 1994. Monitoring of local reflectance changes in boreal forests using satellite data. PhD thesis. Swedish University of Agricultural Sciences, Remote Sensing Laboratory. Report 7.

Peterson, U. 1992. Reflectance factor dynamics of boreal forest clear-cut communities during early secondary succession. *Int. J. Remote Sens.,* 13(12):2247-2262

Peterson, U. and Nilson, T., 1993. Successional reflectance trajectories in northern temperate forests. *Int. J. Remote Sens.* 14(3):609-613.

Av Skogsstyrelsen publicerade Rapporter:

I Skogsstyrelsens författningssamling (SKSFS) publiceras myndighetens föreskrifter och allmänna råd. Föreskrifterna är av tvingande natur. De allmänna råden är generella rekommendationer som anger hur någon kan eller bör handla i visst hänseende.

I Skogsstyrelsens Meddelande-serie publiceras redogörelser, utredningar m.m. av officiell karaktär. Innehållet överensstämmer med myndighetens policy.

I Skogsstyrelsens Rapport-serie publiceras redogörelser och utredningar m.m. för vars innehåll författaren/författarna själva ansvarar.

Skogsstyrelsen publicerar dessutom fortlöpande: Foldrar, broschyrer, böcker m.m. inom skilda skogliga ämnesområden.

Skogsstyrelsen är också utgivare av tidningen Skogseko.

Av Skogsstyrelsen publicerade Meddelanden:

1991:2   Vägplan -90
1991:3   Skogsvårdsorganisationens uppdragsverksamhet
           – Efterfrågade tjänster på en öppen marknad
1991:4   Naturvårdshänsyn – Tagen hänsyn vid slutavverkning 1989–1991
1991:5   Ekologiska effekter av skogsbränsleuttag
1992:1   Svanahuvudsvägen
1992:2   Transportformer i väglöst land
1992:3   Utvärdering av samråden 1989-1990 /skogsbruk – rennäring
1993:2   Virkesbalanser 1992
1993:3   Uppföljning av 1991 års lövträdsplantering på åker
1993:4   Återväxttaxeringarna 1990-1992
1994:1   Plantinventering 89
1995:2   Gallringsundersökning 92
1995:3   Kontrolltaxering av nyckelbiotoper
1996:1   Skogsstyrelsens anslag för tillämpad skogsproduktionsforskning
1997:1   Naturskydd och naturhänsyn i skogen
1997:2   Skogsvårdsorganisationens årskonferens 1996
1998:1   Skogsvårdsorganisationens Utvärdering av Skogspolitiken
1998:2   Skogliga aktörer och den nya skogspolitiken
1998:3   Föryngringsavverkning och skogsbilvägar
1998:4   Miljöhänsyn vid föryngringsavverkning - Delresultat från Polytax
1998:5   Beståndsanläggning
1998:6   Naturskydd och miljöarbete
1998:7   Röjningsundersökning 1997
1998:8   Gallringsundersökning 1997
1998:9   Skadebilden beträffande fasta fornlämningar och övriga kulturmiljövärden
1998:10   Produktionskonsekvenser av den nya skogspolitiken
1998:11   SMILE - Uppföljning av sumpskogsskötsel
1998:12   Sköter vi ädellövskogen? - Ett projekt inom SMILE
1998:13   Riksdagens skogspolitiska intentioner. Om mål som uppdrag till en myndighet
1998:14   Swedish forest policy in an international perspective. (Utfört av FAO)
1998:15   Produktion eller miljö. (En mediaundersökning utförd av Göteborgs universitet)
1998:16   De trädbevuxna impedimentens betydelse som livsmiljöer för skogslevande växt- och djurarter
1998:17   Verksamhet inom Skogsvårdsorganisationen som kan utnyttjas i den nationella miljöövervakningen
1998:18   Auswertung der schwedischen Forstpolitik 1997
1998:19   Skogsvårdsorganisationens årskonferens 1998
1999:1   Nyckelbiotopsinventeringen 1993-1998. Slutrapport
1999:2   Nyckelbiotopsinventering inom större skogsbolag. En jämförelse mellan SVOs och bolagens inventeringsmetodik
1999:3   Sveriges sumpskogar. Resultat av sumpskogsinventeringen 1990-1998
2001:1   Skogsvårdsorganisationens Årskonferens 2000
2001:2   Rekommendationer vid uttag av skogsbränsle och kompensationsgödsling
2001:3   Kontrollinventering av nyckelbiotoper år 2000
2001:4   Åtgärder mot markförsurning och för ett uthålligt brukande av skogsmarken
2001:5   Miljöövervakning av Biologisk mångfald i Nyckelbiotoper
2001:6   Utvärdering av samråden 1998 Skogsbruk - rennäring
2002:1   Skogsvårdsorganisationens utvärdering av skogspolitikens effekter - SUS 2001
2002:2   Skog för naturvårdsändamål – uppföljning av områdesskydd, frivilliga avsättningar, samt miljöhänsyn vid föryngringsav-
           verkning
2002:3   Recommendations for the extraction of forest fuel and compensation fertilising
2002:4   Action plan to counteract soil acidification and to promote sustainable use of forestland
2002:5   Blir er av
2002:6   Skogsmarksgödsling - effekter på skogshushållning, ekonomi, sysselsättning och miljön
2003:1   Skogsvårdsorganisationens Årskonferens 2002
2003:2   Konsekvenser av ett förbud mot permetrinbehandling av skogsplantor
2004:1   Kontinuitetsskogar - en förstudie
2004:2   Landskapsekologiska kärnområden - LEKO, Redovisning av ett projekt 1999-2003
2004:3   Skogens sociala värden
2004:4   Inventering av nyckelbiotoper - Resultat 2003

Reports 8a-8c from the Swedish National Board of Forestry are the proceedings- volumes from the scientific part of the ForestSat conference about "Operational Tools in Forestry Using Remote Sensing Techniques", held in Borås, May 31 – June 1, 2005.

The volumes contains 70 contributions from Europe, Canada and USA, which together gives a picture of the state of the art in research and practice in large area forest remote sensingin Europe and North America.